Yarmouk University

Faculty of Sciences

Geology and Earth Sciences

"Mineralogy, Geochemistry and Engineering Properties of Selected Basaltic flows from Yarmouk River Basalt, North Jordan"

Submitted by

Rawan Mohammad Araydah

Supervisor

Prof. Dr. Rafie Shinaq

Co-Supervisor

Prof. Ahmad Al-Malabeh

Second semester, 2018/2019

© Arabic Digital Library-Yarmouk University

المنارة للاستشارات
www.manaraa.com

"Mineralogy, Geochemistry and Engineering Properties of Selected Basaltic flows from Yarmouk River Basalt, North Jordan"

By

Rawan Mohammad Araydah

Submitted in Partial Fulfillment of the Requirements for the Degree of Master of Science in Applied Geology

Yarmouk University, Irbid, Jordan

Approved by:

Prof. Dr. Rafie A. Shinaq..... **(Supervisor)**

Department of Earth and Environmental Sciences, Yarmouk University

Prof. Dr. Ahmad A. Al-Malabeh.....

.....**(Co- Supervisor)**

Department of Earth and Environmental Sciences, HashemiteUniversity

Pro. Dr. Nizar S. Abu Jaber.....**(Member)**

German Jordanian University

Dr. Sana'a A. Odat.....**(Member)**

Department of Earth and Environmental Sciences, Yarmouk University

May – 2018

© Arabic Digital Library-Yarmouk University

المنارة للاستشارات
www.manaraa.com

Dedication

I dedicate my dissertation work to my family and my friends. A special thanks to my loving parents, the memory of my father "Mohammad" and my loved mother "Arwa", who supported me to finish this work, and for their encouragement and assistance.

© Arabic Digital Library-Yarmouk University

المنارة للاستشارات
www.manaraa.com

Acknowledgment

My heart pulsates with the thrill for tendering gratitude to those persons who helped me in the completion of my master thesis. The most pleasant point of presenting a thesis is the opportunity to thank those who have contributed to complete it. Unfortunately, the list of expressions of thank no matter how extensive is always incomplete and inadequate. Indeed this page of acknowledgment shall never be able to touch the horizon of generosity of those who tendered their help to me.

First and foremost, I would like to express my gratitude and indebtedness to my committee chairman for his countless hours of reflecting, reading, encouraging, and most of all patience throughout the entire process, thank you Prof**. Dr. Rafie Al- Shinaq and** Prof**. Dr. Ahmad Al-Malabeh** for their kindness in allowing me introducing the present topic and for their inspiring guidance, constructive criticism and valuable suggestion throughout the project work.

I am sincerely thankful them for guidance and pain taking efforts in improving my understanding of this project. I am also grateful to **Dr. Sa′eb Al Shrideh** (Head of the Department of Earth and Environmental Sciences) for assigning me this interesting project and for his valuable suggestions and encouragements at various stages of the work.

© Arabic Digital Library-Yarmouk University

المنارة للاستشارات

www.manaraa.com

Inordinate thanks to the Deanship of Scientific Research and Graduate Studies for funding this research at the Yarmouk University. I would like to thank the Department of Civil Engineering in Jordan University of Science and Technology (JUST) for helping me to prepare the core samples and using their machines.

I would like to thank **Dr. Mohammad Al-Qudah**, who helps me to work with the Coral Draw software. I also would like to thank Mrs. Ghusun Zaiter who helped me preparing thin sections professionally. I would to acknowledge and thank Hadeel Herzallah for helping me in the SEM study, Mrs. Abeer Al-Zu'bi for helping me in studding thin section and Mrs. Ameinah Alawneh, Safaa Khashashneh and Qutaiba Al-Rashdan for helping me in using microscope at the Earth and Environmental Science Department in Yarmouk University.

I would like to thank Eng. Nabeel odelat, Heba Naser, Maysoon Khzaei and Kholud Aayyash from Natural Resources Authority for helping me to complete the engineering and chemical tests.

Full thanks to my Colleague and my best teacher (**Ali Smadi**) who helps me in the field work, thin sections preparation and using software.

© Arabic Digital Library-Yarmouk University

المنارة للاستشارات
www.manaraa.com

Table of Contents

© Arabic Digital Library-Yarmouk University

www.manaraa.com

© Arabic Digital Library-Yarmouk University

المنارة للاستشارات

www.manaraa.com

© Arabic Digital Library-Yarmouk University

www.manaraa.com

© Arabic Digital Library-Yarmouk University

المنارة للاستشارات

www.manaraa.com

© Arabic Digital Library-Yarmouk University

www.manaraa.com

© Arabic Digital Library-Yarmouk University

www.manaraa.com

LIST OF TABLES

© Arabic Digital Library-Yarmouk University

المنارة للاستشارات

www.manaraa.com

© Arabic Digital Library-Yarmouk University

المنارة للاستشارات
www.manaraa.com

LIST OF FIGURES

© Arabic Digital Library-Yarmouk University

المنارة للاستشارات
www.manaraa.com

© Arabic Digital Library-Yarmouk University

المنارة للاستشارات
www.manaraa.com

© Arabic Digital Library-Yarmouk University

www.manaraa.com

© Arabic Digital Library-Yarmouk University

www.manaraa.com

© Arabic Digital Library-Yarmouk University

المنارة للاستشارات
www.manaraa.com

© Arabic Digital Library-Yarmouk University

المنارة للاستشارات
www.manaraa.com

© Arabic Digital Library-Yarmouk University

www.manaraa.com

© Arabic Digital Library- Yarmouk University

www.manaraa.com

© Arabic Digital Library-Yarmouk University

www.manaraa.com

© Arabic Digital Library- Yarmouk University

www.manaraa.com

Abbreviations and Acronyms of minerals and study area

Mineral (after Kretz, 1983; and Spear, 1993)

No	Symbol	Description
1.	%A	Abrasion percent
2.	AAR	Alkali-Aggregate-Reaction
3.	Ab	Albite
4.	Afs	Alkali feldspar
5.	An	Anorthite
6.	An%	Anorthite percentage
7.	Ap	Apatite
8.	ASTM	American Society for Testing and Materials
9.	Aug	Augite
10.	BMSL	Below mean sea level
11.	Cal	Calcite
12.	CEA	Chalcophile Elements Abundance
13.	cpx	Clinopyroxene
14.	D	diameter
15.	Di	Diopside
16.	DIM	Digital elevation modal
17.	e	Void ratio
18.	EDXS	Energy dispersive x-ray spectroscopy
19.	EIA	Environmental Impact Assessments
20.	EX	Exfoliated

© Arabic Digital Library-Yarmouk University

المنارة للاستشارات
www.manaraa.com

21.	En	Enstatite
22.	F	Force
23.	Fa	Fayalite
24.	Fo	Forsterite
25.	GH	Golan Height
26.	GPS	Global positioning system
27.	Hy	Hypersthene
28.	HFSE	High - field strength elements
29.	I.A.E.G	International Association of Engineering Geologists
30.	ICP	Inductive coupled plasma
31.	Id	iddingsite
32.	Il	Illmenite
33.	IP	induced polarization
34.	ISRM	Institution Standard for Rocks and Materials
35.	*Iw*	Initial weight of the sample
36.	KD	Distribution coefficient
37.	L	Length
38.	L.A	Los Angeles
39.	LFSE	low - field strength elements
40.	LILE	lithophiles elements
41.	MCM	Muwaqqar Chalk Marl Formation
42.	MPa	Megapascal
43.	MQD	Mudawwara Quwayra Dike

© Arabic Digital Library-Yarmouk University

www.manaraa.com

44.	Mt	Magnetite
45.	Ne	Nepheline
46.	Ol	olivine
47.	Opx	Orthopyroxene
48.	Or	Orthoclase
49.	Ox	Oxides
50.	P	compression wave
51.	PPL	Plane polarized light
52.	Pl	Plagioclase
53.	PM	Polarized microscope
54.	Px	Pyroxene
55.	Q	Quartz
56.	r	correlation coefficient
57.	S	Shear wave
58.	Sdl	Sodalite
59.	SEM	Scanning Electron Microscope
60.	SpG_a	apparent, saturation specific gravity
61.	spG_d	bulk, true or absolute specific gravity
62.	spG_s	bulk specific gravity-saturated surface dried
63.	TEA	Transition Elements Abundance
64.	UCS	uniaxial compressive strength
65.	URC	Umm Rijam Chert Limestone Formation
66.	UTM	Universal transverse mercator

© Arabic Digital Library-Yarmouk University

المنارة للاستشارات
www.manaraa.com

67.	UW	dry unit weight
68.	UWV	Ultrasonic Wave Velocities
69.	ν	volume
70.	V	vesicular basalt
71.	Ves	Vesicles
72.	V_p	the P-wave Velocity
73.	WA	water absorption
74.	Wo	Wollastonite
75.	WSC	Wadi Shallala Chalk Formation
76.	XRD	X-ray diffraction
77.	XRF	X-Ray Fluorescence
78.	γ	unit weight of rock
79.	YB	Yarmouk Blocky
80.	γd	dry unit weight
81.	YE	Yarmouk Exfoliated
82.	YM	Yarmouk Massive

© Arabic Digital Library-Yarmouk University

المنارة للاستشارات
www.manaraa.com

Abstract

Araydah, Rawan Mohammad. Mineralogy, Geochemistry and Engineering Properties of Selected Basaltic flows from Yarmouk River Basalt, North Jordan. Master of Science Thesis Department of Earth and Environmental Science, Yarmouk University, 2018 (Supervisor: Prof. Dr. Rafie Shinaq, Co-Supervisor: Prof. Ahmad Al-Malabeh)

This thesis presents the results of the study conducted on "Mineralogy, Geochemistry and Engineering Properties on selected Basaltic flows from YRB area, North Jordan".

Geologically, the study area is part of Harrat Al shaam that covered the northern part of Jordan.

The exposed formation in the study area is Wadi Shallala Chalk Formation (WSC). Four types of basalt flows are exposed there: sheeted, massive, pahoehoe, a´a and vesicular basalt. The measurable thicknesses of those flows range from few meters up to 122 m.

To study the mineralogical, chemical, physical and mechanical properties, 20 rock samples were collected from different locations of the basalt flows.

© Arabic Digital Library-Yarmouk University

المنارة للاستشارات
www.manaraa.com

Mineralogical data display that the YRB samples consist of the following minerals: plagioclase, olivine, pyroxene, feldspar, alkali feldspar, opaque's, carbonates and iddingsite.

The obtained petrographical data show that the basalt consists of mesocratic and hypocrystalline minerals, and reflects limited variations. They are composed mainly of pyroxene -phyric basalt, olivine- pyroxene phyric basalt and olivine Phyric basalt type. The YRB minerals are arranged and exhibit mainly as porphyritic, glomeroporphyritic, paliotaxitic, vesicular, amygdaloidal and intergranular textures.

Geochemically, all of the inspected YRB display ultrabasic compositions (i.e., bulk rock silica SiO_2 composition is less than 46% and classified as alkaline to sub alkaline basalt.

The basaltic rocks show a variety of textural and mineralogical characteristics, which may affect their physical and mechanical properties as well as their use as construction materials. They have high apparent specific gravity ranging from 2.62 to 2.91 gm/cm^3. The bulk specific gravity ranges (oven dry basis) from 2.54 to 2.89 gm/cm^3. The bulk Specific gravity (S.S.D dry basis) ranges from 2.57 to 2.90 gm/cm^3. The absorption values ranges from 0.14 to 1.38%. The specific gravity is considered to be high and its texture is crystalline.

© Arabic Digital Library-Yarmouk University

المنارة للاستشارات
www.manaraa.com

The porosity values ranges from 0.4 to 3.59% indicating low porous rock. The void ratio ranges from 0.004 to 0.0372%, the uniaxial strength ranges from 353.33 to 611.36 MPa with an average value of 485.40 MPa which is classified as very high strength and extremely hard rock according to class A (>250 MPa) classification.

According to the result of Los Angeles Abrasion test basalt uniformity of wear ranges from 0.195 to 0.198% with an average value of 0.1965%. Following the classification system proposed by Deere and Miller the tested basalt samples display high ultrasonic wave velocity of class 4 ranging from 3141 to5514 m/s giving an average value of 4003 m/s. The relationship between porosity, compressive strength and deformability indicates that the YRB show low porosity of 1.8% and can be classified as extremely strong and slightly deformable as building materials.

Based on field descriptions, petrographical studies, chemical analyses, physical, and mechanical testing this study explained that the genesis of basalt is related to the extension of Harrat Al- Shaam.

Key Words: Porosity, Unconfined compressive strength, Los Angeles Abrasion

© Arabic Digital Library-Yarmouk University

المنارة للاستشارات
www.manaraa.com

ملخص

عرايضة، روان محمد. الخواص المعدنية والجيوكيميائية والهندسية للإنسيابات البازلتية في نهر اليرموك، شمال الاردن. رسالة ماجستير في العلوم، قسم علوم الأرض والبيئة، جامعة اليرموك، ٢٠١٨ (المشرف: أ.د. رافع شناق، المشرف المشارك :أ. د. أحمد الملاعبة)

تقدم هذه الرسالة نتائج الدراسة التي تم الحصول عليها من تحليل الخواص المعدنية والكيميائية والهندسية لمقاطع بازلتية مختارة في منطقة نهر اليرموك، شمال الأردن.

تعتبر منطقة الدراسة جزء من حرة الشام والتي تغطي الجزء الشمالي منها. أما بالنسبة للتكوين المتكشف في منطقة الدراسة فهو تكوين وادي الشلالة

أثبتت الدراسات الميدانية أن بازلت نهر اليرموك يتكون من أربع انسيابات بازلتية هي من الأقدم إلى الأحدث كما يلي: انسيابي ، كتلي، بهاويهو وآآة وبازلت فقاعي، تتراوح سماكاتها من بضعة أمتار إلى ١٢٢م.

تم جمع ثلاثون عينة من مختلف مواقع البحث لأجراء الدراسات المعدنية والكيميائية والهندسية مثل الوزن النوعي وسرعة الصوت.

أظهرت الدراسات المعدنية أن البازلت الموجود في منطقة نهر اليرموك يتكون البلاجيوكليز،البيروكسين، الأوليفين كمعادن أساسية بالإضافة إلى وجود معادن ثانوية مثل المعادن القلوية ومعادن الفلدسبار وأكاسيد الحديد والكربونات والادنغزايت .

بينت الدراسات البتروغرافية والمهجرية إن البازلت متوسط اللون و ٥٠% من البلورات مكتملة النمو. تم تقسيم البازلت بتروغرافيا إلى ثلاثة أنواع : بيرو كسين بازلتي ، أوليفين بازلتي، والاوليفين- بيرو كسين بازلت

© Arabic Digital Library-Yarmouk University

المنارة للاستشارات
www.manaraa.com

تترتب معادن البازلت فيما بينها من خلال النسيج المتباين والكتلي والفقاعي والنسيج الزاوي والممتلئ والبين حبيبي.

تم تصنيف الصخور كيميائيا بأنها ذات مكونات فوق قاعدية ومحتوى السليكا فيها أقل من ٤٦% ، كما وتم تصنيفها أيضا على كونها نوع من البازلت القلوي إلى شبة القلوي.

أظهرت الصخور البازلتية خصائص معدنية ونسيجية مختلفة والتي بدورها تؤثر على الخصائص الفيزيائية والميكانيكية واستخدامها كمواد بناء، حيث تمتلك هذه الصخور وزن نوعي ظاهري يتراوح مابين ٢.٢٦ و ٢.٩١غم/سم^{٣}، ووزن نوعي طبيعي جاف يتراوح ما بين ٢.٥٤ الى ٢.٨٩غم/سم^{٣}،ووزن نوعي مشبع ذو سطح جاف يتراوح ما بين ٢.٥٧ إلى ٢.٩٠غم/سم^{٣}. تتراوح نسبة الامتصاص من ٠.١٤ إلى ١.٣٨% ويعتبر الوزن النوعي عالي وهذا يشير الى أن الصخور متبلورة.

تتراوح نسبة المسامية للصخور ما بين ٠.٤ إلى ٣.٥٩%والتي صنفت على أنها صخور ذات مسامية قليلة، تتراوح نسبة الفراغات ما بين٠.٠٠٤ إلى ٠.٣٧٢%. تتراوح قيم الضغط اللامحصور مابين ٣٥٣.٣٣ إلى ٦١١.٣٦ ميجاباسكال بمعدل يصل إلى ٤٨٥.٤٠ ميجاباسكال وبناء عليه صنفت هذه الصخور بأنها ذات ضغط عالي وصخور قاسية جدا تبعا للتصنف أ(>٢٥٠) ميجاباسكال.

أثبتت نتائج فحص التآكل على عينات البازلت التي تم دراستها باستخدام جهاز لوس أنجلوس بأن هذه الصخور متشابة في درجة التآكل حيث تتراوح نسبة التآكل لها من ٠.١٩٥ إلى ٠.١٩٨ % بمعدل يصل إلى ٠.١٩٦٥%.

تصنف العينات الصخرية البازلتية بأنها ذات سرعة موجية فوق صوتية عالية جدا (من الدرجة الخامسة) وتتراوح قيمها من ٣١٤١ إلى ٥٥١٤ م/ث بمعدل يصل ٤٠٠٣م/ث.

© Arabic Digital Library-Yarmouk University
المنارة للاستشارات
www.manaraa.com

تشير العلاقة بين المسامية والضغط المحصور والتشوه إلى إن بازلت نهر اليرموك له مسامية قليلة ١.٨% ويصنف على انه صخر قوي جدا وذو تشوه قليل.

اعتمادا على الوصف الميداني والدراسات البتروغرافية والتحاليل الكيميائية والفحوصات الفيزيائية والميكانيكية تبين هذه الدراسة أن أصل المنشأ للبازلت يعود لامتداد حرة الشام.

الكلمات المفتاحية :المسامية، الضغط اللامحصور، التآكل بجهاز لوس أنجلس

© Arabic Digital Library-Yarmouk University

المنارة للاستشارات
www.manaraa.com

Chapter One

Introduction

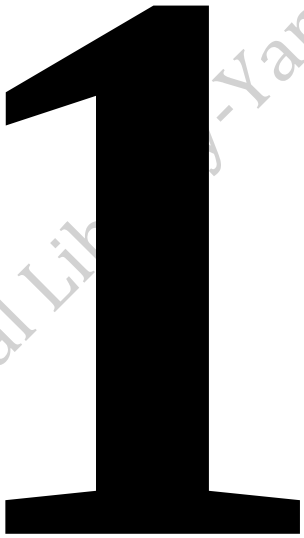

© Arabic Digital Library-Yarmouk University

www.manaraa.com

Chapter one

1.1 Introduction

Basalt is a mafic, melanocritic (dark-toned), aphanitic fine-grained, dense volcanic igneous rock. The mineral grains of basalt are so fine that they cannot be distinguished by naked eye or even by a magnifying glass. Basalt is the most common type of extrusive igneous rocks and the most common igneous rocks found in the earth (Ibrahim et al. 2007). It consists of olivine, plagioclase, and pyroxene and opaque. It's also contains accessory minerals such as, alkali feldspar.

Most magma originate by melting in the Earth's mantle and lower crust, plate tectonic and other geologic setting such as rifting and subduction zones plays a major role in the generation of several magma types such as basaltic, andesitic and rhyolitic . When the shallow mantle undergoes partial melting, the basaltic magma rises and crystallizes to produce earth crust and basaltic rocks (Winter 2001).

According to their mineralogical compositions basaltic rocks originate in various types such as, tholeiitic and alkali basalt, both of these magma types are distinct (Raymond, 2002).

© Arabic Digital Library-Yarmouk University

المنارة للاستشارات
www.manaraa.com

Basaltic rocks and extrusive structures are commonly produced when primary magma undergoes rapid phase of cooling then forced out onto the surface of the earth. Extrusive structures are divided into three groups: major, intermediate and minor. The largest structures lava plateaus and basaltic plains are tabular in overall form and are composed primarily of lava flows of silica – poor (basaltic) volcanic rock. The minor structure is lava flow (magma that lost gas when it erupted at the surface) and formed piles of rock up to several thousand meter thick (Raymond, 2002). The volcanic rocks are mainly widespread in the northwestern part of the Arabian Plate that Jordan considered to be part of it. Basaltic rocks in Jordan are distributed in many localities, including northern, northeastern, central and southern parts of the country (Al-Malabeh, 2009).

According to Bender, (1974) and Al Malabeh, (1993), basaltic rocks in Jordan are mainly Tertiary to Quaternary in age and cover an area up to 18 % of Jordan.

They present the following ages:

- Oligocene to Early Miocene (26.23 - 22.17 million years).
- Middle to Late Miocene (13.97 - 8.94 Ma).
- Late Miocene to Pleistocene (6.95 Ma to < 0.15 Ma).

© Arabic Digital Library-Yarmouk University

المنارة للاستشارات
www.manaraa.com

YRB is part of the Harrat Al-Shaam and exposed on both sides of the Yarmouk River Valley. It is Holocene to Late Pleistocene in age (2.6 million years -100,000 years (Al- Malabeh et al. 2016**).**

Harrat Al-Shaam is believed to be produced from paleo-volcanic activities, accompanied by opening continental rifts since beginning of the Oligocene and frequently in the Miocene, Pliocene and Pleistocene (Ilani et al. 2001). It is considered to be one of the largest basalt field located on the Arabian plate covering approximately 50,000 km^2 and extends in the NW-SE direction over 7000 km long from Saudi Arabia in the south through Jordan and Syria in the north (Coleman and McGuire 1988; Camp and Roobol 1992; and Pick et al. 1999). During the Cenozoic era, basaltic lava poured out from vertical fissures and local vents, and covered large areas in Jordan (Moh`d, 2000). Most of the basalt occurrences are concentrated in the northeastern part as a large volcanic field covering an area of 12,000 km^2 which is considered to be a part of Harrat Al –Shaam as shown in (Figure1.1: a, b).

The Jordanian part of Harrat Al-Shaam north Jordan is known as Jordanian Harrat basalt including the study area (Al-Malabeh, 2003).

Many ancient civilizations developed the use of natural stone to a fine art, and dimension stones. Basalt still occupies an important place in

© Arabic Digital Library-Yarmouk University

المنارة للاستشارات
www.manaraa.com

architecture, particularly in the construction of prestigious buildings. Many historical cities was built from basalt in north and northeast Jordan such as the Greek Roman castles in northeast Jordan (Al-Malabeh, 2004), the Decapolis city of Umm Qays (Gadara) and parts of Abila (Quelebeh).

The physical, chemical, mechanical and the high abrasion resistance properties of basalt make it very significant for industrial applications and building materials (Figure 1.2).

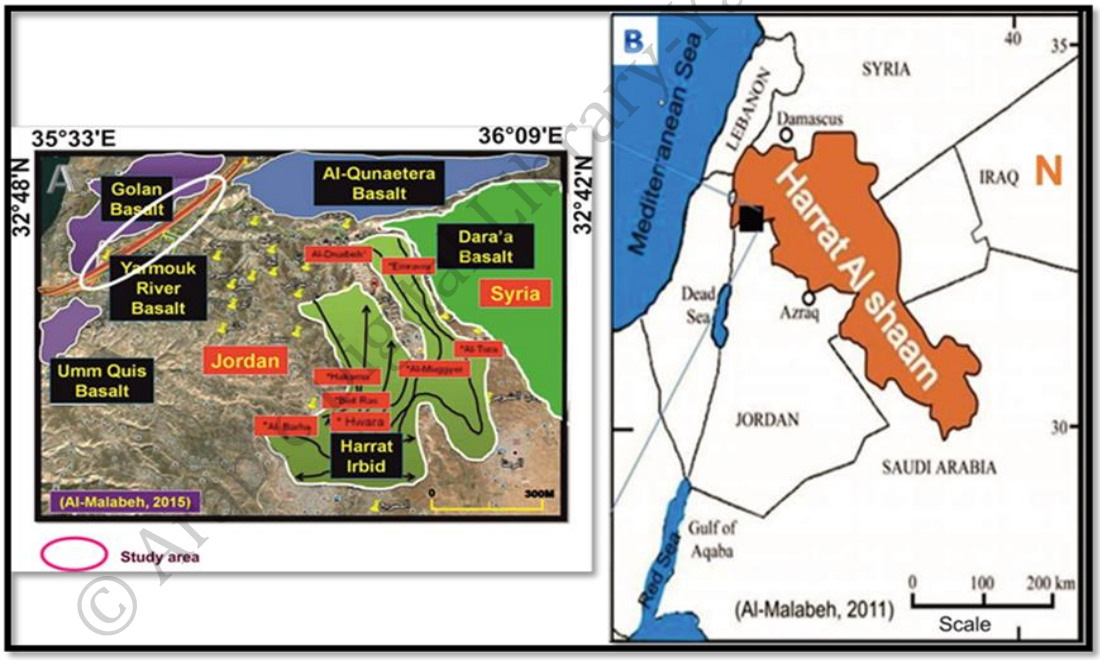

Figure (1.1): A. Harrat Al-Shaam basalt in the north Jordan, and B. Map showing the location of Harrat Al-Shaam.

© Arabic Digital Library-Yarmouk University

www.manaraa.com

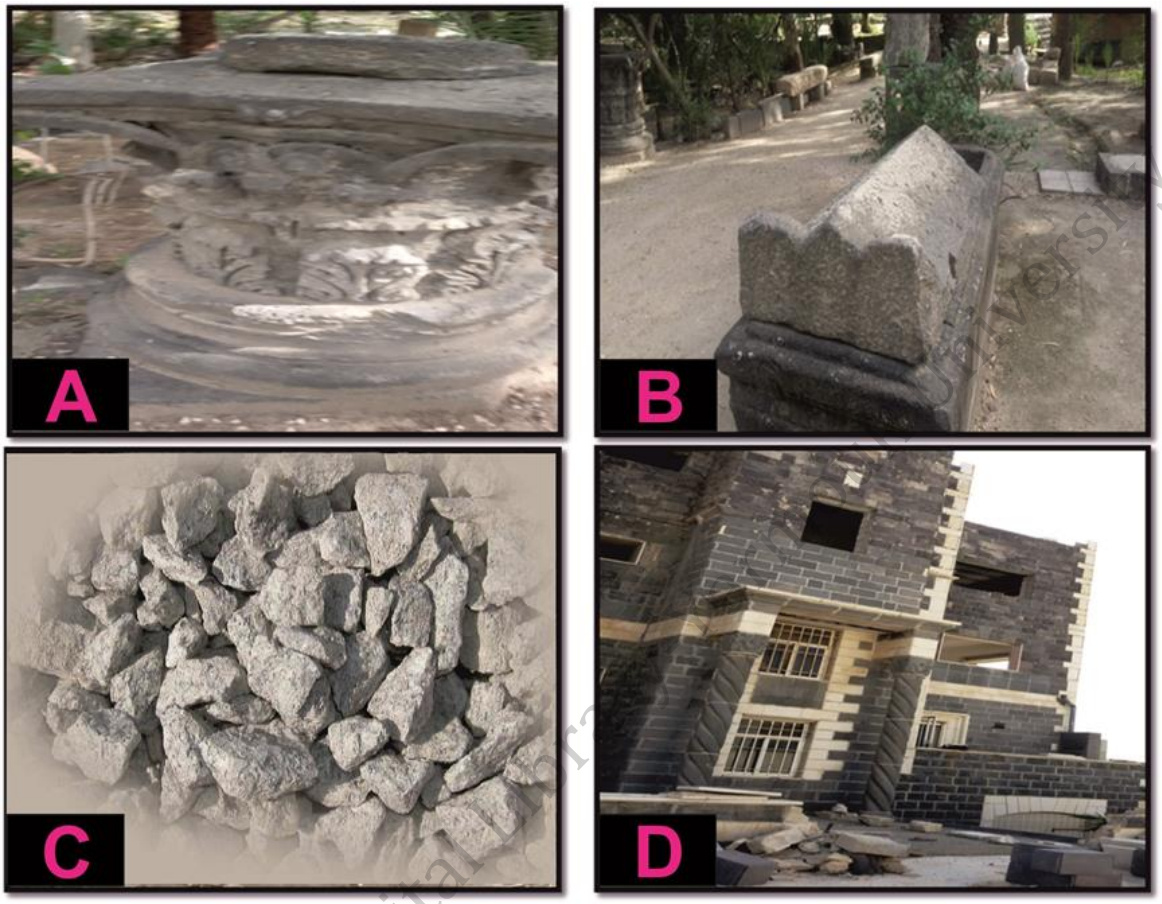

Figure (1.2): Main uses of basalt: (A&B) Basalt used in architectural applications to build columns and ran's in historical places. (C). Aggregate of basalt used in asphaltic concrete mixtures (D).Uses of basalt as construction material.

Dimension modified stones of basalt used for building and decoration. In addition, basalt is used in agriculture - and construction applications, basalt aggregate or crushed basalt is the best reinforcement for concrete due

© Arabic Digital Library-Yarmouk University
المنارة للاستشارات
www.manaraa.com

to its tensile and high compressive strength and natural resistance to deterioration (Al-Malabeh, 2004).

Basaltic rocks are used extensively as engineering materials including aggregates for Portland cement, concrete mix and asphaltic concrete, rock fill for dams and breakwaters, as well as for railroad ballast and highway base courses and cut stones (Goodman, 1993). It is very important in architectural applications and was used in manufacturing process to produce tiles and slabs (Al-Baijat and Benedetti, 2013). However, texture of a basaltic rock is an additional and complex factor affecting its physical and mechanical properties. Changes in mineralogical composition and texture of basalts also affect physical and mechanical properties and their quality as aggregate and other types of uses. Furthermore, basaltic rocks generally have higher unit weight than other rock; therefore, basalt aggregate has a high relative density. It also shows excellent ability in thermal and acoustic insulation, due to its high specific gravity and low porosity values.

© Arabic Digital Library-Yarmouk University

1.2 Previous studies

Studies carried out on the Jordanian Harrat can be divided into old and the new studies.

Old Studies

المنارة للاستشارات
www.manaraa.com

Lartet (1869) was the first scientist who studied the North Arabian Volcanic Province, and Dubertret (1929) was the first scientist who published the geological map.

Wiesmann and Abdullatif (1963) represent the first regional geological and petrological investigation of the basalt northeast of Jordan. Six different basalt flows were identified in the Jordanian Harrat by Van Den Boom and Sawwan (1966) and Bender (1974).

Barberi et al. (1979) and Moffat (1988) used K-Ar dating to provide the absolute ages of the basalt in the Jordanian Harrat.

Ibrahim (1993) subdivided the basaltic flows into five volcanic-stratigraphic groups, consisting of Wisad, Safawi, Asfar, Rimah and Bishriyya Groups.

New Studies

Series of studies on the basaltic flows and tephra volcanic cones accomplished by Al-Malabeh (1989 &1994) and Al-Malabeh et al. (2002). Al-Malabeh (1994) concluded that the Jebal Aritain and Jebal Fahem volcanoes were generated by primary magmas, formed at low degrees of 3-8% due to partial melting of a consolidated and homogeneous garnet peridotite mantle source, at > 100 km depth.

© Arabic Digital Library-Yarmouk University

المنارة للاستشارات
www.manaraa.com

Ibrahim et al. (2003) suggested a new subdivision of the basaltic dike system in north-eastern Jordan depending on geological ages. During the Early Miocene, basalt was characterized by a tholeiitic composition, while in the Middle to Late Miocene it was characterized by an increase in the alkaline character of the magma chamber. In the final stage (around 1.7Ma), the dikes comprises a basanite composition.

Al-Zyoud (2005) modified the evaluation of basaltic rocks in Al-Hashimiyya area, and studied the physico-mechanical properties of these rocks.

Kempe and Al-Malabeh (2005) concluded that the lava field of basaltic plateaus on the Arabian plate may be derived from Asthenosphere and Lithospheric partial melting of the mantle.

El-Hasan and Al-Malabeh (2008) studied the basaltic rocks in El-Lajjoun in central Jordan, and concluded that the basalt is resulted from a low degree of partial melting (10%) of a homogeneous garnet peridotite mantle source in the Asthenosphere at a depth > 100 km.

Al-Malabeh (2009) studied considerable amounts of mantle xenoliths within pyroclastic successions in Al-Harida volcano in the Jordanian Harrat, and concluded that the slight enrichments of some incompatible elements indicate cryptic metasomatism.

© Arabic Digital Library-Yarmouk University

المنارة للاستشارات
www.manaraa.com

Abu-Mahfouz (2009) studied the petrogenesis of basaltic rocks in Irbid district northern Jordan, and their engineering properties as building materials. This study added a new area of about 300 Km^2 to Harrat Al-Shaam and new economic value in building and construction applications.

Bany Yaseen et al. (2010) distinguished low Mg-ratios as an indication of fractional crystallization in tuff samples in northeast Jordan. This study implies derivation from a peridotite source in the upper mantle with low degree of melting.

Al- Oufi et al. (2012) used induced polarization (IP) imaging survey to detect lava caves in the basaltic flows in Harrat Al- Shaam in northeast Jordan. High precision and distinct economic value make IP a very important tool for mapping the extents of lava caves and illustrating the subsurface structures.

Kempe et al. (2012) studied lava caves in Harrat Al-Shaam, North-eastern Jordan, and established that Jordan has a large fraction of pressure ridge caves.

Bany Yaseen (2014) studied petrography and mineral chemistry of the Almandine garnet in Harrat Al-Shaam plateau in north eastern Jordan, and found that the Miocene alkaline basaltic garnet xenoliths are related to lithosphere mantle origin.

© Arabic Digital Library-Yarmouk University

المنارة للاستشارات
www.manaraa.com

Ibrahim et al. (2014) studied the volcano tectonic evolution in central Jordan, and established that the differences in the basalt composition are indicators of different degrees of partial melting and fractionation.

Alnawafleh et al. (2015) studied representative samples from the Mudawwara Quwayra Dike (MQD) and subdivided them into sub-alkaline basaltic rocks.

1.3 Research Question

The previous studies show that no researchers attempts to tackle the problem of studying the mineralogical, petrographical, geochemical, physical and mechanical properties of the basalt rocks at the Yarmouk River area. This study aims to fill this gap and provide a detailed exploration.

1.4 Location of study Area

The study area is located North West of Jordan near Birkat Al Arayes in Al Mokhaba country Figure (1.3 and 1.4). (YRB) is located 25km north of Irbid. The area is bounded by the longitudes 35° 69′ E to 35° 71′ E and Latitudes 32° 67′ N to 32° 69′ N. Basalt flows in the study area are underlain by the Shallala Chalk Formation, which is the main exposure in Wadi Shallala.

© Arabic Digital Library-Yarmouk University

المنارة للاستشارات
www.manaraa.com

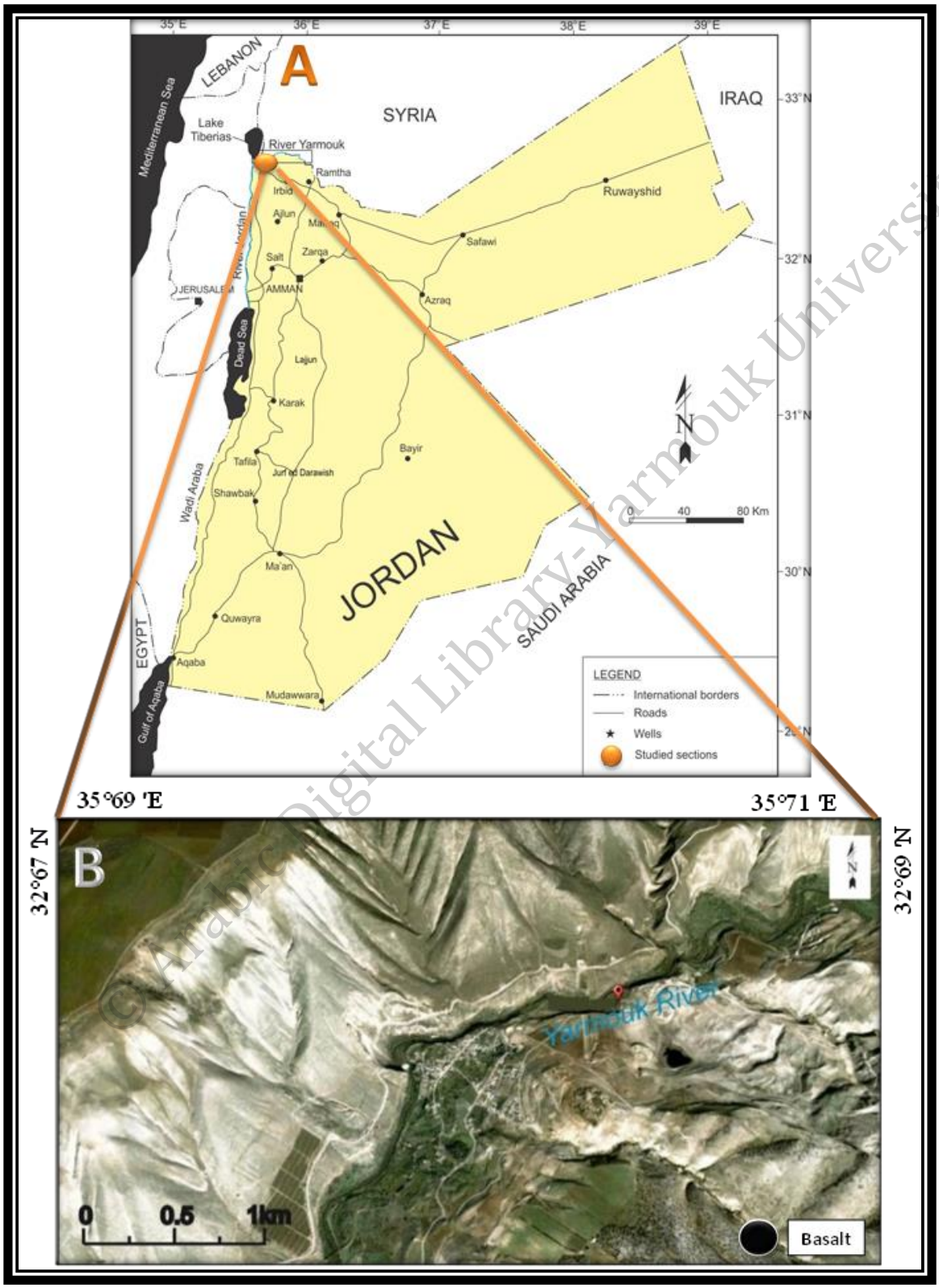

Figure (1.3): Showing: (a). Jordan map (b).Google earth image showing the Location of basalt in the study area North Jordan (www.Googleearth.com).

© Arabic Digital Library-Yarmouk University

المنارة للاستشارات
www.manaraa.com

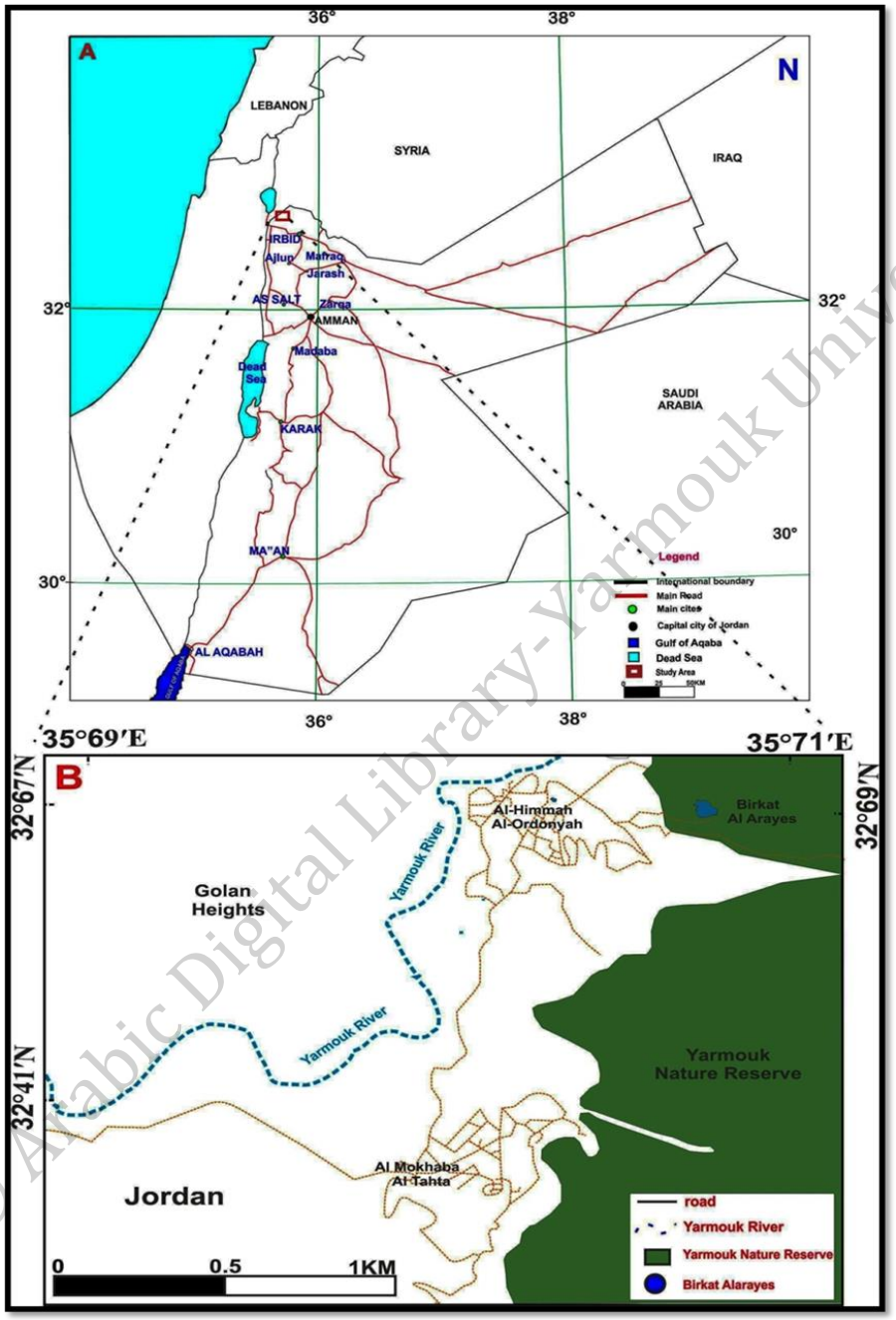

© Arabic Digital Library-Yarmouk University

Figure (1.4): Generalized figure showing: (a). Physiographic map of Jordan and the location of the study area (Modified after Central Intelligence Agency CIA, 2004), (b). Google earth image shows road map in the study area.

المنارة للاستشارات
www.manaraa.com

1.4.1 Geology of the study area

The basalt flows in the study area are underlain by rocks of Balqa Group (Moh'd, 1997). According to Powell, (1989) they crop out in north Jordan along the Yarmouk River and along the eastern margins of the rift. The Balqa Group includes Umm Ghudran Formation, Amman Silicified Limestone Formation, Al-Hisa Phosphorite Formation, Muwaqqar Chalk Marl Formation and Umm Rijam Chert Limestone Formation Figure (1.6).

1.4.1.1 Muwaqqar Chalk Marl Formation (MCM), B3

This formation is Maastrichtian to Paleocene in age and composed of soft, thick-bedded chalky- marl, marl, chalky limestone, marly limestone and hard microcrystalline limestone concretions within clayey marl associated with fossils including bivalve, gastropods and fish teeth. High bitumen content in the Muwaqqar chalk-marl in the local fault -controlled basins such as the Yarmouk river area, due to formation of deeper –water basin with stagnant anoxic basal water-mass which preserved settling planktic and nektonic organic matter, such high kerogenous marls are termed oil shale in Jordan (Powell, 1989). The thickness of this formation ranges from 120 m to 320m (Moh'd, 1997).

© Arabic Digital Library-Yarmouk University

www.manaraa.com

1.4.1.2 Umm Rijam Chert Limestone Formation (URC), B4

URC is Eocene in age, 220m thick and consists mainly of chalky limestone, chalk, marly limestone, kerogenous limestone and chert unit (Moh'd, 1997).

1.4.1.3 Wadi Shallala Chalk Formation (WSC)

The age of this formation ranges from middle to upper Eocene**.** It crops out in north Jordan along Wadi Shallala and the Yarmouk River, (Figure1.5) .The formation is made up of chalk, marl, glauconitic and micritic limestone. The chalk is rich in chert nodules, and covered with marl and marly chalk (Al-Hunjul, 2001).

Figure (1.5): outcrop of Wadi Shallala Chalk Formation covered with basalt flows at the Yarmouk River.

© Digital Library- Yarmouk University

المنارة للاستشارات
www.manaraa.com

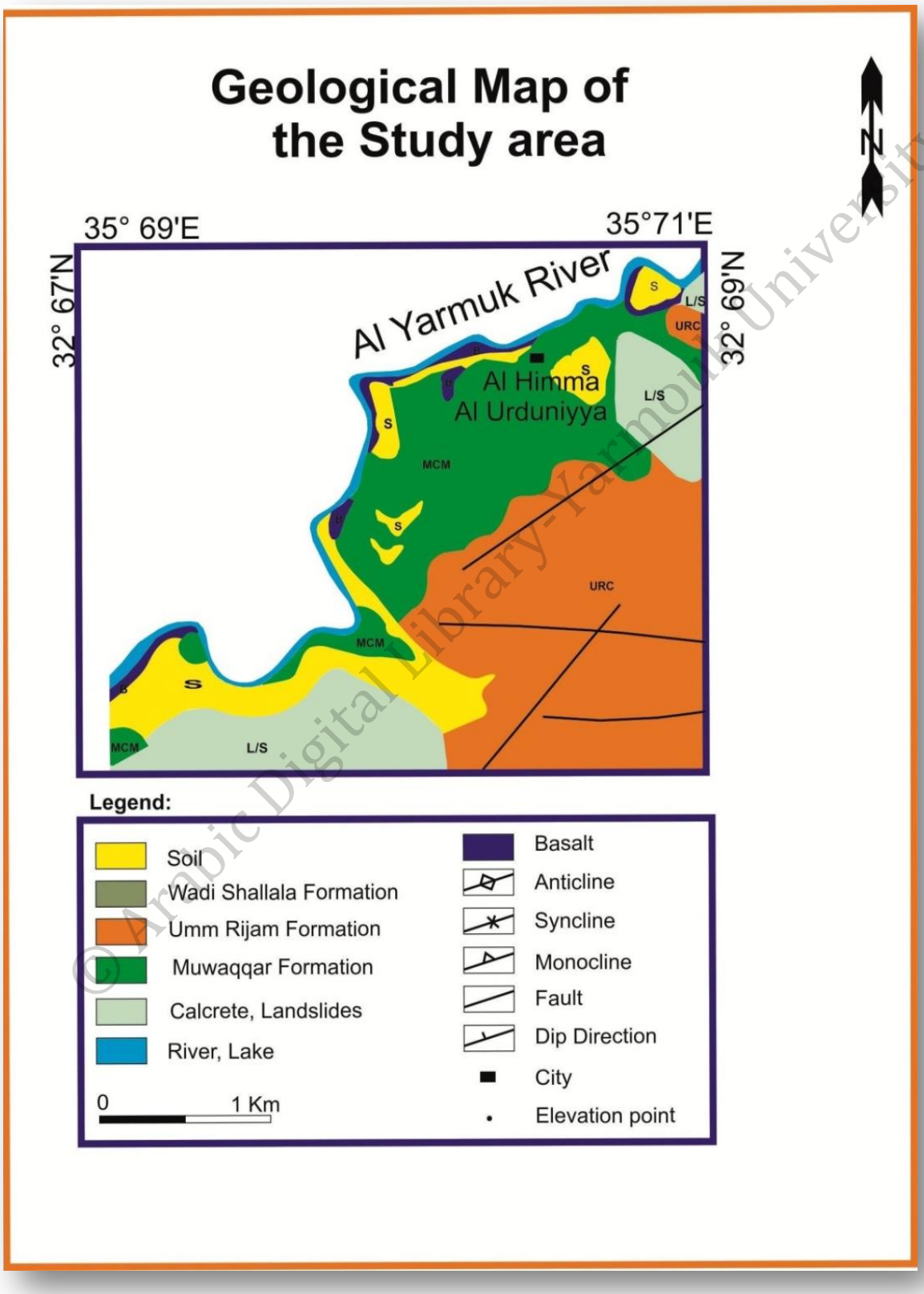

Figure (1.6): Geologic map of the study area (After Moh'd, 1997).

© Arabic Digital Library-Yarmouk University

المنارة للاستشارات
www.manaraa.com

Following is a brief description of the exposed rock formations in the study area (Figure1.7):

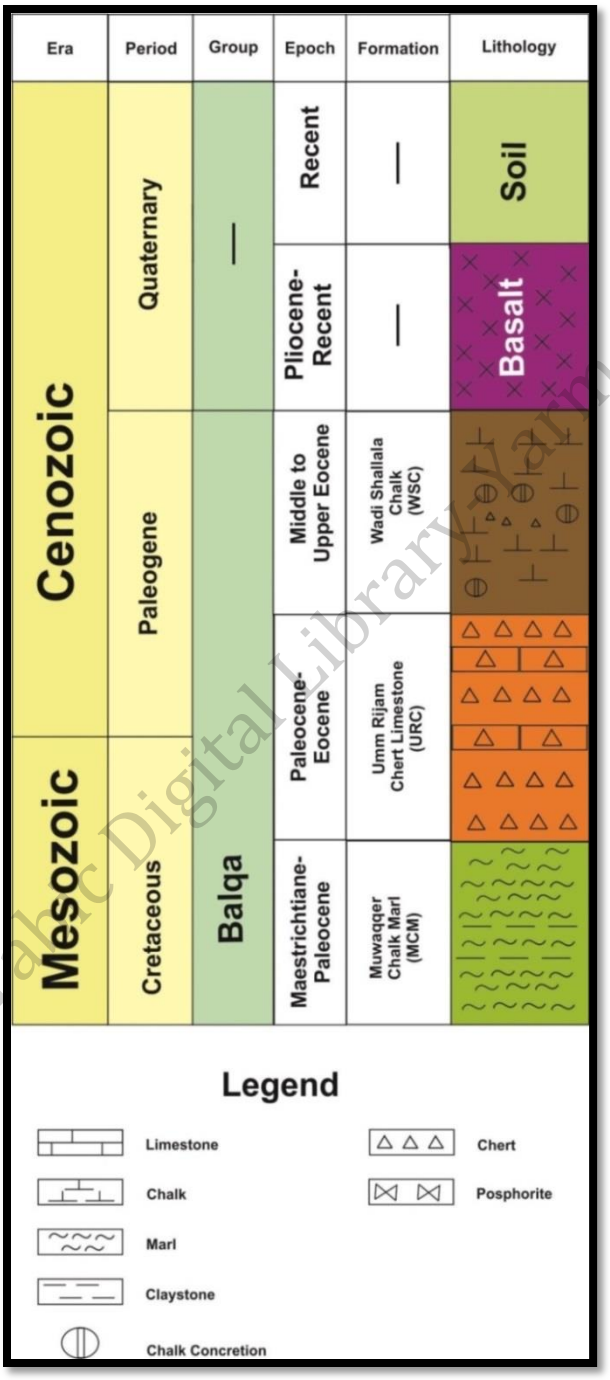

Figure (1.7): Lithostratagraphic columnar section of the major exposed rocks sequences in the study area north Jordan (Modified after Moh'd, 1997).

© Arabic Digital Library-Yarmouk University

www.manaraa.com

1.5 Objectives

Scarcity of studies on the basaltic rocks of the Yarmouk river led to re-evaluating of the basaltic rocks in the region using different methods in order to determine their mineralogical, petrographic, geochemical and petrogenesis properties to obtain a comprehensive knowledge that can be considered as a database for YRB in the study area.

The objectives of this study are as followed:

- Describing lithology, external morphology, occurrences, extension and relations with the surrounding outcrops.
- Mapping the selected basalt outcrops and locating them using topographic maps and satellite images.
- Presenting a full petrography description and complete geochemical analyses of the basalt.
- Determination of physical and mechanical properties of the basalt rock.
- Evaluating basalt rock as industrial material using physico – mechanical tests to determine the engineering properties.

1.6 Geological setting

During the Cenozoic era, basaltic lava poured out from vertical fissures, local vents, and fault - systems and covered large areas in Jordan (Moh`d, 2000) by a process called tephra- genesis or doming. The basaltic

© Arabic Digital Library-Yarmouk University

المنارة للاستشارات
www.manaraa.com

rocks in Jordan are mainly Tertiary to Quaternary in age. They occupy 18 % of Jordan area. They were classified by (Bender, 1974; and Al- Malabeh, 1993 and El-Hasan and Al-Malabeh, 2008) according to their mode of occurrences. Most of which form from Harrat Al-Shaam in the eastern and northern parts of Jordan, in addition to some other basaltic occurrences in Jordan Rift and central Jordan. Areas of extent can be summarized into the followings:

1- Within-rift basalts: Basalt extrusions along and within the Jordan rift (e.g. Suweima, Zarqa – ma` in and Al – Hamma –Adasia- Shuna areas).

2- Rift-proximal basalts: Basalt volcanoes and basalt lava flows in central Jordan (e.g. Al-Tafila basalt).

3- Rift-distal basalts: Basalt sheets and tephra volcanoes and fissure effusion in the northeastern parts of Jordan; the Jordanian Harrat. This basalt covers an area of about (12,000) km², which is part of a large intercontinental volcanic terrain of Harrat Al – Shaam. It covers a total area of more than 50,000 km². Harrat Al – Shaam extends from south Syria through Jordan until North West Saudi Arabia (Al-Malabeh, 1993).

4- Dike basalts: Basalt dikes in the desert of eastern and southern central Jordan (e.g. Qitar Al-Suwan dike) in south Jordan, Qitar Al Abed dike in northeast Jordan.

© Arabic Digital Library-Yarmouk University

المنارة للاستشارات
www.manaraa.com

5- Harrat Irbid basalts: covers an area of 600 km² and are patchy outcrops of basalt in several areas in Irbid District (e.g. Beit Ras, Yarmouk River and Al-Barha and Al-Tura basalt).

Harrat Al-Shaam is believed to be produced from paleo-volcanic activity accompanied by opening of the continental rifts since beginning of the Oligocene and frequently in the Miocene, Pliocene and Pleistocene (e.g. Ibrahim, 1993; Tarawneh et al. , 2000; Ibrahim et al. , 2001; and Ilani et al. , 2001).Results of this study can shed light on the span and duration of the upper-mantle upwelling beneath the western Arabian Plate (Ilani et al., 2001; Al-Malabeh, 2005; and Al-Amoush, 2010). The study area is located to the east of the Jordan valley fault, which is a strike- slip fault. The Golan Heights (GH) is an elevated basalt-covered plateau located at the south-western part of the study area, rising above Sea Level of Galilee on the eastern side of the Jordan River (Meiler, 2011; Meiler et al., 2011). The geology of Irbid area especially Yarmouk River is an extension of the south Syrian geology.

The analyzed basalt samples of the studied area proved that the basaltic rocks exposed in Irbid area are part of Harrat Al-Shaam (Al-Malabeh, 2009 and Abu-Mahfouz, 2009).

© Arabic Digital Library-Yarmouk University

المنارة للاستشارات
www.manaraa.com

Chapter Two

Methodology

2

© Arabic Digital Library-Yarmouk University

المنارة للاستشارات
www.manaraa.com

Chapter Two

Methodology

2.1 Introduction

Office, field and laboratory efforts were used to study the mineralogy, chemical composition and geotechnical properties of the (YRB) exposed in the study area north Jordan. Litological, geochemical and mechanical investigations were used see (Figure 2.1).

2.2 Phases of this study

2.2.1 Office work

It's completed by collecting data from previous works. A topographic map and satellite images were used to locate the basaltic outcrops in the study area.

2.2.2 Fieldwork

Thirty representative basalt samples were collected from outcrops exposed in the study area to analyse them for their mineralogical, petrographical, geochemical, and mechanical properties. Those samples were collected from four different lava flows using either a rock hammer or a sledge hammer to obtain fresh material from basalt rocks situated beneath the ground surface and were broken down into hand-sample size, and placed in sample bags for further analysis.

© Arabic Digital Library-Yarmouk University

المنارة للاستشارات
www.manaraa.com

The sample localities were identified using a UTM coordinates obtained from a GPS receiver, and noted in a field book along with preliminary hand sample descriptions. The basalt outcrops were mapped, columnar sections drawn, and representative samples collected.

© Arabic Digital Library-Yarmouk University

www.manaraa.com

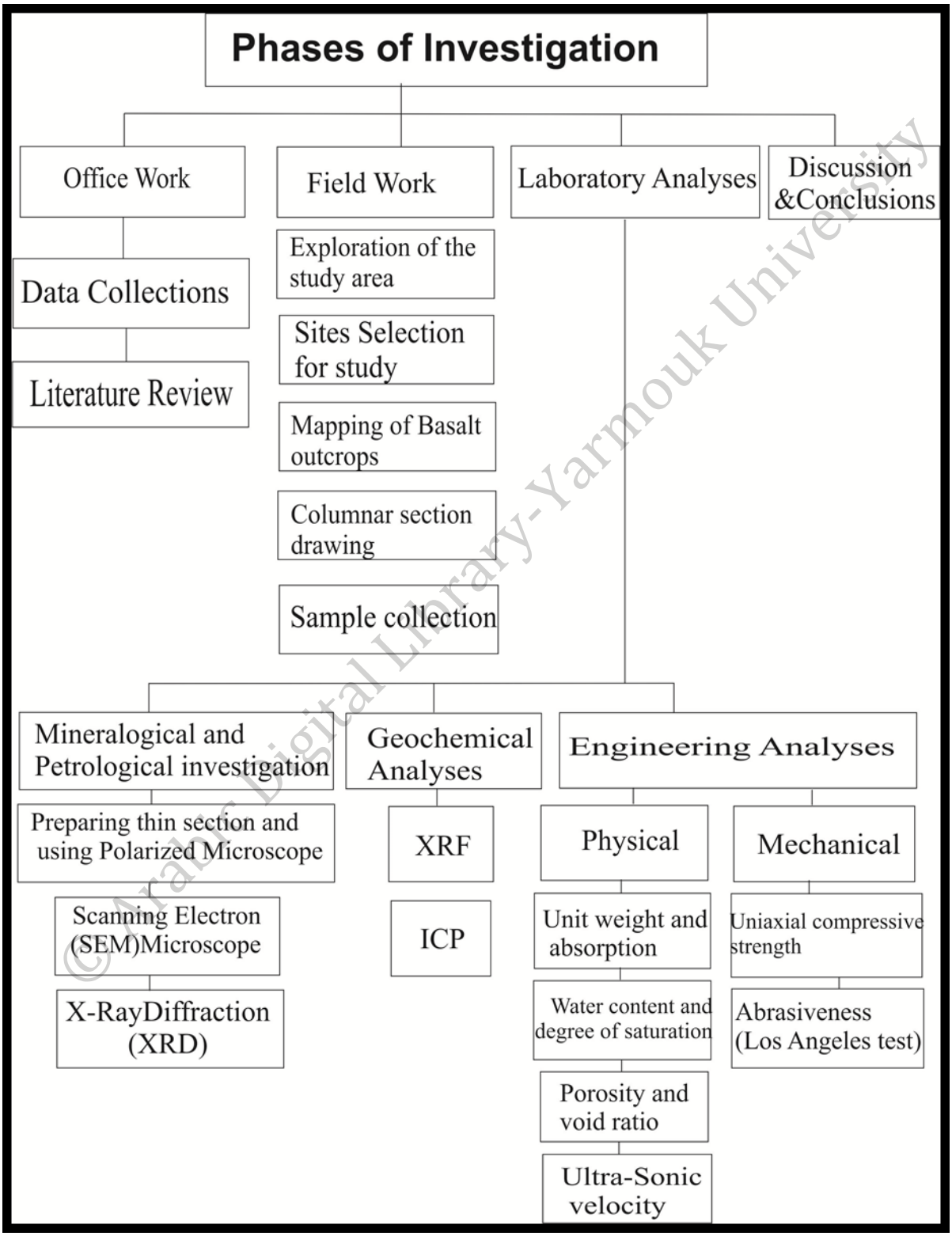

© Arabic Digital Library-Yarmouk University

Figure (2.1): Flow chart illustrating the methods used in the study area.

المنارة للاستشارات
www.manaraa.com

2.2.3 Laboratory work

Thin sections of those samples were prepared and examined using a polarized microscope. Moreover X-ray diffraction (XRD), Scanning Electron Microscope (SEM), X-ray Fluorescence (XRF) techniques and core samples were used.

2.2.4 Analytical techniques

2.2.4.1 Lithological descriptions

The lithology of basalt describes its visible physical characteristics such as color, texture, grain size, or composition at outcrop, in hand samples or with low magnification microscope.

2.2.4.2 Petrological and mineralogical studies

Thirty basalt samples were collected from the YRB in a systematic approach (from bottom to top) and labelled. Those samples were transported to the laboratory at the Department of Earth and Environmental Science to prepare thin sections. Twenty Samples were crushed into a powder and prepared for chemical analysis including X-ray Diffraction (XRD) and X-ray Fluorescence (XRF),

The prepared thin sections were studied with an optical microscope to identify their mineral constituents, texture and petrographical properties. The basalt is composed of several primary minerals such as plagioclase,

© Arabic Digital Library Yarmouk University

المنارة للاستشارات
www.manaraa.com

pyroxene, olivine, iron oxides, and minor minerals such as iddingsite and calcite. A few numbers of vesicles are also present. The main texture is aphanitic.

Petrographic testing is a microscopic examination that evaluate the aggregate and building material (French, 1991) and is used to examine the Alkali-Aggregate-Reaction (AAR) risk in aggregates and building stones which remains to be one of the major cause of damage in concrete

Examining thin sections of aggregates using an optical microscope is helpful in detecting chemical and physical alterations that could cause damage.

The petrography of a rock mass can be of great value in any assessment of its potential suitability for use as aggregate.

Petrographic examination of aggregates in particular uses includes detection of potentially deleterious substances such as porous and frost susceptible particles; weakness or soft particles, or coatings and rock types susceptible to shrinkage and swelling.

2.2.4.2.1 Studying Petrographical and mineralogical properties by using SEM

Scanning Electron Microscope (SEM) is a very useful method used to give information about the sample's surface topography, shape (morphology),

© Arabic Digital Library-Yarmouk University

www.manaraa.com

chemical composition, crystalline structure and orientation of materials and other properties such as electrical conductivity, making up the sample by using thin section and rock fraction. SEMs are equipped with an EDXS detector which measures characteristic energies of elements to determine composition.

2.2.4.2.2 Studying Petrographical and mineralogical properties by using XRD

X-ray Diffraction (XRD) is a significant method for the analysis of solid materials in science. It is often the only powerful tool that allows us to identify and differentiate materials under laboratory conditions; to find the crystal structure of unknown material, measure the size, shape and internal stress of small crystalline regions, determine the orientation of a single crystal or grain (powder). The unique character of the diffraction patterns of crystallized material, the capability to distinguish between elements and their oxides, and the possibility to identify chemical compounds, polymorphic forms, and mixed crystals are crucial advantages of X-ray diffraction methods in the forensic science.

There are many Preparatory procedures that must be wisely selected to prepare sample to X-ray diffraction analysis according to the objectives of the analyst. Accurate assessment of basalt mineralogy requires a thorough

© Arabic Digital Library-Yarmouk University

المنارة للاستشارات
www.manaraa.com

understanding of these procedures and their consequences for data interpretation.

2.3 Geoengineering investigation and characterization methods of basalt rock as building/dimension stone

This analytical techniques deal with the methodologies and principles adopted for physical and mechanical tests and procedures used to describe or evaluate the physical, mechanical, characteristics of building/dimension stone and aggregates. These physical and mechanical properties of the samples include: Physical measurement of specific gravity, water contents, unit weight, porosity, density, permeability, absorption, hardness, abrasiveness, and others. Engineering properties such as the point load test, unconfined compressive strength, indirect tensile strength, Poisson's Ratio (ν), Los Angeles, and slake durability test listed in (Table 2.1).

These tests are available in the published literatures and standards of both the American Society for Testing and Materials **(ASTM)** and Institution Standard for Rocks and Materials **(ISRM)** standards to characterize the basalt rocks in Yarmouk river area as construction materials Therefore, a brief introduction, procedures and equations formulas of these tests/methodologies are presented in this chapter while the results and calculations/specifications are presented in the next chapters (chapter 6).

© Arabic Digital Library-Yarmouk University

المنارة للاستشارات
www.manaraa.com

Basalt samples were collected from active quarries and outcrops; these samples quarried and cut directly from the various flow layers both vertically and laterally. Large sized blocks of the samples have been carried on and transported directly from the field site to the laboratory in Jordanian university of science and technology in civil engineering department. Those samples were used to extract core samples with different diameter and lengths (Figure 2.2).

Those cores were subjected to sawing and grinding processes to prepare them for further physical and mechanical tests Figure (2.3).

Table (2.1): selected physical and mechanical properties of rock

PHYSICO MECHANICAL PROPERTIES	
Physical Properties	**Mechanical Properties**
Mineralogical composition, mineral structure, texture.	Elastic Modulus/Deformation modulus and Poisson's ratio
Specific gravity, density, unit weight	Uniaxial compressive strength
Porosity, void ratio	Tensile strength
Ultra- sonic velocity	Los Angeles test

© Arabic Digital Library-Yarmouk University

www.manaraa.com

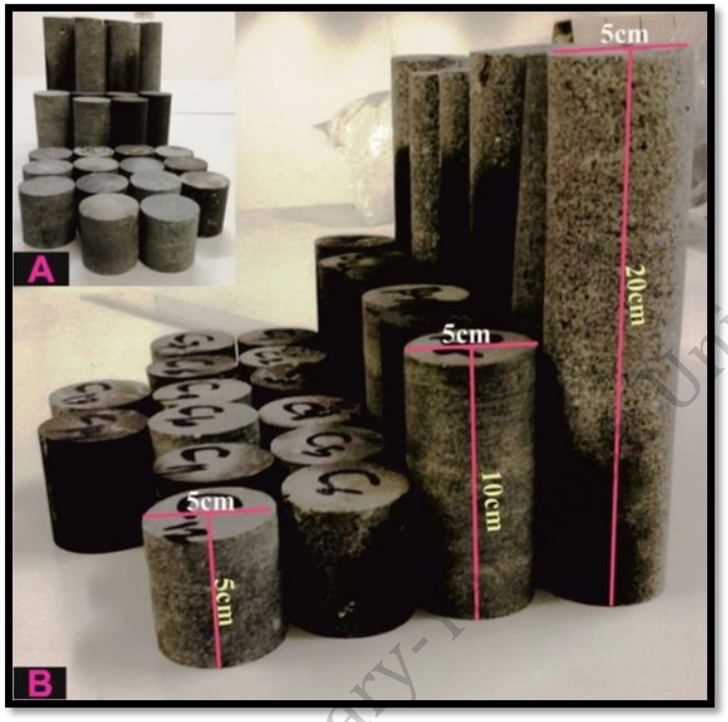

Figure (2.2): A: Showing three size of core sample. B: core samples with different diameter and length suitable for the different tests required.

Figure (2.3): Trimming ends of basalt cores after using sawing machine.

© Arabic Digital Library-Yarmouk University

المنارة للاستشارات
www.manaraa.com

2.4 Engeenering charecteization of rock

2.4.1Studying physical properties by using:

2.4.1.1 Specific gravity and absorption

Specific gravity of a solid substance is generally defined as the ratio of the mass of a given volume of material to the mass of an equal volume of water (at 20°C). However, several variations of this definition exist depending upon the material considered and the purposes for which the value of specific gravity are to be used. The laboratory test for specific gravity and absorption determination requires that the rock specimens be weighted in air in a dry condition, called bulk, true or absolute specific gravity (spG_d). The second type is weighted in air in a saturated condition, this type called bulk specific gravity-saturated surface dried (spG_s) and the third one weighted in water in a saturated condition; called apparent, saturation specific gravity (SpG_a).

Specific gravity procedure and calculations can be used to calculate porosity, void ratio, unit weight and other rock properties. The plagioclase phyric basalt yields the highest specific gravity due to massive and compact nature as well as the presence of magnetite/ilmenite.

© Arabic Digital Library-Yarmouk University

المنارة للاستشارات
www.manaraa.com

2.4.1.2 Absorption

The water absorption is defined as the "difference between the weight of a sample totally immersed in water and its dry weight" (Siegesmund and Dürrast, 2011). It is closely related to its porosity. Water absorption is an indirect measure of the permeability of an aggregate.

2.4.1.3 Unit weight

The unit weight of rock **(γ)** is defined as the ratio of the total weight of rock to the total volume of the rock, dry unit weight (γd) was determined for the YRB, (Derucher& Heinz, 1981).

2.4.1.4 Porosity and void ratio

The porosity of a rock is defined by the ratio of the pore volume (e.g. pores, open cracks) to the volume of the whole rock. It represents the relative proportion of solid grains and voids in the rock. It is also a measure of the interconnected pore space. Two different types of porosity can be distinguished, a primary porosity which is defined as the porosity of the rock after sedimentation and lithification and secondary porosity formed after lithification of the sediments.

The first type called the effective porosity or often called "accessible porosity or the apparent porosity" and the second type also called the total porosity. The first one comprises and measure of the volume of all

© Arabic Digital Library-Yarmouk University

المنارة للاستشارات
www.manaraa.com

interconnected pores and cracks linked to the external surface of the rock, where fluids and gases can access, whereas the latter one includes all pores even the isolated ones, which cannot be accessed (Siegesmund and Dürrast, 2011).

The porosity of some rock is increased through structural deformations fractures, solution of the material itself, dolomitization or diagenetically. This is known as secondary porosity. Usually igneous rocks such as basalt rock will have very low porosity (0-2%). Porosity and absorption of aggregate will affect the water/cement ratio.

2.4.1.5 Void ratio

Void ratio its can be defined as the ratio of the volume of void to the volume of solids of the rock, expressed in decimal fraction. It is dimensionless number which simply shows how many times there are amount of voids than solids in the rock (Derucher& Heinz, 1981).

2.4.1.6 Ultra-Sonic Velocity.

Ultrasonic methods have been used as a non-destructive method, which can inform about the behaviour of these mass rocks during exploitation works in basalt (McCann &Fenning, 1995). It is possible to repeat the test at the same point at different times to determine changes of Vp with time. P and S-wave measurements were made on all the cores in longitudinal mode (Z

© Arabic Digital Library-Yarmouk University

المنارة للاستشارات
www.manaraa.com

direction) (Figure 2.4), P-wave velocity measurements were conducted on samples having a diameter of 5cm and a length of 20 cm.

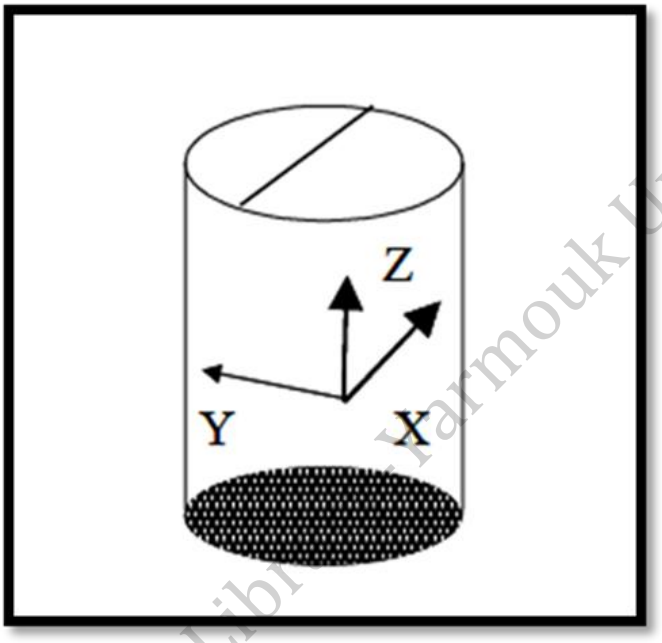

Figure (2.4): Show the P and S-waves direction on the studied cores in longitudinal mode (Z direction).

2.4.2 Studying mechanical properties by using:

2.4.2.1 Uniaxial compression strength (UCS)

The uniaxial compression strength (UCS) is measured in terms of compressive, tensile, and shear strength by applying dynamic compressive loading on the surface of a core sample with repeated loading to initiate brittle cracks, which grow slowly until failure occurs(Siegesmund and Dürrast, 2011).

© Arabic Digital Library-Yarmouk University

المنارة للاستشارات
www.manaraa.com

This test done using straight circular cylindrical samples particularly depends on the length-diameter-ratio, having height 10 cm and diameter preferably 5cm. The longitudinal constant stress (load) is applied continuously to the end-faces of the specimen until failure and final break reached (Figure 2.5). The maximum load is defined as the uniaxial compressive strength.

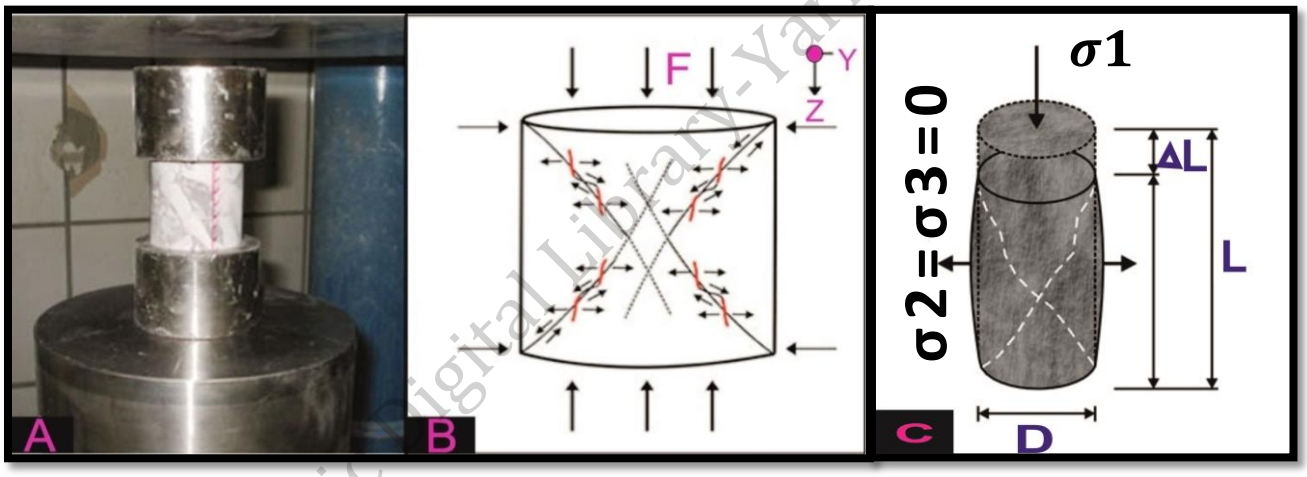

Figrue (2.5): laboratory testing for uniaxial compressive strength on **(a)** cylindrical specimen). **(b)** Rock failures occur through a combination of tensile and shear cracks. F=loading force**. (c)** Core with failure under unconfined compression.

2.4.2.2 Los Angeles Abrasion test

The Los Angeles **(L.A.)** abrasion test is a common test method used to indicate aggregate toughness and abrasion characteristics. The Significance of this test is to indicate relative quality of aggregate sources having similar

© Arabic Digital Library-Yarmouk University
المنارة للاستشارات
www.manaraa.com

mineral compositions due to abrasion value and to calculate the hardness of aggregates (Swain, 2010).

2.5 Geochemical investigations

Geochemical analysis shows the processes that have occurred for magma in the past and led to form the basaltic rocks. Geochemical analysis depends mainly on the analysis of trace elements present in basalt such as: Ba, B, Nb, Pb, Sn, Sr, P, Zn, La, Li, Y, Cu, Mo, Cr, Co, Ce, V, Cu and Ni.

The reason for analyzing trace elements is that they can be used as testing models for magmatic differentiation, determination of the depth of generation of a primary magma, determination of the paleotectonic settings of the volcanic rock.

2.5.1 Studying Petrological and mineralogical properties by using XRF

The X-ray Fluorescence **(XRF)** analysis is typically used for bulk analyses of larger fractions of geological materials. The relative ease and low cost of sample preparation make this one of the most widely used methods for analysis of major and trace elements in rocks and minerals. The samples were analyzed for major oxides (SiO_2, Al_2O_3, $(Fe_2O_3)_t$, MgO, CaO, Na_2O, K_2O, P_2O_5 and Cl) and trace elements (Cr, Ni, Zn, Cd, Li, Mo, Co and Rb).

© Arabic Digital Library-Yarmouk University

www.manaraa.com

2.5.2 Studying Petrological and mineralogical properties by using ICP

The Atomic Inductive coupled plasma **(ICP)** is used for determining the concentration of a particular element in a sample to be analysed. ICP was carried to determine the abundances of SiO_2, TiO_2, Al_2O_3, $(Fe_2O_3)_t$, MnO, MgO, CaO, Na_2O, K_2O, and P_2O_5 oxides.

© Arabic Digital Library-Yarmouk University

المنارة للاستشارات
www.manaraa.com

Chapter Three

Field Investigation

3

© Arabic Digital Library-Yarmouk University

المنارة للاستشارات
www.manaraa.com

Chapter Three

Field Investigation

3.1 Introduction

The main aim of this chapter is to observe and collect data about the Yarmouk River Basalt (YRB), to investigate the basalt distribution in the field and collect rock samples from different new basaltic outcrops in the study area, which will further help to understand the physical, chemical and mechanical processes that have occurred over geological time.

Fieldwork investigations involve making careful observations and measurements in the field, collection and precise recording of the position of the collected samples for laboratory analysis.

The basalt flows don't appear obviously in all areas. Field characters of basalt flows give clues of the nature of the YRB, their thickness, lateral extent, jointing pattern. etc.

3.2 Exploration of the study area

Field work was carried out in the period between September, 2015 and February 2016 to study YRB. Field characteristic and classification of this basalt were identified and photographed. Field description in Al-Hamma area of YRB area provides the necessary basis for different characteristic such as mineralogical, chemical and technical properties in the different flows of the

© Arabic Digital Library-Yarmouk University
المنارة للاستشارات
www.manaraa.com

studied rocks. It also aims to identify the history of the volcanic flows in this area and to know lithostratagraphic sequences exposed in it. These include steps like collecting representative samples from each flow of the four phases for petrographical and mineralogical studies, chemical analysis and technical properties to evaluate basalt rock using many techniques. YRB is located between 142 m and 20 m (BMSL), with a total thickness of 122 m

3.3 Elevation determination and Mapping of Basalt samples locations

Based on the field survey, geographic position system (GPS) and Google Earth images, thirteen samples were selected on location map to find out the spatial relationships of basalt in the study area (Figure. 3.1 and 3.3). The highest elevation in the study area ranges from 350 to 320 m above sea level, while the lowest elevation ranges from 100 to 200 m above mean sea level (Figure. 3.2 and 3.4).

© Arabic Digital Library-Yarmouk University

المنارة للاستشارات
www.manaraa.com

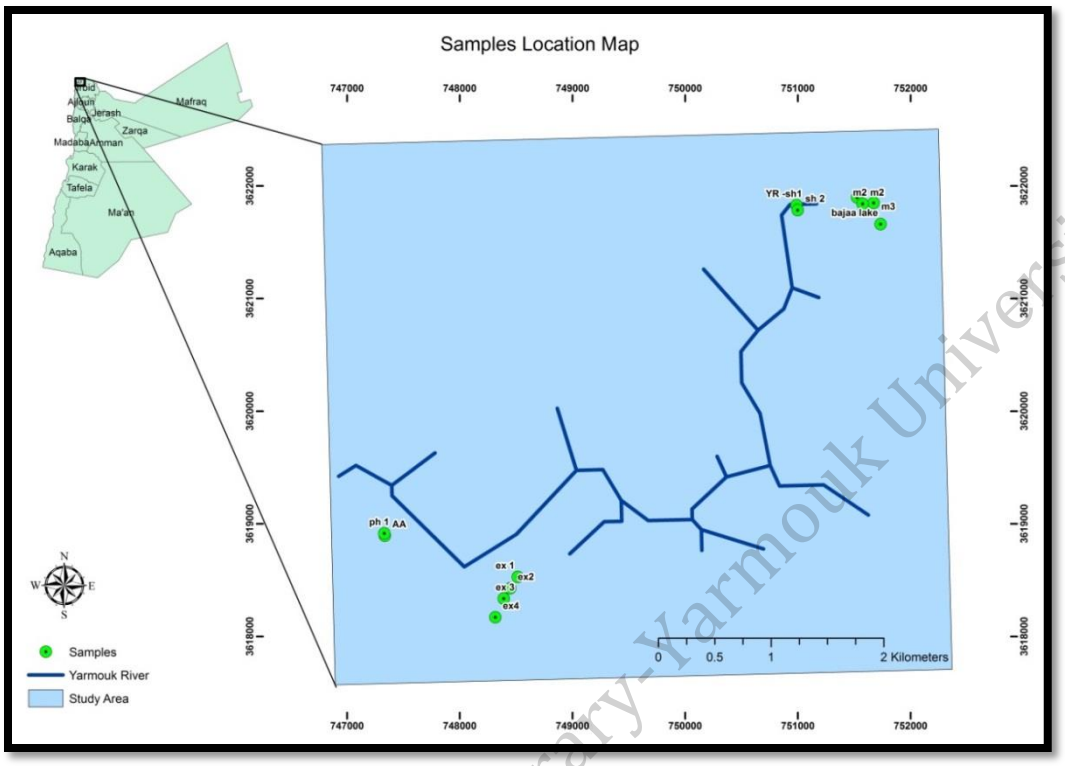

Figure (3.1): Location map of study area showing the representative selected basaltic samples.

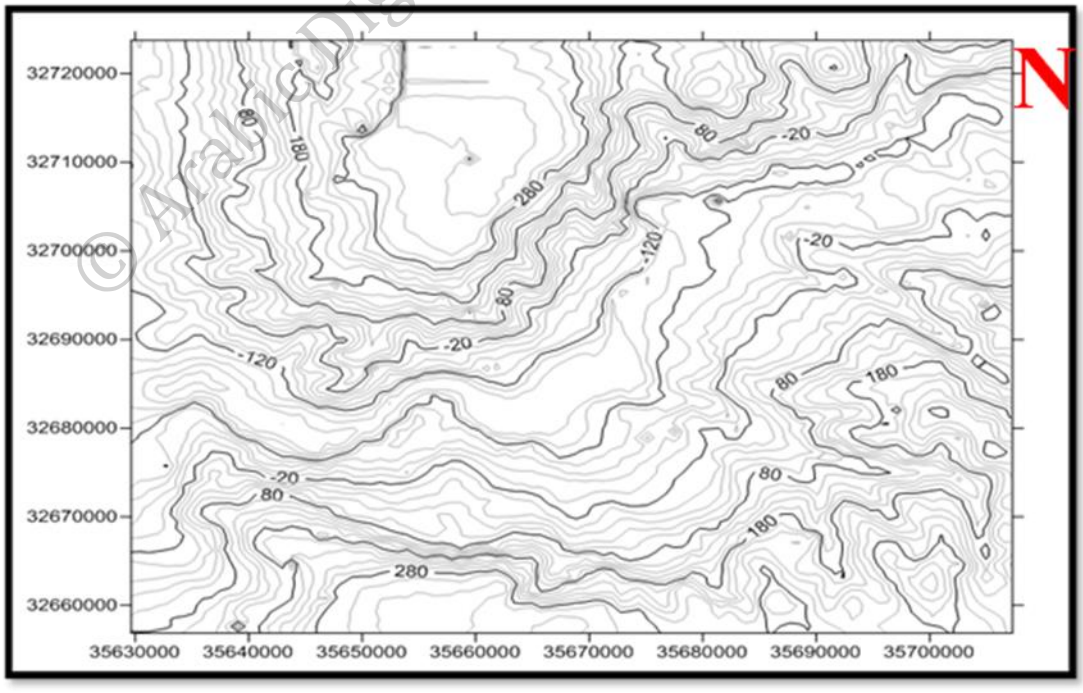

Figure (3.2): Contour map of study area shows the elevation

© Arabic Digital Library-Yarmouk University
المنارة للاستشارات
www.manaraa.com

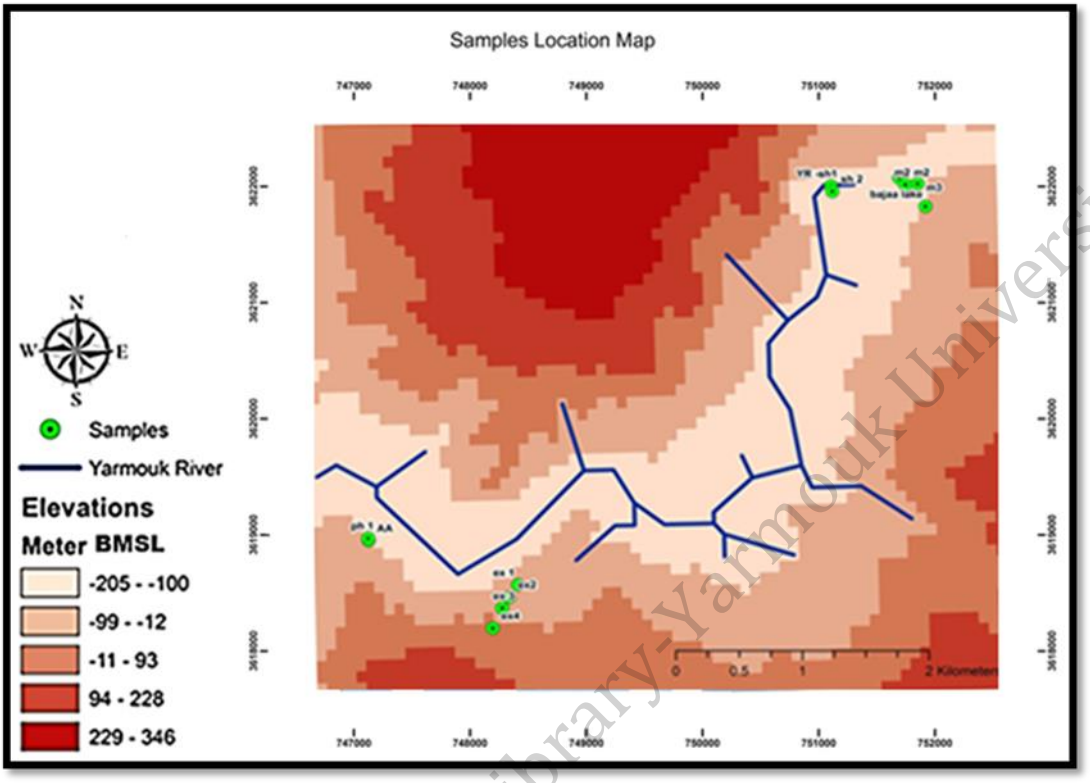

Figure (3.3): DIM map of study area shows the elevation and sample locations.

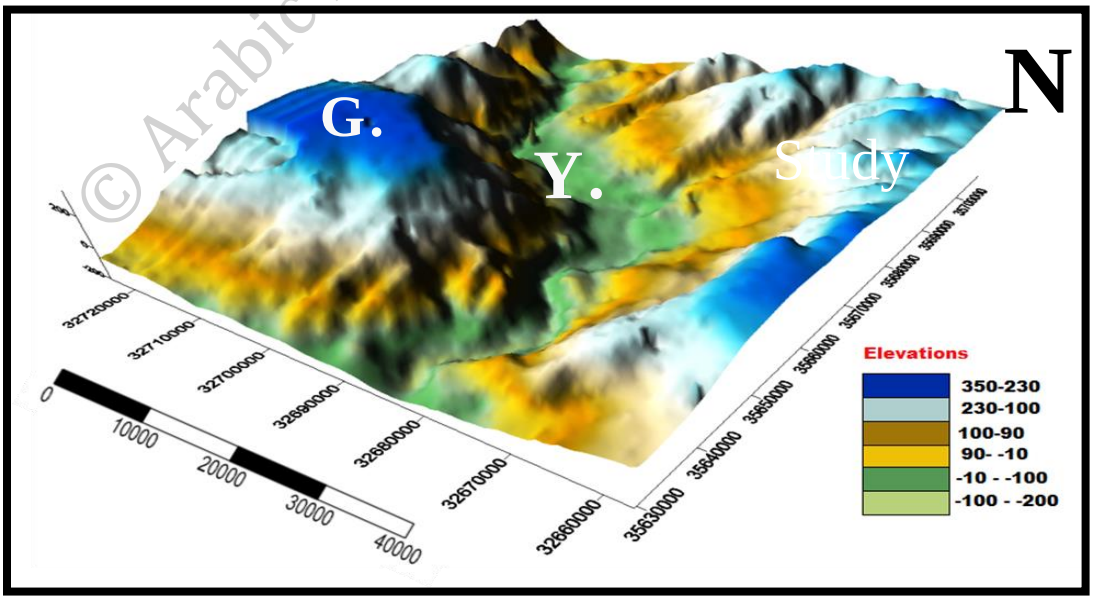

Figure (3.4): 3 D map representing the study area topography.

© Arabic Digital Library-Yarmouk University

www.manaraa.com

3.4 Field observations and flows descriptions

Field investigations show that the Basaltic flows of YRB resulted from four flows .These flows extended along both sides of the Yarmouk river valley with a distance of about 50 km long. The basalt occupies an area of 70 km² in both sides' with an average thickness of 122m. However, it is noted that the flows have a limited variety of composition and textures. These basalt flows have large extensions and thicknesses in the study area.

3.4.1 Description of the basaltic flows

The stratigraphy of YRB was studied a long a vertical section in the west side of the flows. According to field observations the YRB are classified into four major flows from the bottom to top as follow:

4. Exfoliated and vesicular basalt
3. Pahoehoe and a'a basalt
2. Massive and blocky basalt
1. Sheet basalt

In general, description most of the basaltic rocks in the study area are highly weathered, sheeted basalt in the first flow massive, rounded , blocky, basalt in the second flow, pahoehoe and a'a basalt in the third flow and Exfoliated and vesicular basalt with some columnar basalt in the fourth flow.

© Arabic Digital Library-Yarmouk University

المنارة للاستشارات
www.manaraa.com

This outcrop characterized by fine grained, grey and black color and calcite filled the vesicles.

3.4.1.1 Yarmouk Sheet basalt (YS)

It's the first flow and it's also called terrace basalt**.** This phase was named and described by Harza Engineering Company in (1955). The most important characteristics of this phase are the arrangement of the basalt in sheet form. It is also distinguished by different lithological and stratigraphic features such as joints and fractures. The total thickness of this flow is 35 m. The basalt is black in color and mostly fine grained in hand sample. It shows some vesicles which increases gradually from the first towards the last flow (Figure 3.5 and 3.6). The detailed coordinates and elevation of each flow is given in (Table 3.1).

Table (3.1): Field classification of YS basalt: flows, samples and GPS

Phase	Flow	Sample.no	Latitude (N)	Longitude (E)	Elevation(BMSL)(m)
Yarmouk Sheet basalt	1	YS1	32°42'21.60"N	35°40'40.80"E	134
		YS2	32°42'18.00"N	35°40'40.80"E	138

© Arabic Digital Library-Yarmouk University

www.manaraa.com

Figure (3.5): Field photograph, showing steep sheeted basalt in the terraces flow near the Al-Himmah Al-Ordonyah.

Figure (3.6): Field photograph, showing a side view of the cliff-sheeted basalt in the YS flow in the other side of the river 32°72'73.60"N, 35°62'9942.4"E from Al-Hardan restaurant.

www.manaraa.com

3.4.1.2 Yarmouk Blocky (YB) and Massive basalt (YM)

The blocky and massive basalt second phase covered the YS-Basalt. The layered sediment and soil is marked by the presence of a non-conformity plane. This flow has a total thickness of 27 m. The basalt is characterized by the occurrence of blocks of basalt. These blocks are scattered on the top of each flow and range in diameter from 0.5 m up to 2 m. They have black to gray in color and highly weathered (Figure 3.7, 3.8 and 3.9). The detailed coordinates and elevation of each sample is given in (Table 3.2).

Table (3.2): Field classification of YB and YM flows, samples and GPS.

Phase	Flow	Sample.no	Latitude (N)	Longitude (E)	Elevation(BMSL)(m)
Yarmouk Massive basalt	2	M1	32°42'21.60"N	35°40'58.80"E	121
		M2	32°42'21.60"N	35°41'2.40"E	110
		M3	32°42'21.60"N	35°41'6.00"E	103
		M4	32°42'14.40"N	35°41'6.00"E	101

© Arabic Digital Library-Yarmouk University

www.manaraa.com

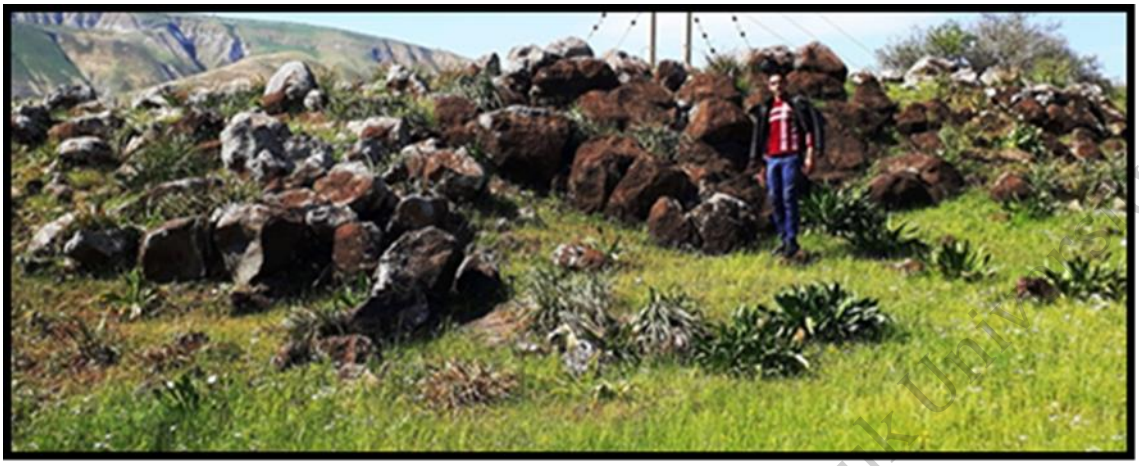

Figure (3.7): Field photograph, showing blocky and massive basalt in the YB & YM flows of YRB near Al-Bajaa Lake.

Figure (3.8): Field photograph, showing the massive basalt in the YB &YM flow near Al-Bajaa Lake.

© Arabic Digital Library-Yarmouk University
المنارة للاستشارات
www.manaraa.com

Figure (3.9): Field photograph, showing vesicular massive of basalt rock in the YE & V flow near Al-Bajaa lake.

3.4.1.3 Pahoehoe and a'a flow

The third flow that appears as Hawaiian term of pahoehoe and a'a lava is characterized by blocky basalt. Sometimes pahoehoe lava characterized by high thickness and fractured layer. The total thickness of this flow is about 15 m, its light dark grey in color, it's more fluid and old in age and it's

www.manaraa.com

overlain by a'a basalt is scoria lava which is rough, irregular flow jagged, rubbly, and has a broken surface and lose fragments. It's more vesicular and younger than pahoehoe basalt (Figure 3.10 and 3.11). The total thickness of this flow is 8 m. The detailed coordinates and elevation of each flow is given in (Table 3.3).

Table (3.3): Field classification of Yarmouk pahoehoe and a'a basalt: flows, samples and GPS.

Phase	Flow	Sample. no	Latitude (N)	Longitude (E)	Elevation(BMSL)(m)
Yarmouk pahoehoe and a'a basalt	3	a'a	32°40'48.00"N	35°38'16.80"E	106
		PH	32°40'48.00"N	35°38'16.80"E	107

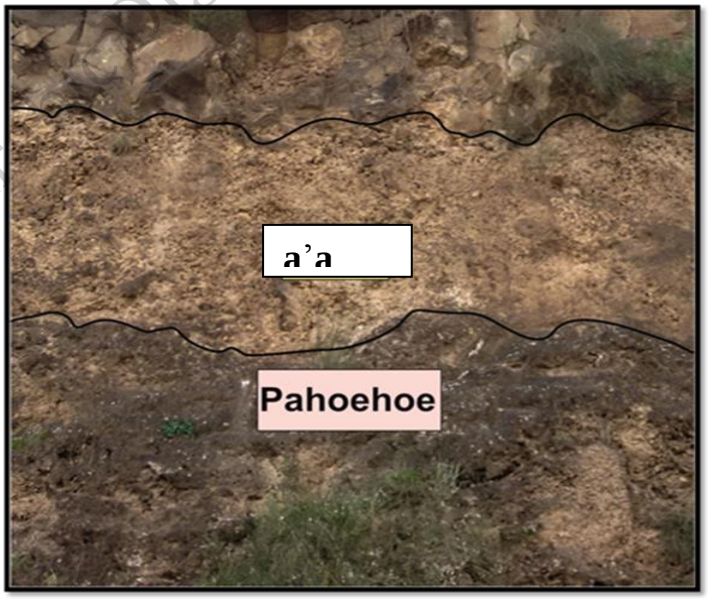

Figure (3.10): Field photograph, showing the pahoehoe and a'a basalt in the pahoehoe and a'a flow from Al-Adassiyah country.

© Arabic Digital Library-Yarmouk University
المنارة للاستشارات
www.manaraa.com

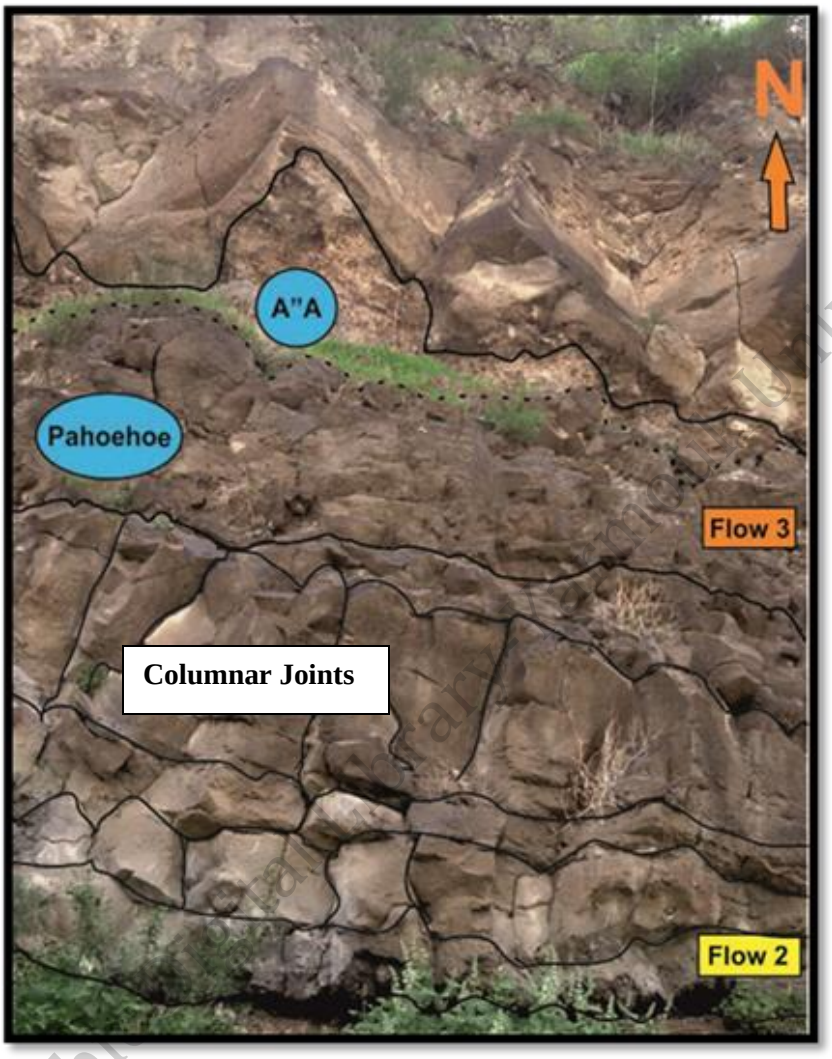

Figure (3.11): Field photograph, showing the blocky, massive and pahoehoe and a'a basalt with fractures in the YB ,YM and pahoehoe and a'a flow from Al-Adassiyah country.

3.4.1.4 Yarmouk Exfoliated and vesicular basalt (YE&V)

YE&V basalt forms the last phase of basalt outcrop in the study area. The basalt is distinguished by exfoliation feature and looks like onion structure and present as spherical weathered basalt (Figure 3.12). This phase

© Arabic Digital Library-Yarmouk University
المنارة للاستشارات
www.manaraa.com

has five weathered and ex-foliated layers of basalt, and measure about 35 m in total thickness. The flows crop out on the upper slopes and are underlies by the chalk rocks (which one) and overlain by some columnar and vesicular basalt. The basaltic rocks of this phase are slightly too moderately altered columnar and vesicular basalt measure about 6 and 14 m in total thickness respectively. Flow four it appears also as columnar and vesicular basalt, its dark grey to black in colour (Figure 3.13 and 3.14). The detailed coordinates and elevation of each flow is given in (Table 3.4).

Table (3.4): Field classification of Yarmouk Exfoliated: basalt flows, samples and GPS.

Phase	Flow	Sample no.	Latitude (N)	Longitude (E)	Elevation(BMSL)(m)
Yarmouk Exfoliated and Vesicular basalt	4	EX1	32°40'37.20"N	35°38'60.00"E	91
		EX2	32°40'33.60"N	35°38'56.40"E	73
		EX3	32°40'22.80"N	35°38'52.80"E	10
		EX4	32°40'22.80"N	35°38'52.80"E	12

© Arabic Digital Library-Yarmouk University

www.manaraa.com

Figure (3.12): Spherical basalt appears as onion-like exfoliated structures above the pahoehoe and a'a flow near army chick point.

Figure (3.13): Field photograph, showing the highly columnar basalt in the YE &V flow with vesicles at its top near to samara restaurant (Al-Mokhaba Al Tahta).

www.manaraa.com

Figure (3.14): Field photograph, showing the direction of vesicles at the top of basalt in the YE & V flow from (Al-Mokhaba Al Tahta).

3.4.1.5 Wadi Shallalah Chalk Formation (WSC)

Wadi Shallalah Chalk Formation is exposed at the upper slopes of the Yarmouk River area and underlain by the YRB. It is about 70 meters thick and the chalks are generally white to greyish white in color and have massive nature (Figure 3.15).

© Arabic Digital Library-Yarmouk University

المنارة للاستشارات
www.manaraa.com

Figure (3.15): Field photograph, showing a chalk horizon underlain by the YRB 32°39'59.34"N, 35° 40' 33.32"E.

© Arabic Digital Repository - Yarmouk University

3.4.1.6 Soil Cover

The YRB is covered by thinly to moderately thick beds of soil. The soil thickness increases gradually from the bottom towards the top above the basalt flows. They range in thickness from 50 cm above the first basaltic phase to several meters above the upper fourth phase. The soil is reddish brown to dark brown in color (Figure 3.16).

المنارة للاستشارات
www.manaraa.com

Figure (3.16): Field photograph showing a red brown soil horizon overlain the Yarmouk Blocky Basalt from Al-Mokhaba Al Tahta 32°42'18.37"N 35°40' 37.51"E.

A brief description of the four flows show in (figure 3.17).

© Arabic Digital Library-Yarmouk University

www.manaraa.com

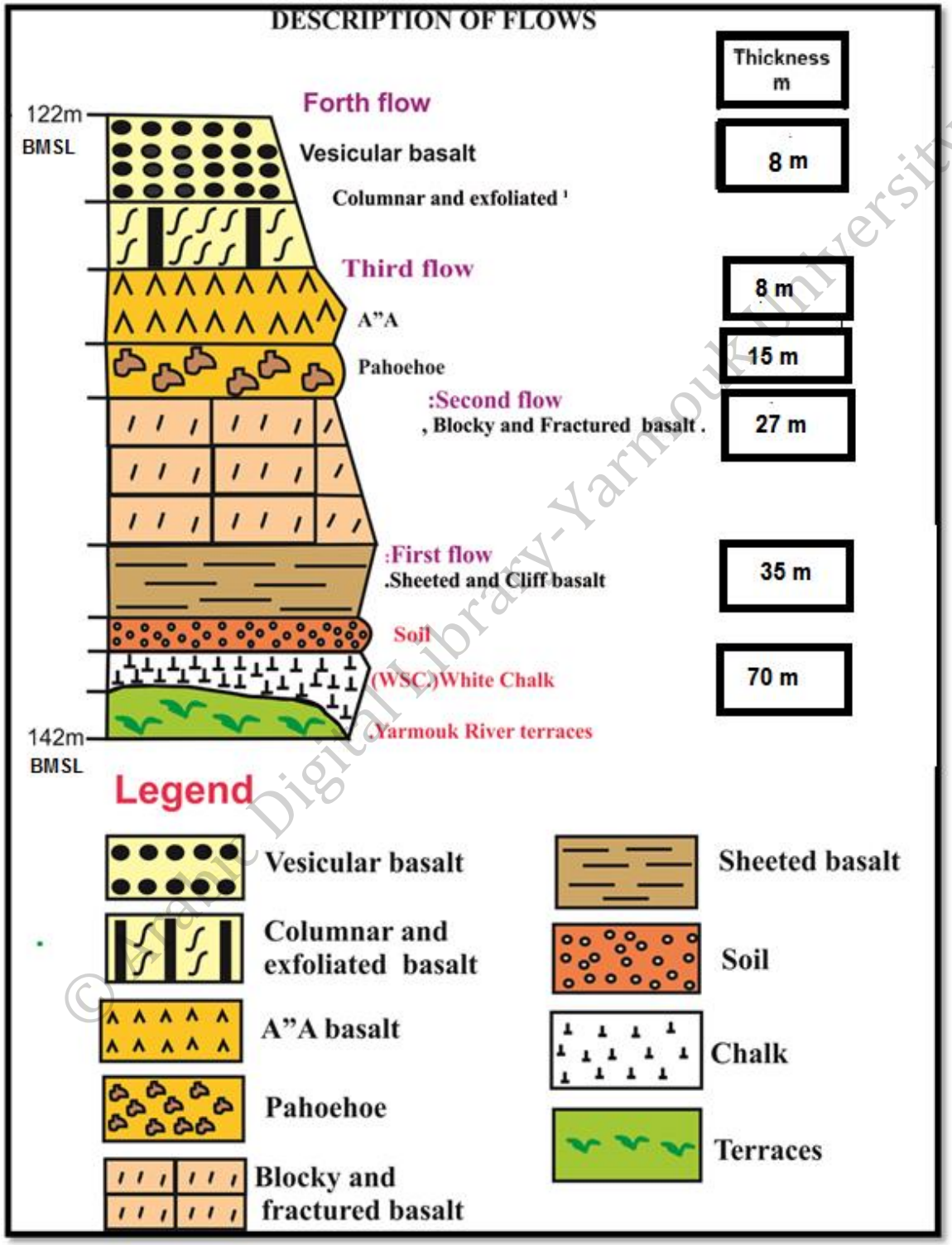

© Hani Digital Library-Yarmouk University

Figure (3.17): Columnar section showing the complete lithological successions of all basalt flows in the study area.

www.manaraa.com

Chapter Four

Petrography and Mineralogy

4

© Arabic Digital Library-Yarmouk University

www.manaraa.com

Chapter Four

Petrography and Mineralogy

4.1 Introduction

This chapter focused on the mineralogical composition of basaltic rock which collected from Yarmouk river outcrops in order to investigate the primary and secondary minerals properties with their textural characteristics.

Thirteen representative fresh samples were taken from the studied flows of the study area (Yarmouk river area); those samples were analysed using X-ray Diffraction (XRD), polarizing microscopy (PM) and Scanning Electron Microscope (SEM) respectively.

The basalt rocks in all locations of the study area are composed of several primary minerals such as olivine, plagioclase, pyroxene, oxides, and secondary minerals such as iddingsite, orthoclase, nepheline, barite and calcite crystals. Some vesicles were also present, the aphanitic and porphyritic texture dominated. The microscopic description of the studied samples of YRB is presented in (Tables 4.1).

Different equipment and techniques such as XRD, CIPW norm calculation method and SEM were used to identify and study the petrography of the indefinite minerals in the basalt rocks.

© Arabic Digital Library-Yarmouk University

المنارة للاستشارات
www.manaraa.com

Table (4.1): description of the studied samples of YRB

Flow number		**Flow one 1**	**Flow two 2**	**Flow three 3**	**Flow four 4**
Texture		Aphanitic			
Primary minerals	Olivine	Most abundant as phenocrysts and in groundmass. The crystals occur both as individuals and glomeroporphyritic aggregate of more than six crystals. Olivine presents in most samples.			
	Plagioclase	Plagioclase occurs in two generations as felty to microlites in the groundmass in all samples.			
	Pyroxene	Pyroxene moderately abundant as anhedral clinopyroxene (cpx) and orthopyroxene (opx) crystal.			
	Alkali feldspar	Slightly abundant			
	Feldspathoids	Slightly abundant as leucite, nepheline			
Secondary minerals	Iddingsite	Abundant at the rim of olivine crystal.			
	Calcite, barite and Zeolite	Slightly abundant as filling material.			
Vesicles		Moderately abundant as subrounded to void and elongated vesicle. The vesicles were filled with secondary minerals, calcite, barite and zeolite.			
Opaque		Abundant such as magnetite, chromite and illmenite.			

© Arabic Digital Library-Yarmouk University

المنارة للاستشارات
www.manaraa.com

4.2 Determinations of minerals by using XRD analysis

Minerals show a wide diversity in diffraction patterns based on d-spacing, and relative peak intensities which are a result of their diversity in crystal and molecular structure .Many minerals have characteristic peaks at very high d- spacing (low angles) and other minerals have characteristic peaks at very low d- spacing (high angle). This variety dictates a wide analysis range for each crystalline component phase of an unknown specimen and produces its own powder diffraction pattern by using x powder12 software to process and identify phase assemblages.

Seven samples were analysed using XRD analysis method; these samples are (R1, phase 2A, phase 2-2, phase 2-3 phase 4-6 phase 4-5 and A'A). The indicated main minerals were Plagioclase and pyroxene (clinopyroxene) especially augite, pigeonite, sodalite and diopside. Olivine (forsterite) also appeared as primary rock forming minerals. Calcite and zeolite also appeared as secondary rock forming mineral. XRD also indicated that plagioclase, feldspathoids, opaque minerals are present. As well as sodalite, magnetite, illmenite as trace minerals (Figure 4.1).

© Arabic Digital Library-Yarmouk University

المنارة للاستشارات
www.manaraa.com

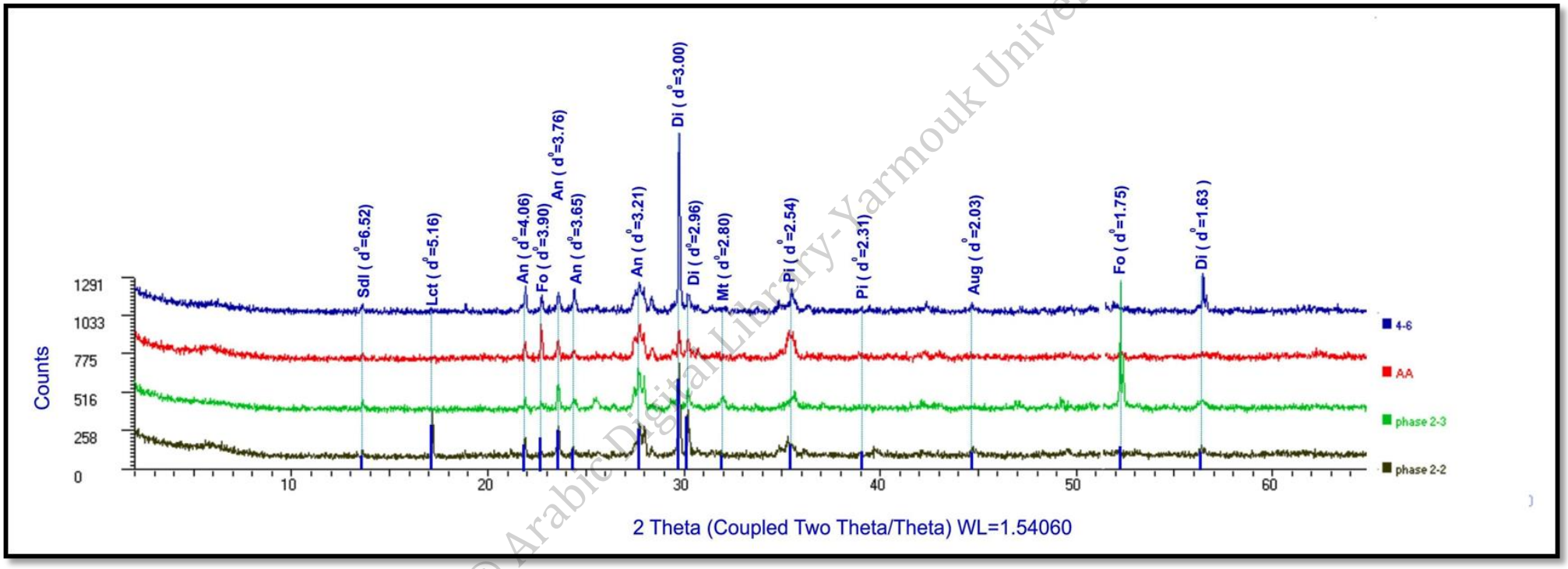

Figure (4.1): Correlation of XRD data between four basaltic samples each sample from different flow (phase2-2, phase 2-3, phase 4-6 and a'a) and their minerals with d-spacing by using xPowder12 program.

© Arabic Digital Library- Yarmouk University

www.manaraa.com

4.3 Determinations of minerals by using CIPW Norm Calculation

According to the CIPW norm, the average of analyzed rocks are characterized by a high normative hypersthene , diopside and olivine content, with at most a low or no content of normative nepheline. The CIPW norm calculation of YR samples shows also high average content of albite, anorthite and low average percent of orthoclase, magnetite, apatite, and illmenite (Table 4.2).

Table (4.2): Analytical data for calculated CIPW norms of different basalts samples from YR area.

Sample	Or	Ab	An	Di	Hy	Ol	Mt	Il	Ap	An%
R1	3.84	20.099	23.78	13.6	17.66	7.71	5.36	3.56	0.6	53.13
R4	6.6	21.64	24.55	17.72	10.83	9.95	3.89	3.46	1.36	53.15
R6	3.84	23.52	23.8	22.23	3.19	12.82	5.22	3.44	0.56	50.29
Phase2-1	3.84	18.53	24.54	19.85	12.26	7.21	5.26	4.37	0.97	56.98
Phase2-4	5.74	21.66	23.95	19.86	27	13.4	3.91	3.35	0.94	52.52
Phase3	8.1	22.59	20.8	17.64	7	8.54	5.09	5.2	2.27	47.94
Phse4-3	4.02	24.88	22.45	20.54	3.62	12.5	5.44	3.51	0.56	47.43

The CIPW well matches with results obtain by modal petrographically. For compares see (Table 4.3, 4.4, 4.5 and 4.6) and see (Table 4.2) for CIPW analysis.

© Arabic Digital Library-Yarmouk University

www.manaraa.com

4.4 General petrographic and mineralogical description

The selected YRB samples from four flows in the study area consist mainly of primary and secondary minerals displaying aphanitic to porpherytic texture with elongated and oval –shaped vesicles, melanocraitic, holocrystalline, and hypidiomorphic fine to medium grained. The main mineral constituents were plagioclase, olivine, pyroxene, and barite minerals. The secondary minerals included calcite, zeolite, Iddingsite and serpentine. Opaque also exist. The common textures of the YRB were trachytic, glomeroporphyritic, vesicular, and amygdaloidal, porpherytic, ophitic to sub ophitic texture, intergranular and taxitic texture.

Olivine and pyroxene form the main phenocrysts phases with high amounts of plagioclase in the groundmass in these rocks. Three petro-types were studied, Olivine- Pyroxene Phyric Basalt, Pyroxene Phyric Basalt and Olivine Phyric Basalt. The microcrystalline matrix is dominated by plagioclase, augite, olivine and magnetite. Plagioclase euhedral or subhedral in shape, present in different cooling and growths rates and show no zonation. Which are generally small-to medium taxitic or intergranular microlites within matrix phase consisting of (30-40%) of the basaltic rocks. Olivine is the second dominant mineral phase in the basalt, its forming about (18-20%). They occurred as euhedral to subhedral crystal shape. Pyroxene

© Arabic Digital Library-Yarmouk University

المنارة للاستشارات
www.manaraa.com

form about (10-15%), occur as euhedral to subhedral phenocrysts and intersected with plagioclase to form ophitic to sub-ophitic texture.

Accessory minerals like nepheline, orthoclase and magnetite and secondary minerals such as (calcite), zeolite, iddingsite in addition to vesicles filled with secondary minerals such as calcite and zeolite.

4.4.1 Yarmouk Sheet basalt (YS)

The name of flow one basalt rocks according to abundance of phenocrysts is **pyroxene - phyric basalt.** Olivine crystals not recorded, Plagioclase is the dominant mineral phase of this basalt, it forms (45.2) vol %its tow type basalt identified by microcrystalline matrix of small crystals of microlites range from(0.1-0.7mm) in 10x*10x magnitude due to high cooling rate and intermediate crystal due to low cooling rate . Augite and magnetite also found .Pyroxene crystals form (35.8) vol. % in the rock in this flow mostly pigeonite.

Elongated iridescent albite, anorthite, plagioclase, pale brown subhedral hypersthene and subhedral to euhedral pink- violate to blue augite and pigeonite mostly (70º-80º), pigeonite (10º -20º) as well as presence of accessory and secondary minerals such as orthoclase, magnetite and chlorite.

© Arabic Digital Library-Yarmouk University

www.manaraa.com

The main textures appeared obviously in this basalt of flow one include porphyritic, glomeroporphyritic, ophitic and sub-ophitic, intergranular and pilotaxitic textures. See (Table 4.3).

© Arabic Digital Library-Yarmouk University

www.manaraa.com

Table (4.3): Mineral and textural description of YS basalt samples.

Texture description		**Mineral description**						
Rock type	**Textures**	Grain Diameter			(%) in sample	Colour (Under XPL)	Crystal shape	Other characteristics
		Minerals	Phenocryst (mm)	Groundmass (mm)				
pyroxene Phyric Basalt	**Porphyritic, Glomeroporphyritic, Ophitic to Subophitic, Intergranular, , Paliotaxitic**	Olivine	-	-	0	-	-	Olivine not exist in samples its pyroxene basalt.
		Pyroxene	0.1-2.1	0.1-0.8	35.8	Pinkish blue to reddish brown	Subhedral -Anhedral	Two types (orthopyroxene parallel extinction, clinopyroxene inclined extinction. greenish yellow colour in PPL view.
		Plagioclase	-	0.1-0.7	45.2	Iridescent grey	Subhedral -Euhedral	Intermediate and microlites Plagioclase tabular shape, colourless crystals exhibit two sets of cleavage.
		Alkali feldspar	0.22-0.6	-	4	Pale grey to dark grey	Subhedral -Euhedral	Mostly orthoclase(Carlsbad twining)
		Carbonates	-	-	0	-	-	Not recorded.
		feldspathoids	0.1-0.4	-	7	Pale grey to dark grey	Subhedral -Anhedral	Nepheline: The most common feldspathoids. Grey colour.
		Opaque	-	0.03-0.15	5.2	Dark black	anhedral	Oxide such as Magnetite the most common
		Vesicles	-	-	0	-	-	No vesicles.

© Arabic Digital Library-Yarmouk University

المنارة للاستشارات
www.manaraa.com

4.4.2 Yarmouk Blocky (YB) and Massive basalt (YM)

This flow is characterized by different mineralogical and textural characteristics are consisting primarily of pale brown subhedral to euhedral olivine altered partly to iddingsite, subhedral to euhedral pink to pale purplish clinopyroxene (augite) inclined mostly (55º) and altered partly at the rim as a phenocrysts and groundmass. Plagioclase consists of small size microlites (needle -like shape) due to rapid rate of cooling of lava and to large tabular phenocryst with lamellar twinning due to slow rate of cooling of lava. Therefore, the name of basalt in this flow is **Olivine-Pyroxene- Phyric basalt**. A few crystals of calcite as phenocrysts and as a filling malarial, feldspathoids are not recorded in this flow but intermediate amount of alkali feldspar are present as subhedral shape such as orthoclase. Clinopyroxene and opaque appear clearly in this flow. Vesicles have circular random shape (Table 4.4).

Porphyritic, glomeroporphyritic, amygdaloidal, vesicular, radiate, and intergranular and pilotaxitic are the major textures emerged in basaltic samples beside less visible textures such as, aphanitic and embayment textures.

© Arabic Digital Library-Yarmouk University

www.manaraa.com

Table (4.4): Mineral and textural description of YB and YM sample.

Texture description		Mineral description						
Rock type	Textures	Grain Diameter			(%) in sample	Colour (Under XPL)	Crystal shape	Other descriptions
		Minerals	Phenocryst (mm)	Groundmass (mm)				
Olivine – pyroxene Phyric Basalt	Porphyritic, Glomeroporphyritic, Intergranular, vesicular, Paliotaxitic and Amygdaloidal texture.	Olivine	0.2-2.1	0.02-0.09	12.5	colourless to pale yellow in thin section, orang, yellowish, or reddish brown	Subhedral-Euhedral	Altered to iddingsite partially at the rims. Highly fractured with no cleavage. Two Generations.
		Pyroxene	0.1- 2.7	0.03-0.10	26.3	Pinkish blue to reddish brown	Subhedral	Mostly clinopyroxene (augite) inclined 20-55extinction. Greenish yellow colour in PPL view.
		Plagioclase	-	0.3-1.2	30.3	grey	Subhedral – Euhedral	Plagioclase polysynthetic twinning , tabular and needle Shape, colourless crystals exhibit two sets of cleavage.
		Alkali feldspar	0.035-0.8	-	4.5	Pale gray to dark gray	Subhedral – Euhedral	Mostly orthoclase
		Carbonates	0.1-1.2	-	7.4	Light pinkish to pale blue	Subhedral – Anhedral	Mostly calcite perfect cleavage
		feldspathoids	-	-	-	-	-	Feldspathoids not recorded.
		Opaque	-	0.01-0.2	8.3	Dark black	Anhedral	Oxide such as Magnetite the most common
		Vesicles	0.012-2	-	6.5	Dark black	-	ellipsoidal to void and elongated vesicle Random shape.

© Arabic Digital Library-Yarmouk University

www.manaraa.com

4.4.3 Pahoehoe and a'a flow

According to petrographic characteristics of this flow it is described as olivine - pyroxene -phyric basalt. Plagioclase is the dominant mineral phase of this basalt, it forms 30.3 vol. %, as a groundmass, phenocrysts are slightly recorded. Olivine forms about (12.5) vol. %. Pyroxene crystals range from (26.7) vol. % (Table 4.5).

The petrographic study of basalt represent high proportions of medium grains of subhedral to euhedral olivine and anhedral crystals are recorded, some phenocrysts clusters as glomeroporphyritic texture with abundance of vesicles and microcrystalline matrix of plagioclase, augite, olivine and opaque, and arranged by porphyritic, amygdaloidal, Vesicular and intergranular textures.

Olivine crystals characterized by medium to large-grained crystal pinkish to pale brown colour, and by high relief, parallel extinction crystals. Olivine crystals also give an evidence of the affection of stresses by presence of fractures. Olivine minerals was subjected to alteration processes, such as hydration and oxidation, the processes represented by a slight chlorite and much iddingsite that occur at the rims, along the fractures of the crystals of the olivine rarely in the core and completely at the whole olivine crystal. It's

© Arabic Digital Library-Yarmouk University

المنارة للاستشارات
www.manaraa.com

called altered olivine. Iddingsite appears as a dark red, slightly pleochroic brown colour.

Pyroxene can be identified by comparing it with olivine crystals in PPL view; olivine has much pale colour than pyroxene.

Plagioclase described as medium and small-microlites within matrix phase, arranged randomly (intersected) between crystals and 0.33-0.55 mm in diameter with few phenocrysts.

© Arabic Digital Library-Yarmouk University

www.manaraa.com

Table (4.5): Mineral and textural description Pahoehoe and a'a samples.

Texture description		Mineral description						
Rock type	**Textures**	Grain Diameter			(%) in sample	Colour (Under XPL)	Crystal shape	Other characteristics
		Minerals	Phenocryst (mm)	Groundmass (mm)				
Olivine Phyric Basalt	**Porphyritic, Glomeroporphyritic, Ophitic to Subophitic, Intergranular, vesicular, Paliotaxitic**	Olivine	0.25-1.8	0.02-0.09	12.5	colorless to pale yellow in thin section, orangish, yellowish, or reddish brown	Subhedral-Euhedral	Altered to iddingsite completely .core and at rims. Fractured with no cleavage. Two Generations.
		Pyroxene	0.33-0.68	0.04-0.10	26.3	Pinkish blue to reddish brown	Subhedral	Two types (orthopyroxene parallel extinction, clinopyroxene inclined extinction. greenish yellow colour in PPL view.
		Plagioclase	Find	0.33-0.55	30.3	grey	Subhedral - Euhedral	Plagioclase phenocrysts exist, tabular shape, colourless crystals exhibit two sets of cleavage.
		Alkali feldspar	0.25-0.6	-	4.5	Pale grey to dark grey	Subhedral - Euhedral	Mostly orthoclase
		Carbonates	0.3-0.6	-	7.4	Light pinkish to pale blue	Subhedral - Anhedral	Mostly calcite perfect cleavage
		feldspathoid	0.3-0.4	-	6	Pale grey to dark grey	Subhedral-Anhedral	Nepheline: The most common feldspathoid. Grey colour.
		Opaque	-	0.02-0.4	8.3	Dark black	anhedral	Oxide such as Magnetite the most common
		Vesicles	0.3-0.7	-	6.5	-	-	ellipsoidal to void and elongated vesicle

© Arabic Digital Library-Yarmouk University

www.manaraa.com

4.4.4 Yarmouk Exfoliated and vesicular basalt (YE&V)

In general representative samples of this flow are composed mainly of large crystals of euhedral to subhedral, tabular pinkish olivine phenocrysts and small proportions of olivine as a groundmass. Some sample phenocrysts are completely and partially altered to iddingsite in the core and at the rims. Small amount of euhedral to subhedral pale brown and green pyroxene phenocrysts and pyroxene groundmass may be clinopyroxene. There are high present of calcite phenocrysts or at the rim of vesicles. Intermediate amount of accessory minerals such as nepheline and alkali feldspar, vesicles and opaque also appear clearly in this flow. The name of basalt in this flow is **Olivine – pyroxene Phyric** basalt based on phenocrysts (Table 4.6). Groundmass crystals include medium-grained crystals of elongated prism plagioclase with multiple, lamellar twinning, sub-rounded olivine and augite, subhedral opaque minerals and vesicles.

Porphyritic, glomeroporphyritic vesicular and amygdaloidal are the most common textures present in basalt in this flow. It consist also, sup-ophitic, pilotaxitic, radiated and intergranular textural.

© Arabic Digital Library-Yarmouk University

www.manaraa.com

Table (4.6): Mineral and textural description of YE&V samples.

Texture description		**Mineral description**						
Rock type	**Textures**	Grain Diameter			(%) in sample	Colour (Under XPL)	Crystal shape	Other descriptions
		Minerals	Phenocryst (mm)	Groundmass (mm)				
Olivine – pyroxene Phyric Basalt	**Porphyritic, Glomeroporphyritic, amygdaloidal, Ophitic to Subophitic, Radiated, Seriate, Intergranular, vesicular, Pilotaxitic texture.**	Olivine	0.11-1.8	0.04-0.08	8-10	colourless to pale yellow in thin section, orangish, yellowish, or reddish brown	Subhedral-Euhedral	Altered to iddingsite completely .core and at rims. Fractured with no cleavage. Two generations.
		Pyroxene	0.2-0.71	0.02-0.22	30.3	Pinkish blue to reddish brown	Subhedral	Two types (orthopyroxene parallel extinction, clinopyroxene inclined extinction. greenish yellow colour in PPL view.
		Plagioclase	-	0.12-1.0	35.3	Grey	Subhedral - Euhedral	Plagioclase ,tabular shape , colourless crystals exhibit two sets of cleavage with lamellar twinning and large crystal.
		Alkali feldspar	0.35-0.8	-	7	Pale grey to dark grey	Subhedral - Euhedral	Mostly orthoclase
		Carbonates	0.33-1.6	-	7.4	Light pinkish to pale blue	Subhedral - Anhedral	Mostly calcite perfect cleavage.as phenocrysts and at the rim of vesicles.
		feldspathoid	0.07-0.9	-	5	Pale grey to dark grey	Subhedral-Anhedral	Nepheline: The most common feldspathoids. Grey colour.
		Opaque	-	0.05-1.2	10	Dark black	anhedral	Oxide such as Magnetite the most common
		Vesicles	0.12-0.92	-	6.5	Dark black	anhedral	Sub rounded to void and elongated vesicle

© Arabic Digital Library-Yarmouk University

www.manaraa.com

4.5 Petrography and Mineralogy

4.5.1Minerals description

The YRB samples were melanocraitic, idiomorphic to hypidiomorphic, holocrystalline, fine to medium grained. Minerals were described as; primary minerals that formed during the original crystallization when the rock first form including (plagioclase, olivine, pyroxene, minerals, barite and accessory minerals characteristically minerals are formed during the solidification of the rocks from the magma and present in small amounts (Best, 2003). Common minor accessory minerals include alkali feldspar, feldspathoids and opaques and secondary mineral that form later via alteration or weathering including calcite, iddingsite and serpentine.

4.5.1.1 Primary minerals

4.5.1.1.1 Plagioclase

Plagioclase is the most abundant mineral phase in the studied samples, rates between 8 vol % and 45 vol %. They occur as fine to medium elongated plagioclase and needle microlites in the groundmass (Figure 4.2). Arranged randomly (intergranular) or arranged subparallel to parallel (pilotaxitic) (Figure 4.3). Plagioclase phenocryst exists(Figure 4.3).

The main properties of plagioclase are colourless, euhedral to subhedral, tabular and needle shape. The cleavage shows multiple and lamellar twinning. The crystals are slightly fractured. Plagioclase crystals are clear in plain polarized light (PPL) and grey interference colour in (XPL). Some of

© Arabic Digital Library Yarmouk University

www.manaraa.com

plagioclase crystals enclosed in pyroxene occurs ophitic to subophitic texture. Five crystals of plagioclase stand out from a central point to give a radiated texture. Microlites appear in different size. The average diameter range from 0.12-0.3 mm and the other range from 0.4-0.5mm due to difference in cooling rate.

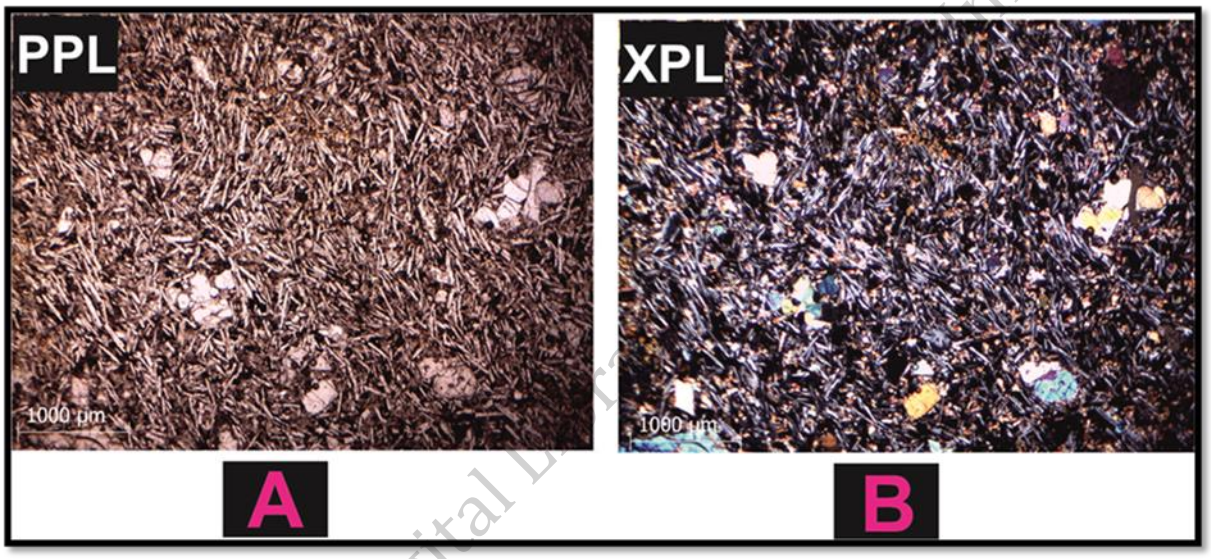

Figure (4.2): Microphotograph shows needle like plagioclase as groundmass, (a) under ppl2.5x magnitude (b) under xpl2.5x magnitude.

© Arabic Digital Library-Yarmouk University

المنارة للاستشارات
www.manaraa.com

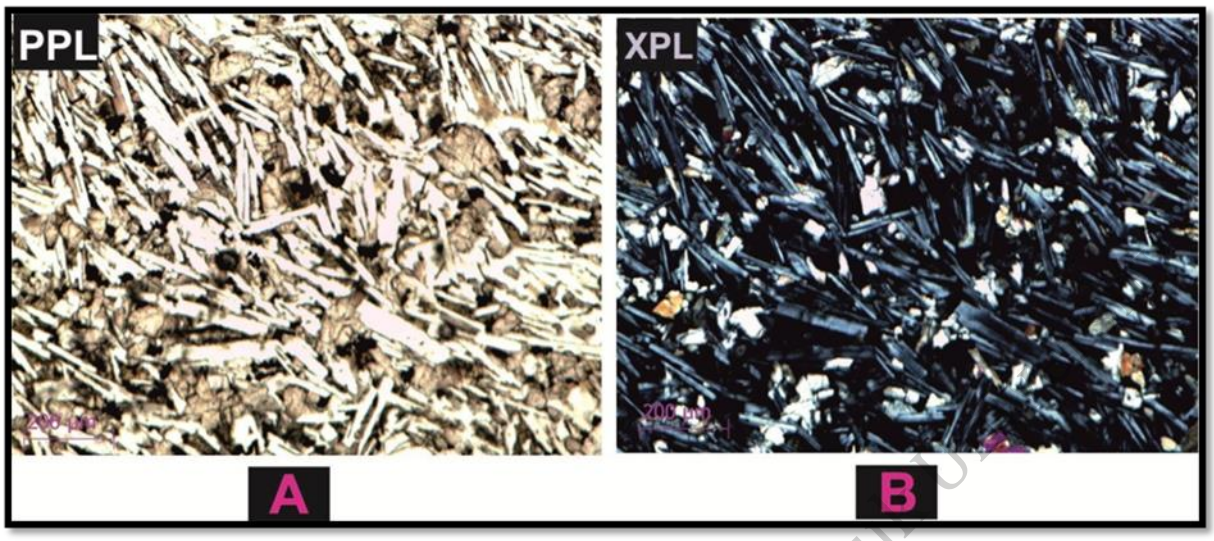

Figure (4.3): Thin sections of YRB. (a) Plane light photomicrograph of intergranular microphenocryst of plagioclase crystals in groundmass, (b) Crossed polarized photomicrograph of intergranular plagioclase crystals10x*10x magnitude.

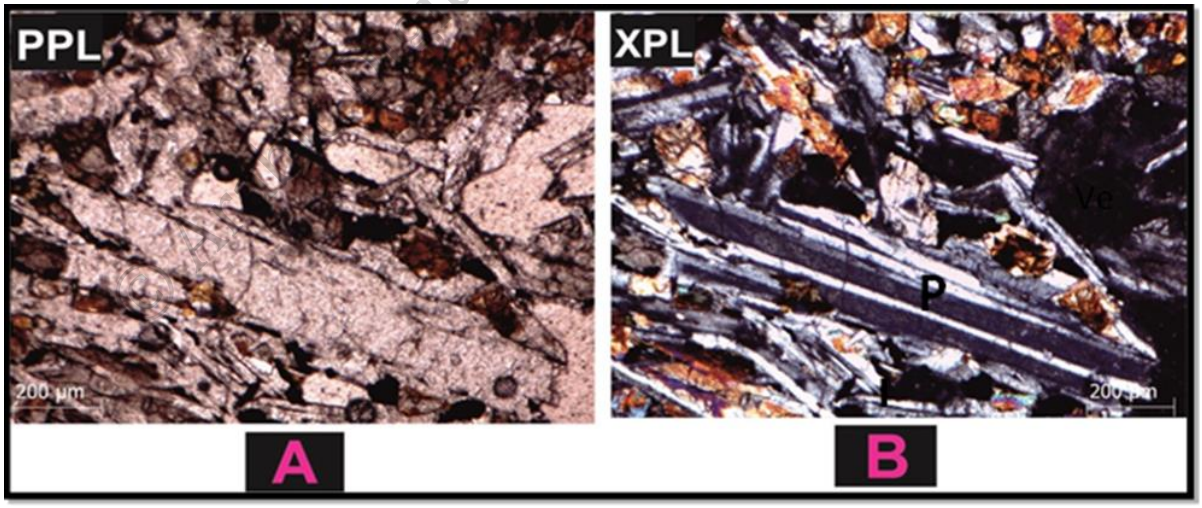

Figure (4.4): Thin sections of YRB. (a) Plane light photomicrograph of phenocryst of plagioclase crystals multiple twinning surrounded by vesicles, (b) Crossed polarized photomicrograph of plagioclase crystals10x*10x magnitude.

www.manaraa.com

Three points were selected on rock fraction to determine the chemical composition and crystal shape of this points Figure (4.5 and 4.6) Table (4.7and 4.8).

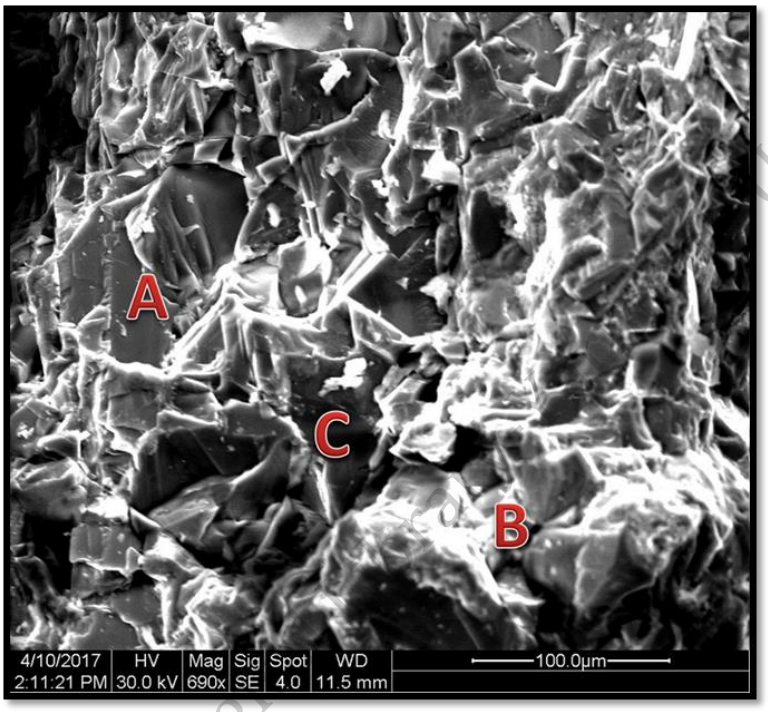

Figure (4.5): Electron micrograph image of rock fraction showing a: orthorhombic clinopyroxene (pigeonite) crystal (Sample No 6(002b), and plagioclase (a, c).

© Arabic Digital University

www.manaraa.com

Table (4.7): Electron microprobe chemical analyses wt% and calculation formula Mol % components of plagioclase and pyroxene sample**.**

Chemical analysis/ YRB sample		**Sample 6 (002)A**	**Sample 6 (002)B**	**Sample 6 (002)C**
Percentages of Oxides (wt %)	**SiO_2**	54.73	50.08	60.56
	TiO_2	0.14	2.46	0.17
	Al_2O_3	28.19	4.76	23.26
	Cr_2O_3	0.05	0.34	0.28
	Fe_2O_3	0.96	10.14	1.03
	MnO	0.08	0.45	0.37
	MgO	0.67	14.03	0.93
	CaO	9.02	16.41	4.98
	Na_2O	5.80	1.14	6.17
	K_2O	0.35	0.24	1.44
Norm Calculation (Mole %)	**An**	46.2	-	27
	Ab	53.76	-	62
Name of pyroxene and plagioclase mineral		andesine	pigeonite	Andesine

© Arabic Digital Library-Yarmouk University

www.manaraa.com

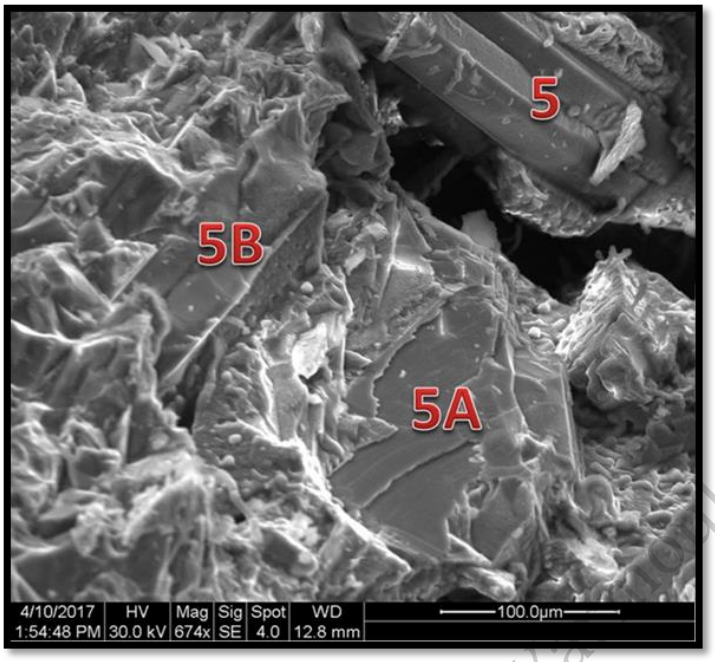

Figure (4.6): Electron micrograph image of rock fraction showing a: orthorhombic clinopyroxene (pigeonite) crystal (Sample No 5, 5b), and plagioclase (5a).

© Arabic Digital Library-Yarmouk University

www.manaraa.com

Table (4.8): Electron microprobe chemical analyses wt% and calculation formula Mol % components of plagioclase and pyroxene sample**.**

Chemical analysis/ YRB sample		**Sample 5**	**Sample 5A**	**Sample 5B**
Percentages of Oxides (wt %)	**SiO_2**	53.71	52.68	49.93
	TiO_2	0.95	0.77	2.41
	Al_2O_3	9.80	24.26	6.10
	Cr_2O_3	0.34	0.51	0.21
	Fe_2O_3	6.65	1.97	8.62
	MnO	0.36	0.59	0.53
	MgO	18.50	2.99	14.28
	CaO	7.10	12.63	15.34
	Na_2O	2.22	3.38	2.18
	K_2O	0.36	0.23	0.41
Name of pyroxene and plagioclase mineral		pigeonite	Plagioclase	Pigeonite

© Arabic Digital Library-Yarmouk University

4.5.1.1.2 Olivine

Olivine is one of the main mineral phases in the studied basalts, rating 8 vo l% and 12 vo l%. It's occurred as phenocrysts and in groundmass with different petrotypes euhedral to subhedral, tabular, fine grained and fractured. Olivine crystals usually present as light grey to colourless crystals, pale yellow in thin section, displays parallel extinction, fractures, higher relief and no cleavage. They range in size from 0.1 to 1.8 mm. Olivine subjected to alteration, hydration or oxidation process that form secondary minerals such as

www.manaraa.com

iddingsite by a process called iddingtization that present partially at high degree along the edge, the fractures and the core of the crystals or completely at the whole olivine crystal.

Iddingsite appears as a dark red, slightly pleochroic brown colour. Groundmass olivine is also iddingtized. Some olivine crystals exhibit oxides (magnetite) inclusions in it. Some of olivine crystal with sizes varies gradually or in a continuous series from the smallest to larges display seriate texture, and the aggregate crystal more than six exhibit glomeroporphyritic texture.

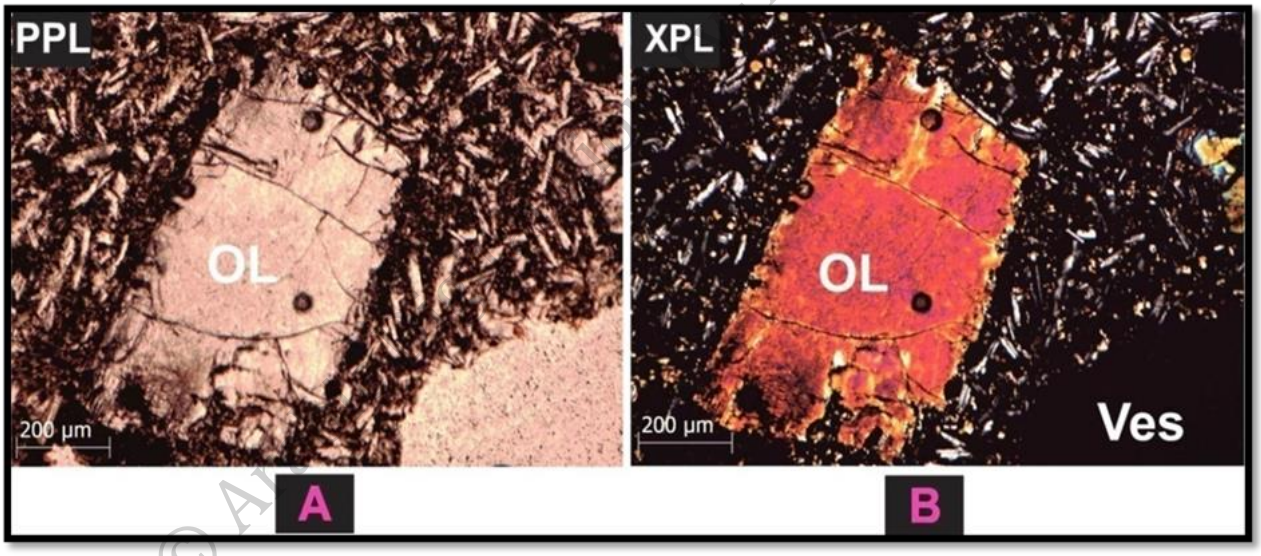

Figure (4.7): Thin sections of YRB. (a) Plane light photomicrograph of euhedral and tabular Microphenocryst of four sided Olivine crystals with needle elongated plagioclase in the groundmass surrounding it and (b) Crossed polarized photomicrograph of euhedral Microphenocryst of Olivine. Crystal 10*10x magnitude.

© Al-Yarmouk University

www.manaraa.com

There are three type of olivine alteration at the rim, core and complete alteration as phynocrysts or in a groundmass. See Figure (4.9, 4.10, 4.10, 4.11 4.12 and 2.13).some olivine crystals show resorbtion Figure (4.14).

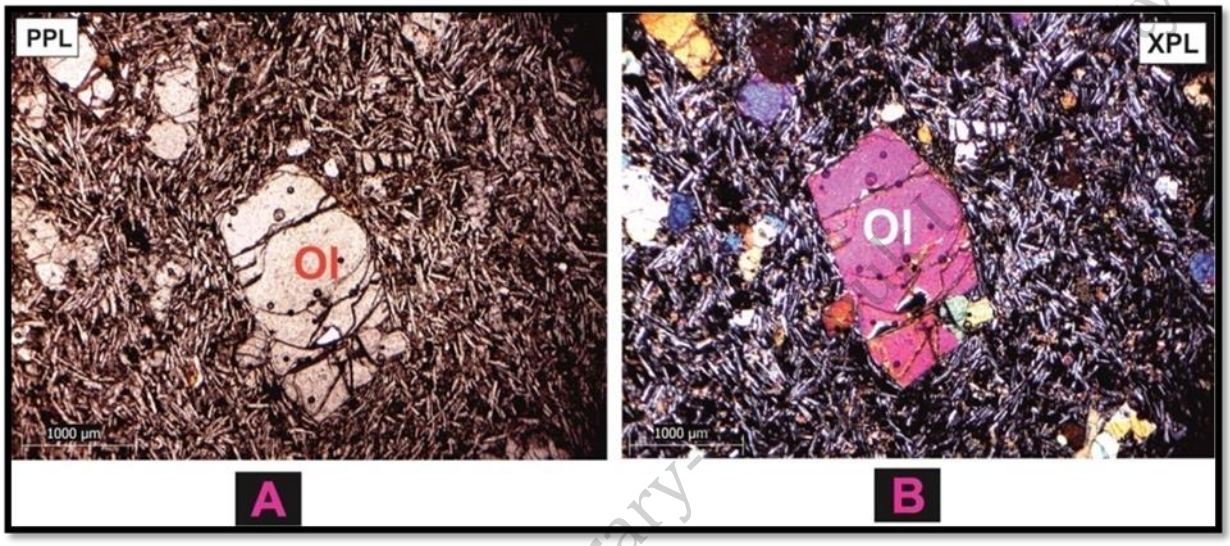

Figure (4.8): Thin sections of Olivine - phyric basalt. (a)Plane light photomicrograph of euhedral microphenocryst of fractured Olivine crystals with needle elongated plagioclase in the groundmass surrounding it and (b) Crossed polarized photomicrograph of euhedral microphenocryst of Olivine. Crystals 2.5 x*10x magnitude**.**

© Arabic Digital Library-Yarmouk University

www.manaraa.com

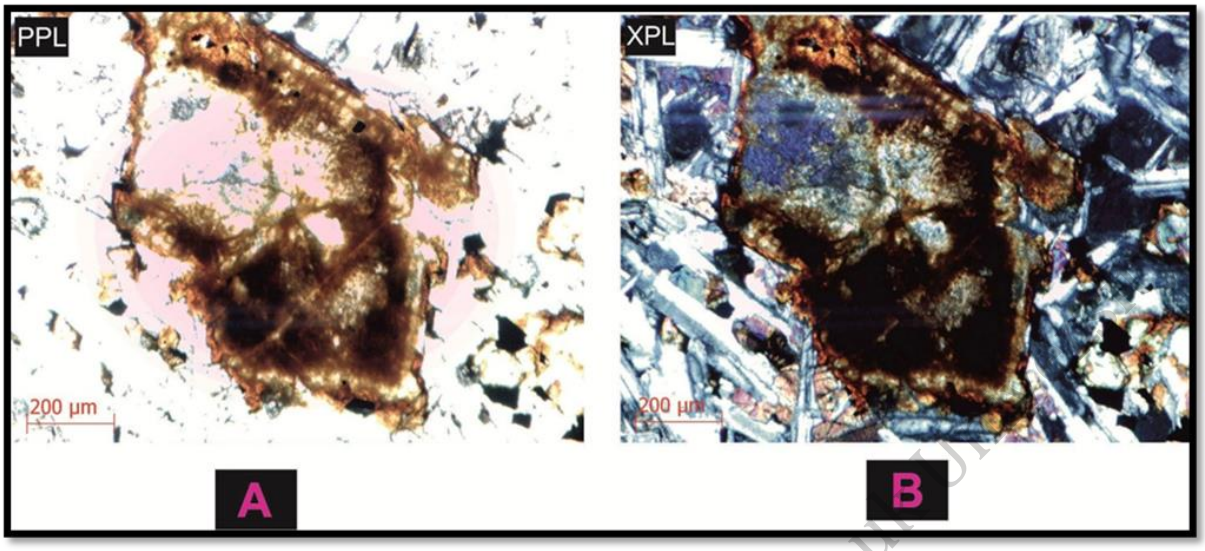

Figure (4.9): Microphotograph shows complete alteration of olivine phenocrysts to iddingsite, (a) under ppl 10 x magnitudes (b) under xpl 10x magnitude.

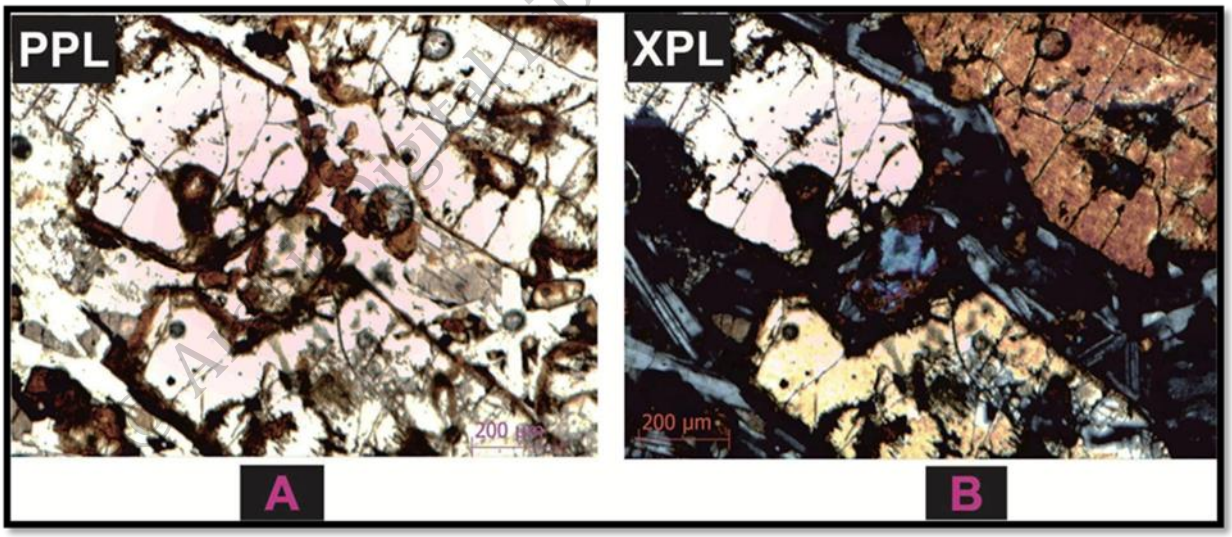

Figure (4.10): Microphotograph shows partialy alteration of olivine phenocrysts to iddingsite at the rims of crystals, (a) under ppl 10 x magnitudes (b) under xpl 10x magnitude.

www.manaraa.com

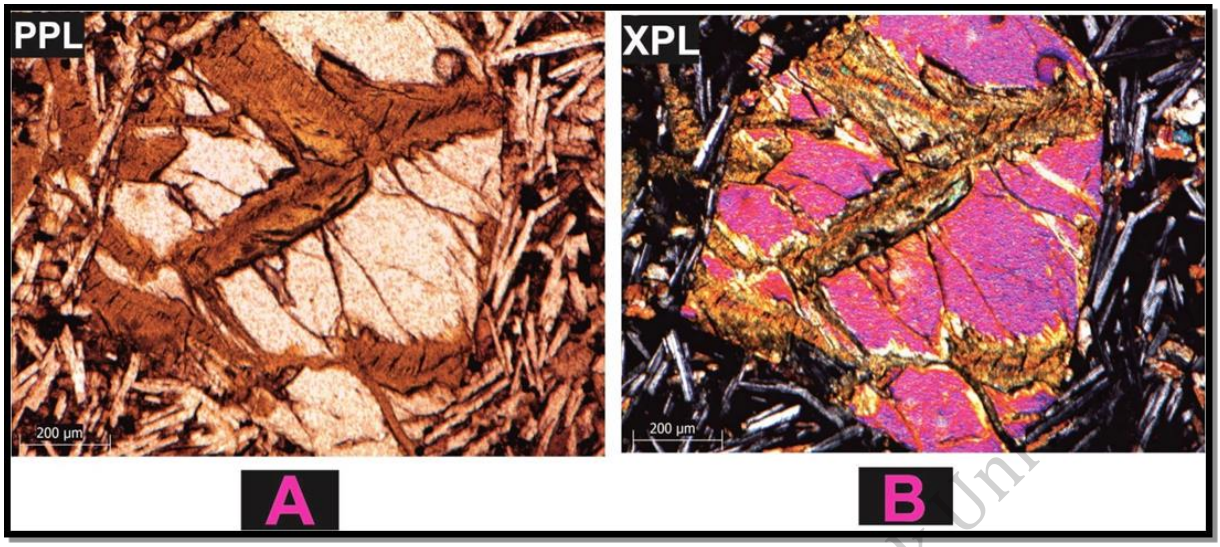

Figure (4.11): Microphotograph shows partially alteration of olivine phenocrysts to iddingsite at the fractures of crystals, (a) under ppl 10 x magnitudes (b) under xpl 10x magnitude.

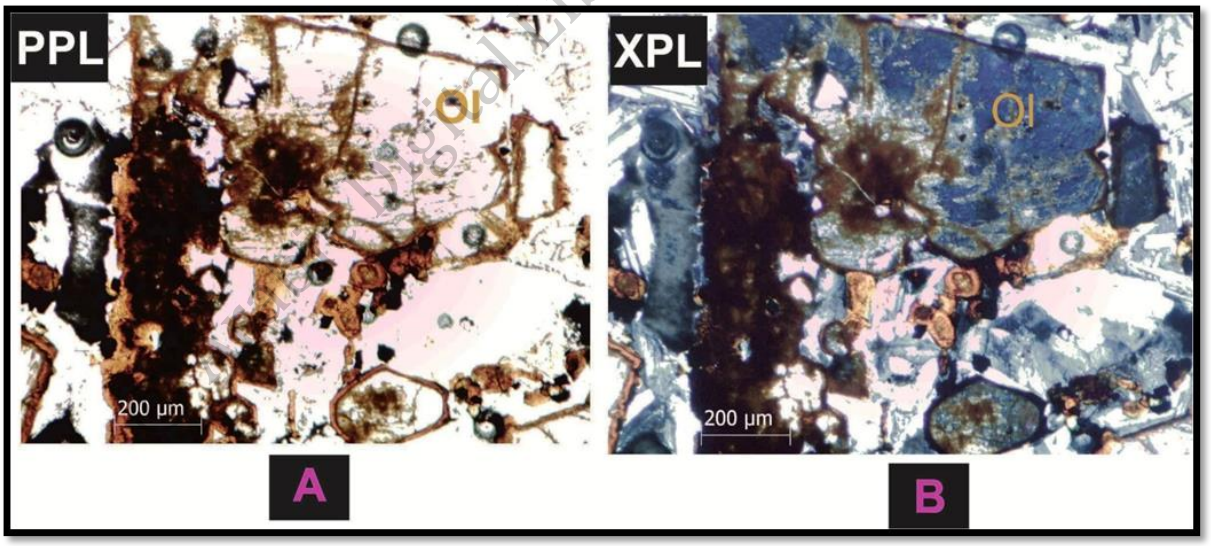

Figure (4.12): Microphotograph shows Incipient serpentinization along internal cracks and core in olivine phenocrysts (alteration of olivine phynocrysts to iddingsite at the fracture of crystals), (a) under ppl 10x magnitude (b) under xpl 10x magnitude.

www.manaraa.com

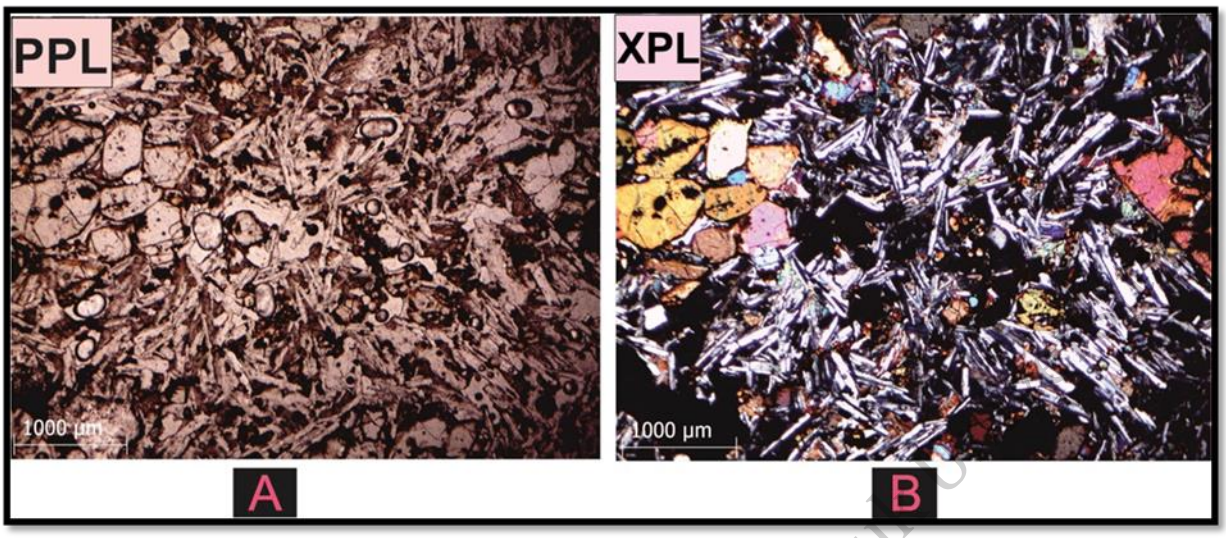

Figure (4.13): Microphotograph shows completely alteration of olivine groundmass to iddingsite with pilotaxitic groundmass of plagioclase, (a) under ppl2.5x magnitude (b) under xpl 2.5x magnitude.

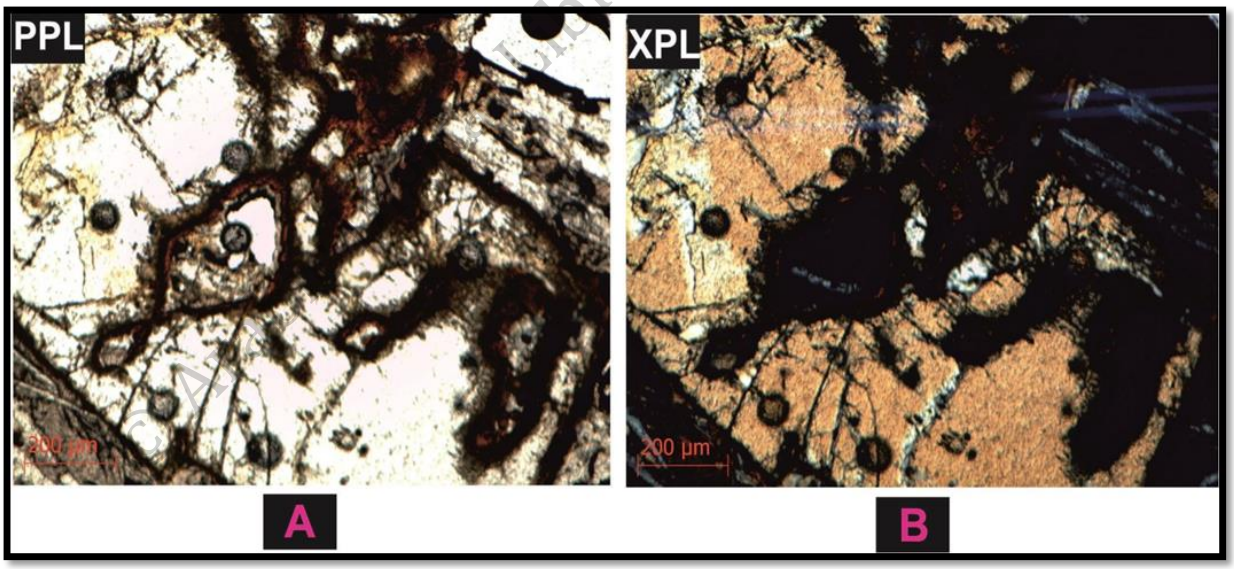

Figure (4.14): Microphotograph showing resorbtion of olivine crystals, (a) under ppl10x magnitude (b) under xpl10x magnitude.

www.manaraa.com

EDX results of olivine crystal shown in (Table 4.9) and (Figure 4.15).

Table (4.9): Electron microprobe chemical analyses wt% and calculation formula Mol% components of olivine sample**.**

Chemical analysis/ YRB sample		**Sample 5a**
Percentages of Oxides (wt %)	**SiO_2**	38.09
	TiO_2	0.62
	Al_2O_3	1.06
	Fe_2O_3	17.33
	MgO	40.27
	CaO	1.57
	Na_2O	1.06
Norm Calculation (Mole %)	**Fo (Forsterite)**	80.01
	Fa (Fayalite)	20.0

© Arabic Digital Library-Yarmouk University

www.manaraa.com

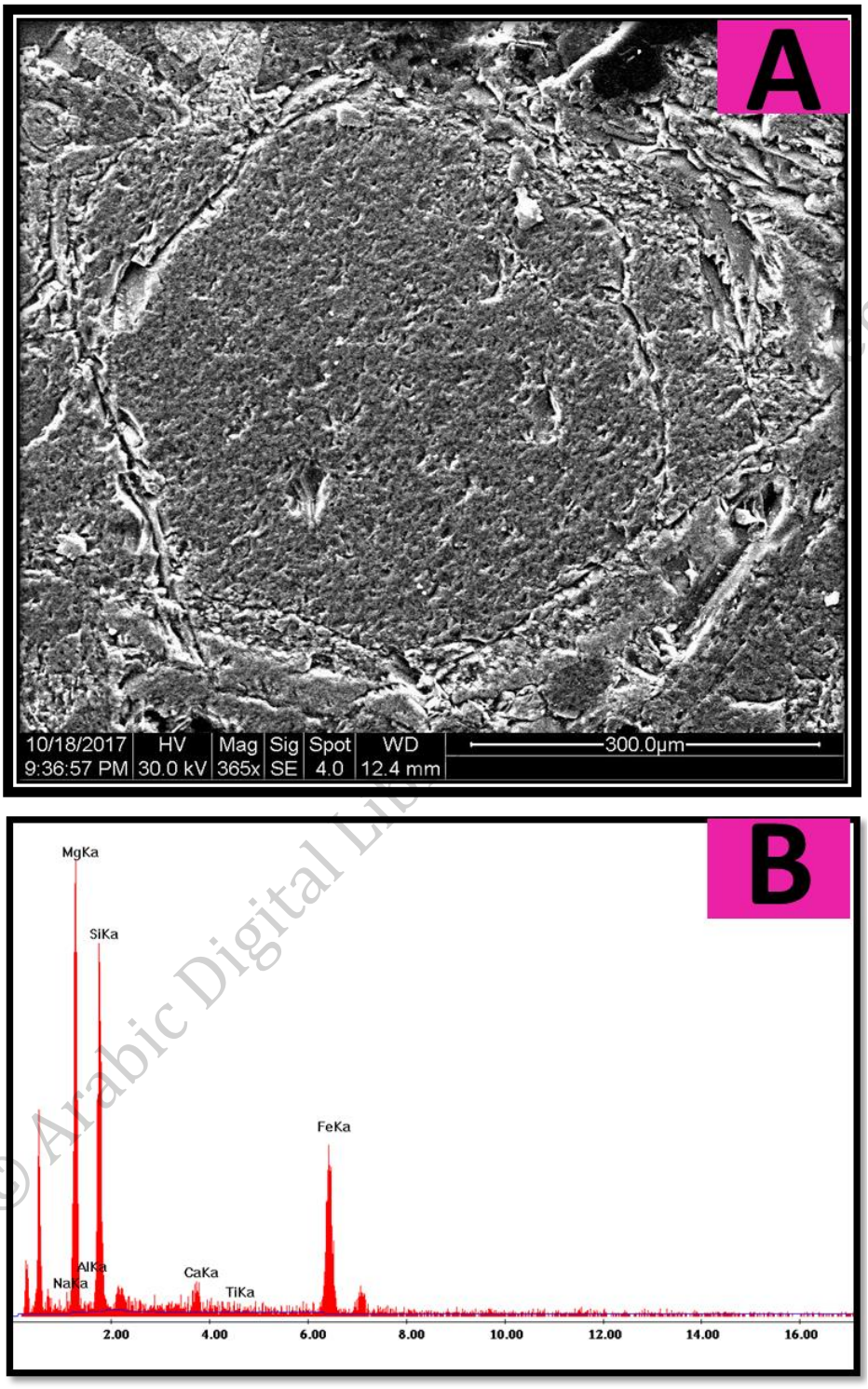

Figure (4.15): Electron micrograph image of rock slide showing a: orthorhombic olivine crystal (Sample No. 5a), b: EDX Results of the olivine of Sample (5b).

© Arabic Digital Library-Yarmouk University

المنارة للاستشارات
www.manaraa.com

4.5.1.1.3 Pyroxene

Is the second dominant mineral it occurred as colourless at (PPL) with subhedral to anhedral crystal with pale green to greyish brown interference colour. Its shows perfect tow set of cleavage in the cross section. The abundance pyroxene ranges between 26 vol % to 35 vol % as two generations as phenocryst (Figure 4.16) and in groundmass (Figure 4.17). pyroxene crystal have an inclined extinction which represents clinopyroxene mineral with inclination is measured to be between (35^{o}-55^{o}).pyroxene crystals affected by alteration process which appear as green chlorite on the cleavage sets or at the rims. Pyroxene minerals forms as intergranular texture, also pyroxene interact with plagioclase crystals to give ophitic and sub-ophitic textures. Diopside, augite, pigeonite, hypersthene mineral and opaque minerals inclusions are common.

© Arabic Digital Library Yarmouk University

www.manaraa.com

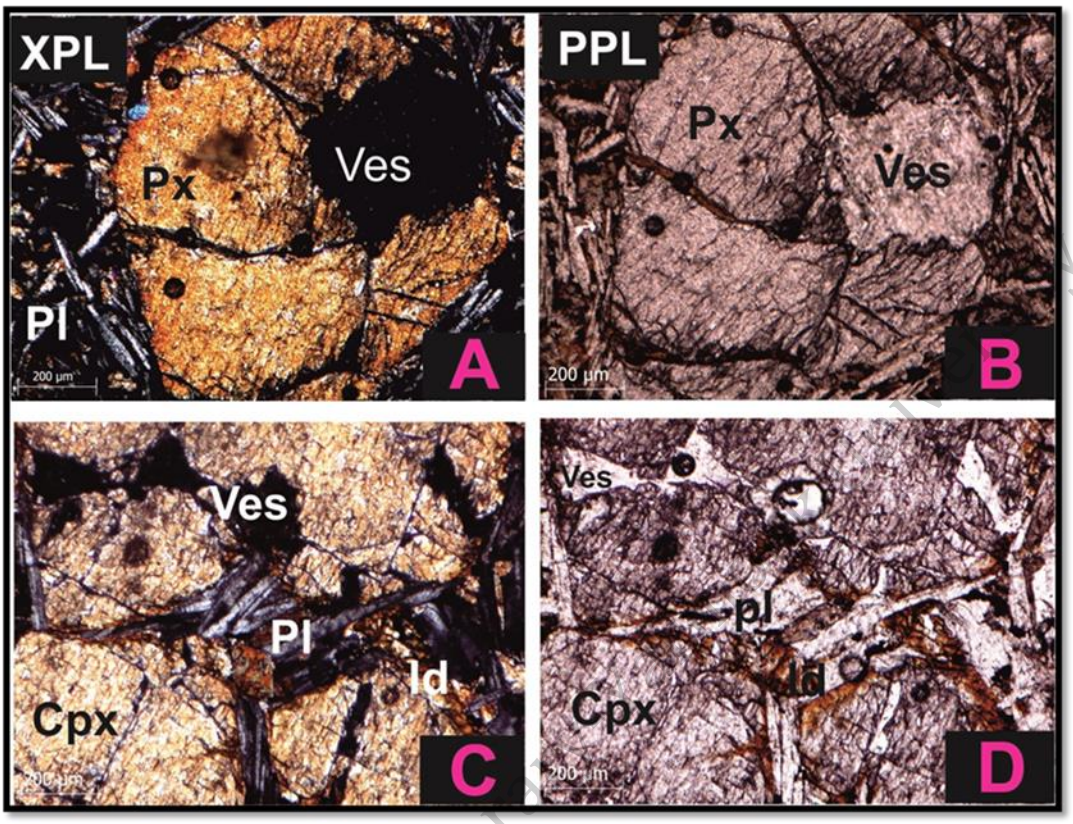

Figure (4.16): Microphotograph shows (A, C): subhedral pyroxene phenocrysts with intergranular groundmass of plagioclase, under xpl 10x magnitude (B, D) under ppl 10x magnitude.

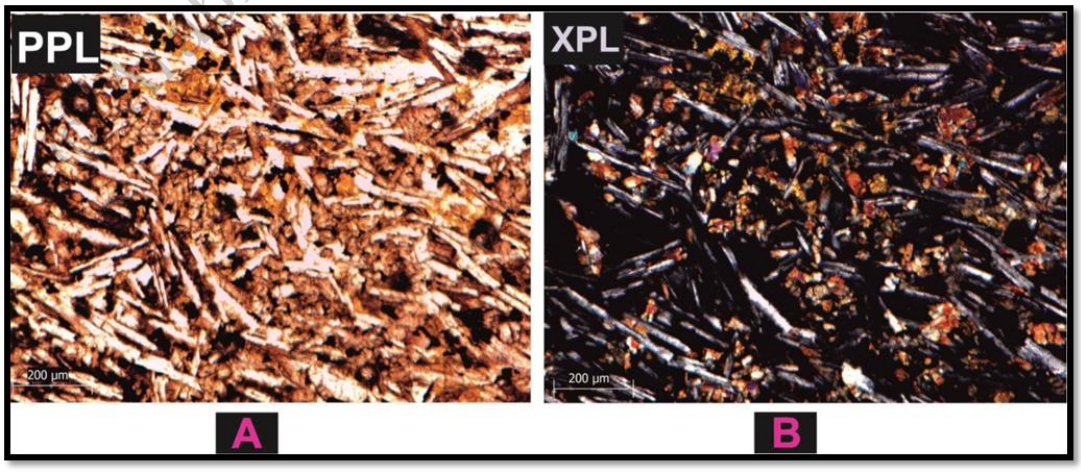

Figure (4.17): Microphotograph showing pyroxene groundmass crystals with pilotaxitic texture, (a) under ppl 10 x magnitudes (b) under xpl 10x magnitude.

www.manaraa.com

SEM analysis is very important in order to identify the chemical composition (Figure 4.18 & Table 4.10). Results of SEM analysis established that the clinopyroxene minerals consist commonly from hypersthene. SEM picture displays the orthorhombic crystal system of orthopyroxene (hypersthene) (Medium ratios of Fe & Mg) (Figure 4.18), compared with orthopyroxene (enstatite) (high Mg) (Figure 4.19).

Table (4.10): Electron microprobe chemical analyses wt% and calculation formula Mol% components of clinopyroxene in YR sample**.**

Chemical analysis/ YRB sample		**Sample 5b**	**Sample 6(001)**
Percentages of Oxides (wt %)	**SiO_2**	60.34	42.96
	TiO_2	0.32	0.17
	Al_2O_3	6.86	8.47
	Cr_2O_3	-	0.50
	Fe_2O_3	21.50	15.06
	MgO	9.77	29.98
	CaO	1.21	0.83
	BaO	-	0.46
	Na_2O	0.00	0.80
	K_2O	0.00	0.17
Norm Calculation (Mole %)	**Wo (Wollastonite)**	4.5	1.56
	En (Enstatite)	45	78.53
	Fs (Forsterite)	50	19.91
Name of orthopyroxene mineral		Hypersthene	Enstatite

©Arabic Digital Library-Yarmouk University

www.manaraa.com

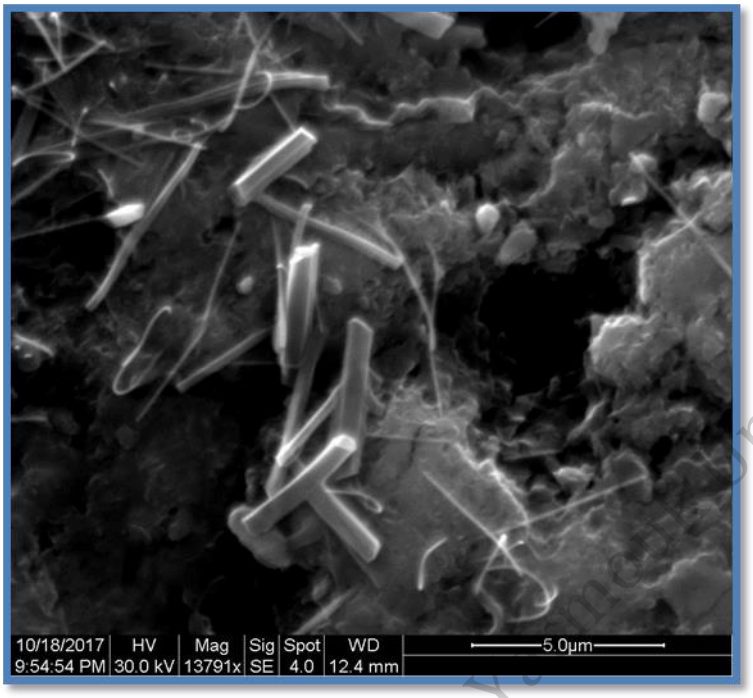

Figure (4.18): Electron micrograph image of slide sample showing orthorhombic orthopyroxene (hypersthene) crystal (Sample No. 5b).

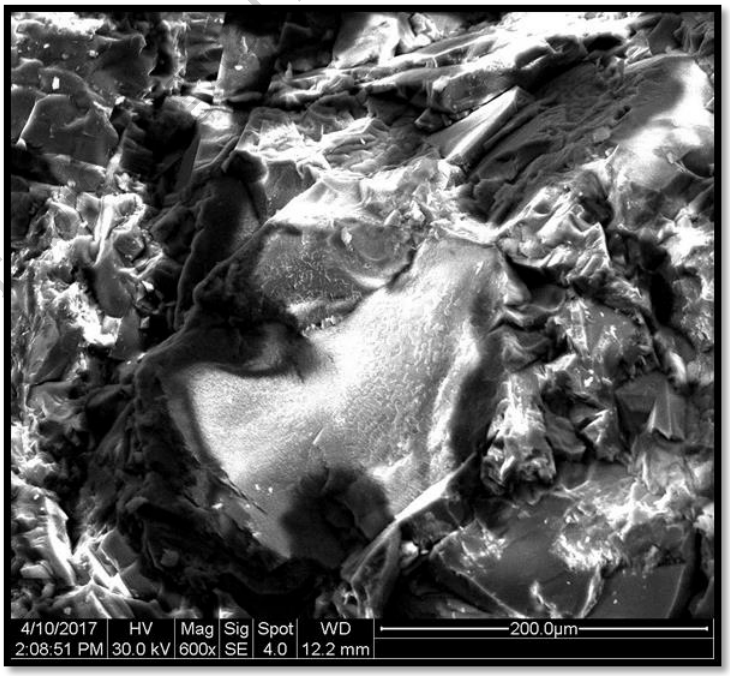

Figure (4.19): Electron micrograph image of rock fraction showing orthorhombic orthopyroxene (enstatite) crystal (Sample No. 6(001).

© Arabian Gulf University Library-Yemeni Branch
المنارة للاستشارات
www.manaraa.com

4.5.1.2 Accessory minerals

Accessory minerals characteristically are formed during the solidification of the rocks from the magma and present in small amounts less than 5%. Common minor accessory minerals include alkali feldspar, feldspathoids and opaques.

4.5.1.2.1 Alkali feldspar

Commonly forms euhedral to subhedral crystals .Orthoclase is the common alkali feldspar. It shows simple twinning (figure 4.20), it's grey or cloudy in colour like plagioclase but without uniform shape at the rim it presents in the groundmass. Orthoclase crystal surrounds plagioclase crystal ranges from 4-7% in volume.

© Arabic Digital Library-Yarmouk University

www.manaraa.com

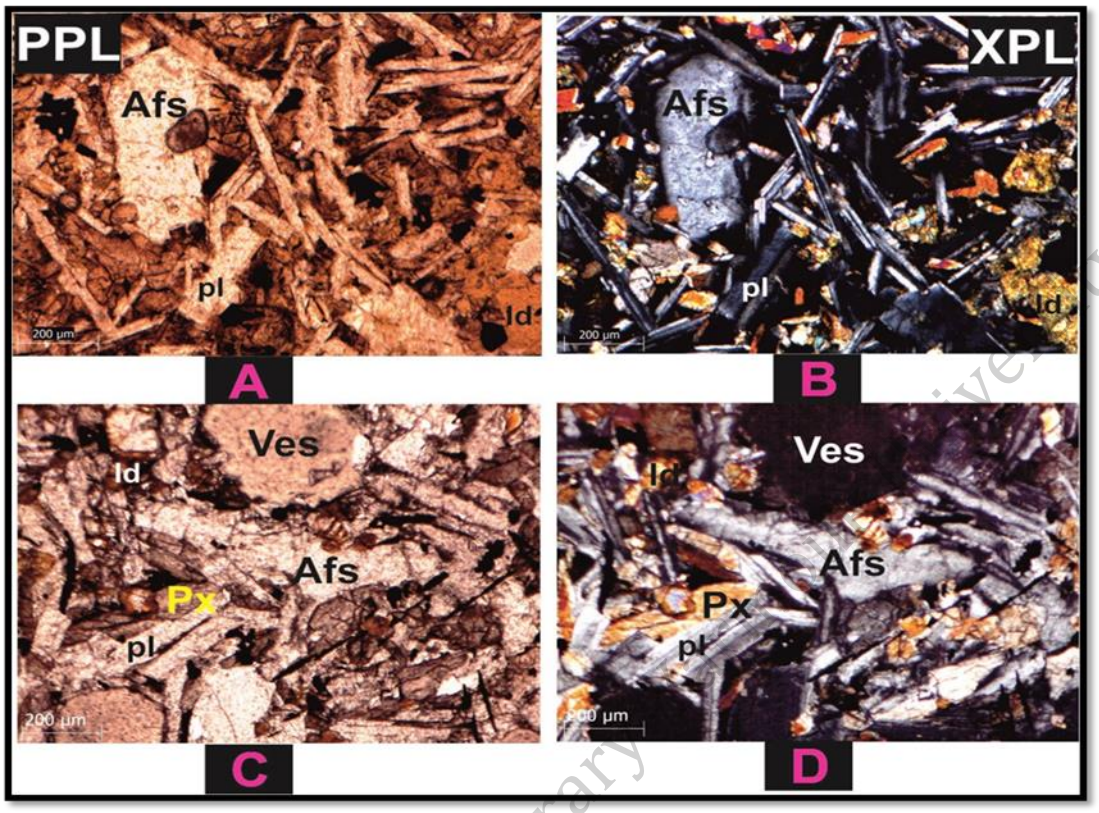

Figure (4.20): Microphotograph shows (b, d): Anhedral alkali feldspar phynocrysts with intergranular groundmass of plagioclase, under ppl 10x magnitude (a, c) under xpl 10x magnitude.

4.5.1.2.2 Feldspathoids minerals

Those minerals are less abundant than feldspar minerals. Leucite, nepheline and sodalite are alkali aluminosilicates minerals in this group. Nepheline the most common of the feldspathoids occurs typically as euhedral to anhedral grains in undersaturated rocks (figure 4.21); leucite is quite rare occurring as euhedral phenocrysts in rocks, sodalite is rare constituents of silica –undersaturated rocks .Sodalite identified by XRD analysis, but nepheline and leucite defined by optical microscope. Nepheline is colourless in PPL and

© Arabic Digital Library

www.manaraa.com

cloudy to grey in XPL, low birefringence and maximum interference colours are first-order grey. It ranges from 5 to 7% in thin section.

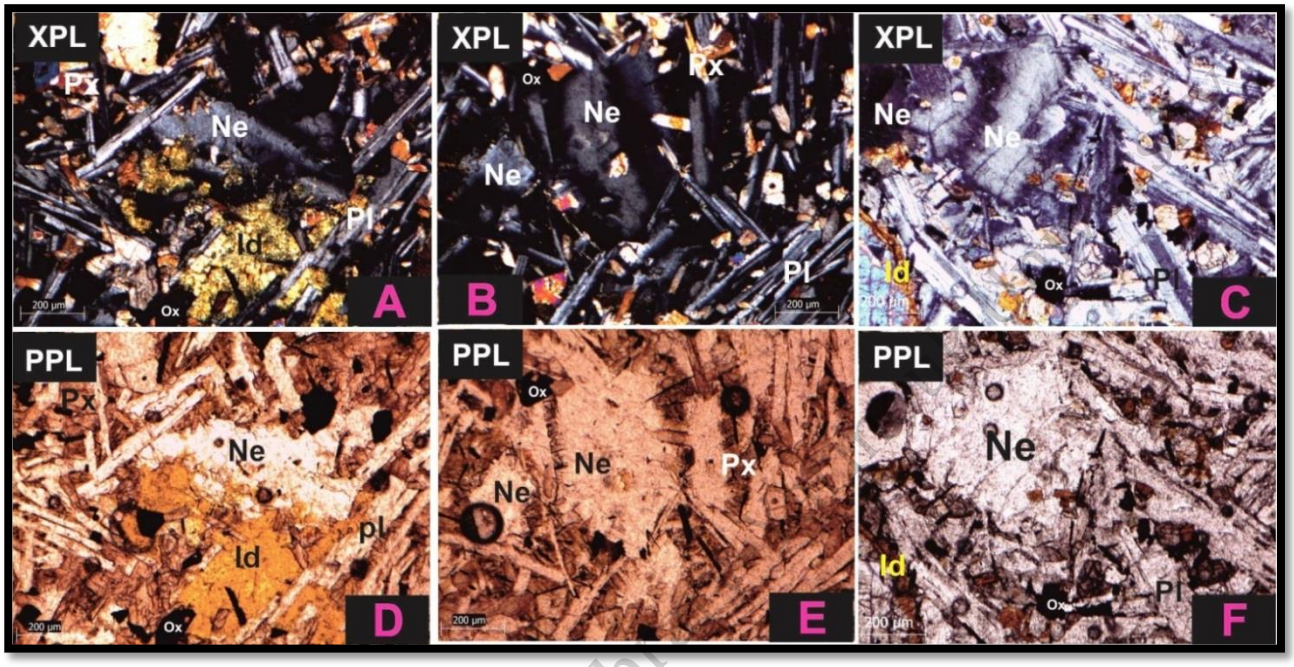

Figure (4.21): Microphotograph shows (A, b, c): Anhedral nepheline phynocrysts with intergranular groundmass of plagioclase, oxides and pyroxene under xpl 10x magnitude (d, e, f) under ppl 10x magnitude.

4.5.1.2.3 Opaques

Opaque minerals were commonly found as large to small dark euhedral crystals of iron oxides and include of magnetite, chromite and illmenite phenocrysts scattered throughout the rock and throughout inclusions within olivine and pyroxene crystals in YR sample (Figure 4.22). its forming about 5 % - 7% of the rocks and ranging from0.01 to 1.2 mm in size. Generally, magnetite is black; and shows homogeneous optical properties. Most of it is anhedral to subhedral, but crystals with square outline are also presented.

© Arabic Digital Library

المنارة للاستشارات
www.manaraa.com

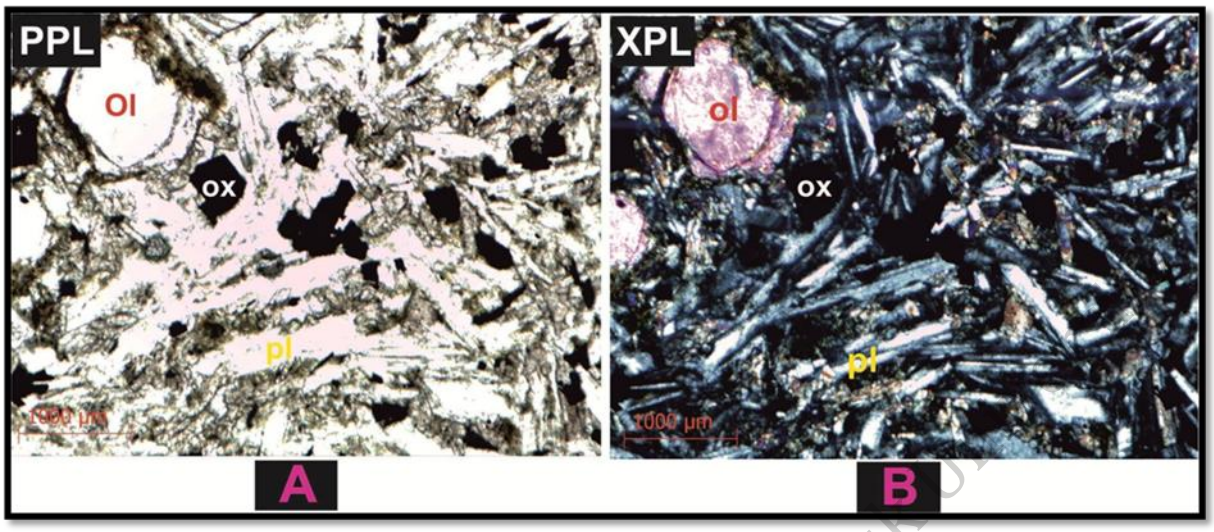

Figure (4.22): Microphotograph shows Anhedral oxides phynocrysts with intergranular groundmass of plagioclase, the optical properties of magnetite were black colour with PPL and XPL Crystals 2.5 x*10x magnitude.

4.6 Groundmass

The groundmass consists mainly of plagioclase (labradorite), olivine, pyroxene (diopside, augite and pigeonite), and opaque. Calcite, iddingsite and chlorite are secondary minerals. Nepheline is recorded.

4.7 Vesicles

YR samples shows spherical to void and elongated vesicles (Figure 4.23). The long axis ranges from 0.1 to 9 mm. Most of the vesicles are empty, but some are filled with calcite and other secondary minerals (probably calcite and zeolites). They form about 3-6.5 vol % of the rock.

© Arabic Digital Library-Yarmouk

المنارة للاستشارات
www.manaraa.com

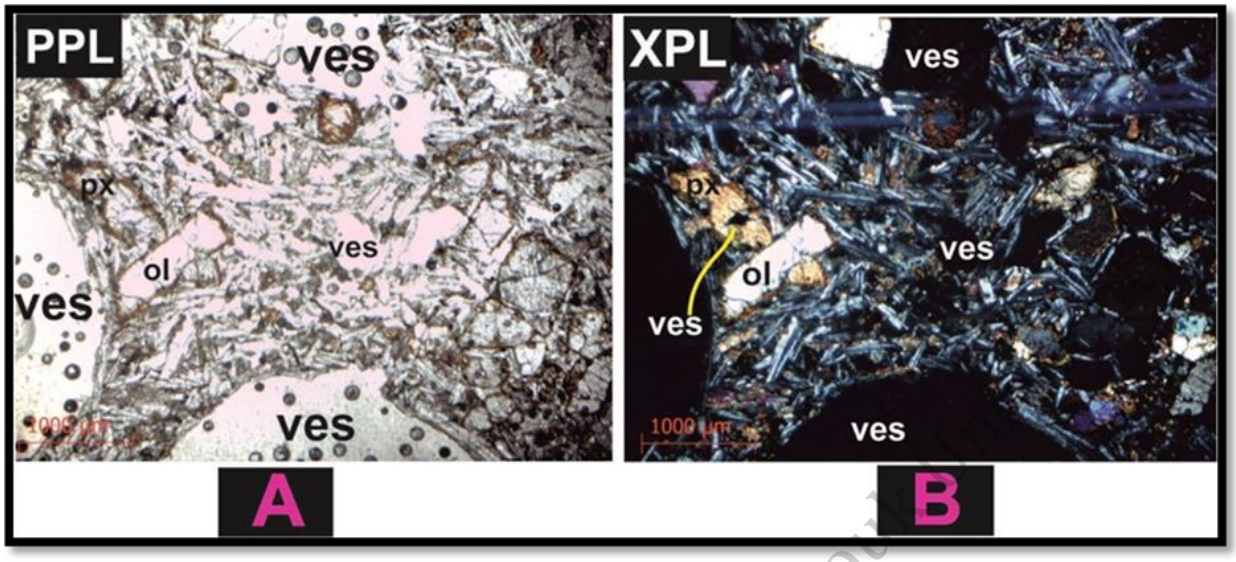

Figure (4.23): Microphotograph showing vesicles in groundmass exhibit vesicular texture, embayed pyroxene phenocrysts (a) under ppl 10x magnitudes white (b) under xpl 10x magnitude is black.

4.8. Secondary minerals

That never crystallizes directly from magma and is never found in fresh igneous rocks, its hydrothermal alteration of the original pyrogenic igneous minerals that are form later via alteration or weathering processes replacing original minerals. The overall shape of the igneous grains is preserved during replacement (Raymond, 2002). Common secondary minerals consist of carbonates, iddingsite and chlorite. With their alterations processes includes:

• Serpentine or iddingsite replacing olivine or oxidation of olivine

• Chlorite replacing pyroxene or chloraitisation of pyroxene

• Sericite or epidote replacing plagioclase or seritization.

© Arabic Digital Library Yarmouk

المنارة للاستشارات
www.manaraa.com

4.8.1 Iddingsite

Iddingsite is a mixture of iron and magnesium and characterized by dark brown to reddish brown to yellowish orange pseudomorphous replacement of olivine of basaltic rocks to iddingsite, its highly birefringent replacement of olivine, and spatially in lavas see (Figure 4.9). Iddingsite is a deuteric mineral derived during the final cooling of the lavas in which it occurs by a reaction between gases, water, and olivine, under oxidizing conditions (Sun, 1957).its recorded at the rims, core ,at the fractures of crystals and in groundmass .

4.8.2 Carbonate and sulfate Minerals

Found as calcite and barite. Calcite: is mainly recorded in the fractured and vesicles most show white to turbid color pink or green colour, and three set of cleavage (Fig. 4.24, 4.25 and 4.26) and by SEM (Figure 4.27) (Table 4.11).with forth order interference colour, perfect rhombohedra cleavage and shows pal red colour under PPL. Calcite is recognized by its cleavage, extreme birefringence, change of relief with rotation, and reaction with weak acid. By using SEM analysis, barite identified by chemical composition compared with calcite (Figure 4.28 a & b) (Table 4.12).

© Arabic Digital Library-Yarmouk University

www.manaraa.com

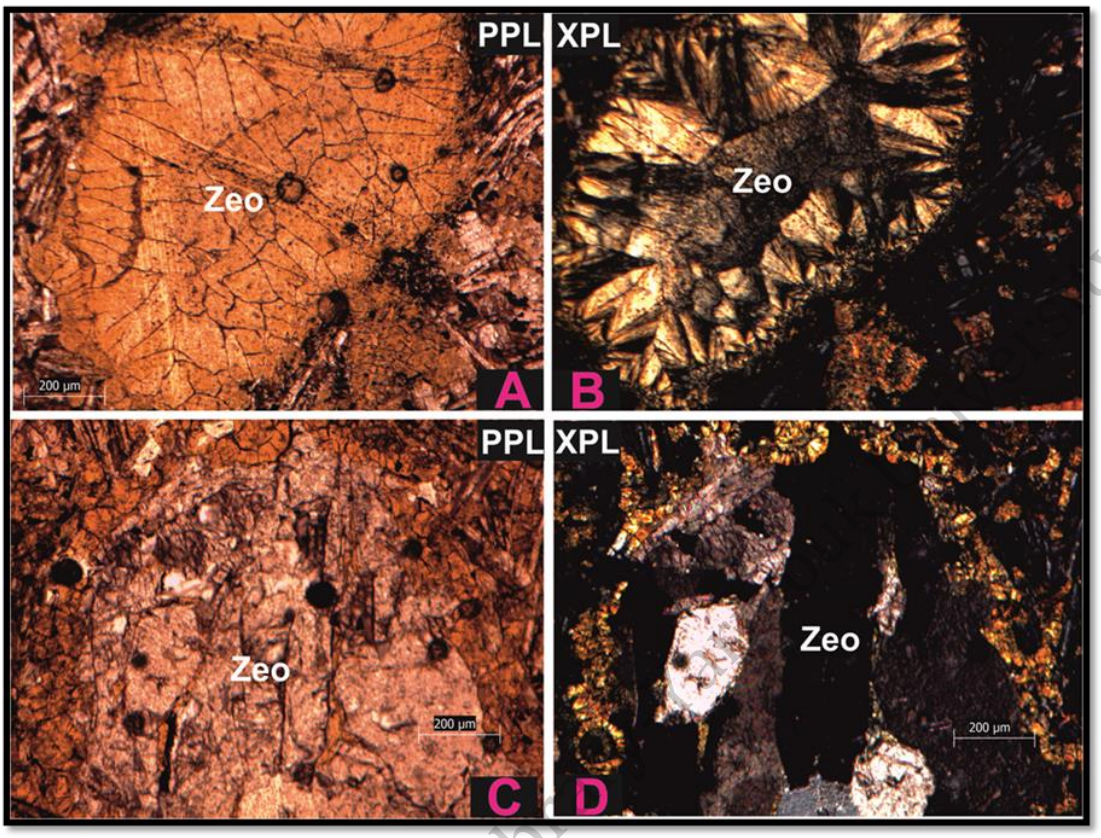

Figure (4.24): Microscopic photo of YR sample shows zeolite with first order interference color filled the vesicles in amygdaloidal texture, (a, c) under ppl 10x magnitude (b, d) under xpl 0x magnitude.

© Arabic Digital Library-Yemeni

المنارة للاستشارات
www.manaraa.com

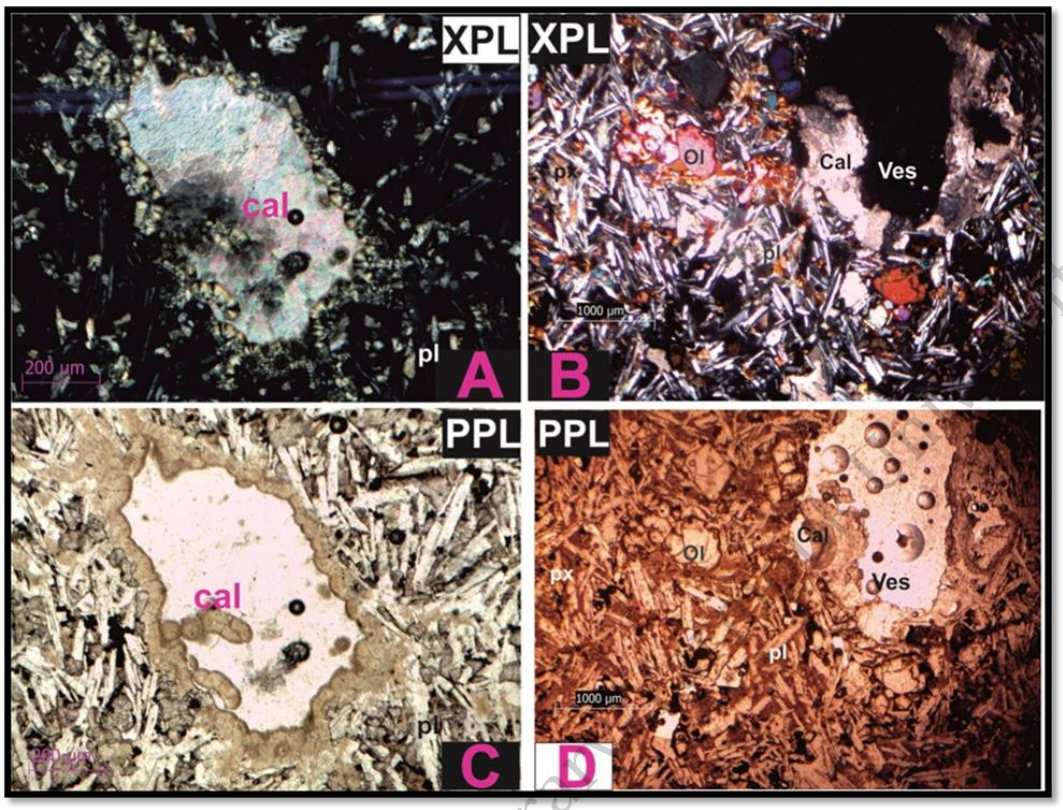

Figure (4.25): Microscopic photo of YR sample shows Carbonates with third order interference colour filled the vesicles in amygdaloidal texture, (a, b) under ppl2.5x magnitude (c, d) under xpl 2.5x magnitude.

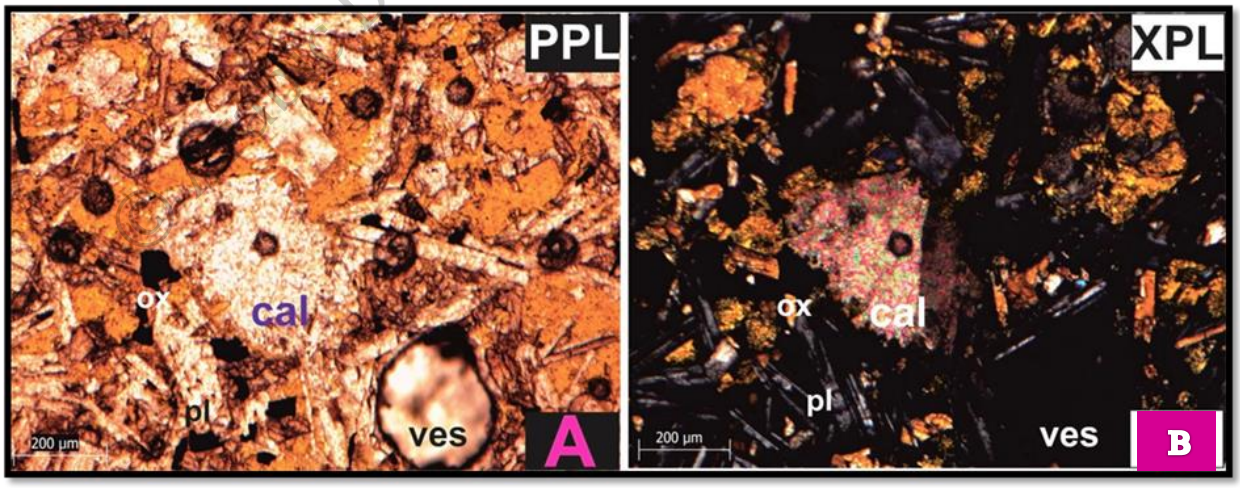

Figure (4.26): Thin sections of YRB. (a) Plane light photomicrograph of anhedral calcite crystals with felty elongated plagioclase in the groundmass surrounding it and (b) Crossed polarized photomicrograph of anhedral Microphenocryst of calcite crystal 10*10x magnitude.

www.manaraa.com

Table (4.11): Electron microprobe chemical analyses wt% and calculation formula Mol% components of calcite in YR sample**.**

Chemical analysis/ YRB sample		**Sample 5(001)**
Percentages of Oxides (wt %)	**SiO_2**	5.48
	TiO_2	1.16
	Al_2O_3	2.43
	Cr_2O_3	0.61
	Fe_2O_3	1.60
	MgO	4.27
	CaO	82.28
	Na_2O	1.22
	K_2O	0.45
Name of carbonate mineral		calcite

© Arabic Digital Library-Yarmouk University

www.manaraa.com

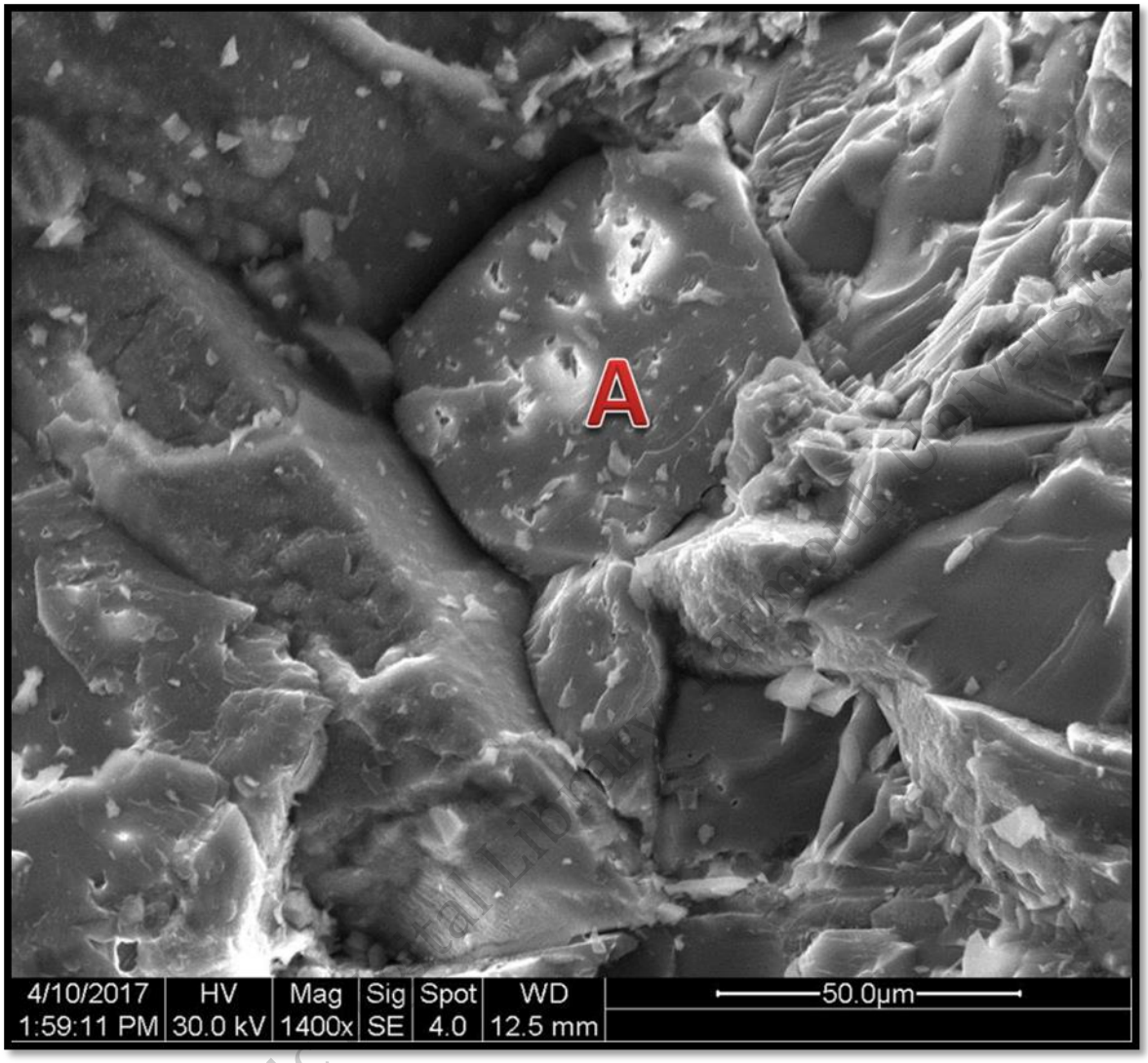

Figure (4.27): Electron micrograph image of rock fraction showing trigonal calcite crystal (Sample No. 5(001).

© Arabic Digital Library-Yarmouk

المنارة للاستشارات
www.manaraa.com

Table (4.12): Electron microprobe chemical analyses wt% and calculation formula Mol % components of barite in YR sample.

Chemical analysis/ YRB sample		**Sample Pahoehoe 001(A)**	**Sample Pahoehoe 004(B)**
Percentages of Oxides (wt %)	**SiO_2**	3.89	3.71
	SiO_4	32.37	36.32
	TiO_2	11.86	8.22
	Al_2O_3	1.32	2.79
	Cr_2O_3	0.24	0.85
	Fe_2O_3	2.10	1.79
	MnO	0.52	1.30
	MgO	1.17	1.93
	CaO	0.51	1.05
	BaO	43.87	38.31
	Na_2O	1.83	3.10
	K_2O	0.32	0.62
Name of sulfate mineral		Barite	Barite

© Arabic Digital Library Yarmouk University

www.manaraa.com

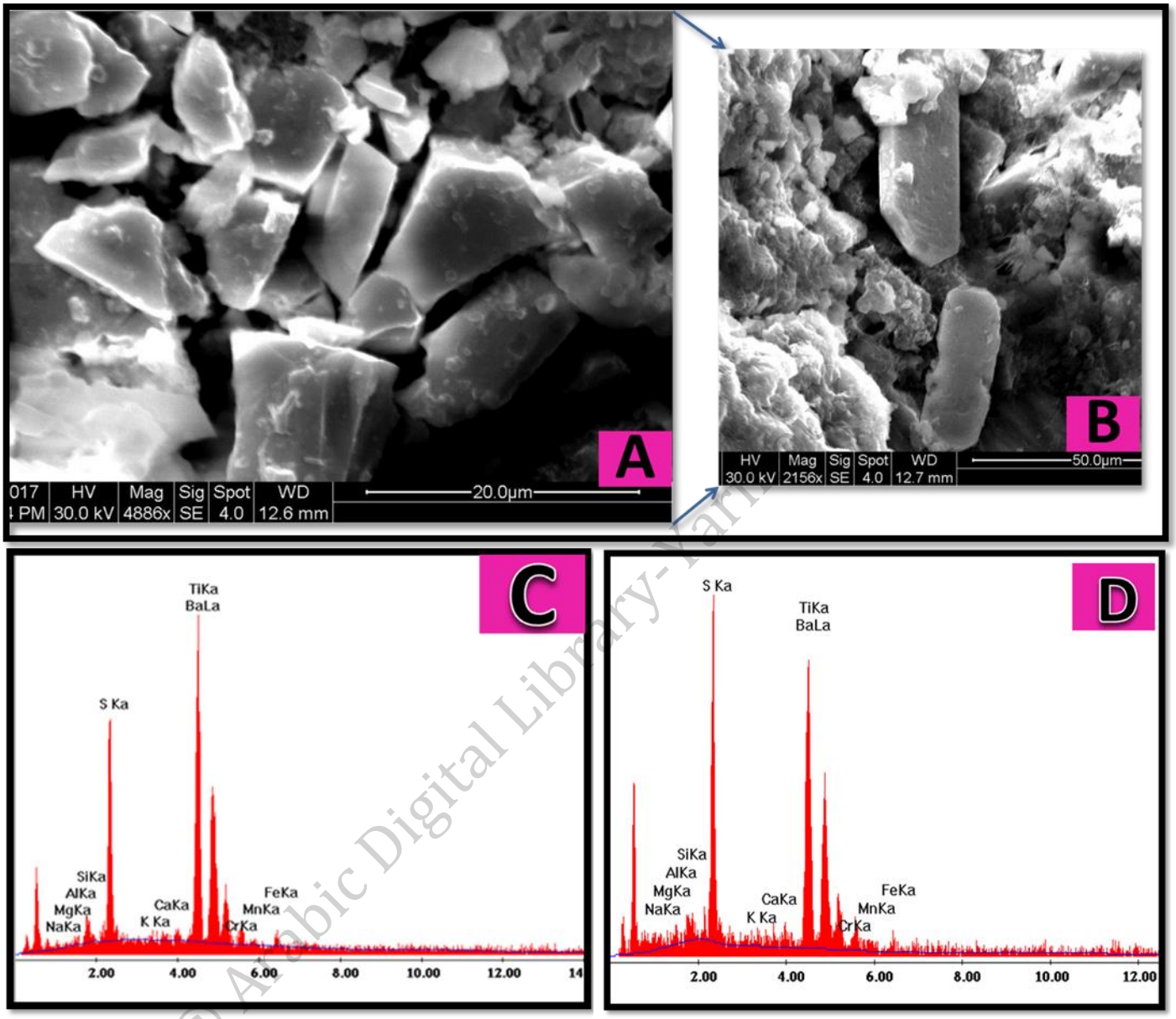

© Arabic Digital Library-Yarmouk

Figure (4.28): Electron micrograph images showing: (a, b) orthorhombic euhedral crystals of barite (SampleNo.Pahoehoe 001(A,B)); (c, d) Energy-dispersive X-ray results of barite samples**.**

المنارة للاستشارات
www.manaraa.com

4.9 Textural Description

Igneous rocks are recognized, described, named and classified on the base of structure, texture and composition or mineral and chemical composition). The texture is the physical character of the rock, including the size, shape, orientation, and distribution of grains and the inter grain relationships (Raymond, 2002). The texture of rock is a result of various processes that controlled the rock genesis and along with mineralogy and chemical composition provides the information that we used to interpret the rocks origin and history (winter, 2001).

4.9.1 Porphyritic texture

This texture produced when two –stage cooling can create bimodal distribution of grain sizes. Slow cooling produced large grains are termed phenocrysts at high depth (intrusive) followed by rapid cooling produced finegrains are termed matrix or groundmass near the surface depth (extrusive). The euhedral phenocrysts embedded in a finer-grained groundmass. Three type of this textures:

a. **Porphyritic - hyaline** (**vitrophyric**): Phenocrysts surrounded by glassy groundmass. Indicates an initial period of slow (intrusive) crystallization followed by quenching of the remaining magma.

b. **Porphyritic-aphanitic**. Phenocrysts surrounded by aphanitic groundmass. Indicates an initial period of slow (intrusive) crystallization followed by rapid

© Arabic Digital Library-Yarmouk University

www.manaraa.com

(extrusive) crystallization of the remaining magma. The most common texture for common volcanic rocks (i.e. basalts).

c. Porphyritic-phaneritic: Phenocrysts surrounded by phaneritic groundmass. Indicates two stages of slow crystallization, i.e. intrusion at two different levels.

Figure (4.29): Microscopic photo of basalt sample shows porpherytic, pilotaxitic and glomeroporphyritic texture of olivine phenocrysts and a groundmass of plagioclase, pyroxene and opaques (a) under ppl 10x magnitudes (b) under xpl 10x magnitude

4.9.2 Glomeroporphyritic texture

A term used to describe a porphyritic texture in which phenocrysts are clustered into aggregates called glomerocrysts or crystal clots (Figure 4.30) in a finer-grained matrix or groundmass.

© Arabic Digital Library-Yarmouk University

المنارة للاستشارات
www.manaraa.com

Glomeroporphyritic textures are common and often included plagioclase and pyroxenes in basic rocks. They form by processes known as synneusis, where accumulation of crystals occurs by surface tension and fixing by interpenetration due to crystal growth.

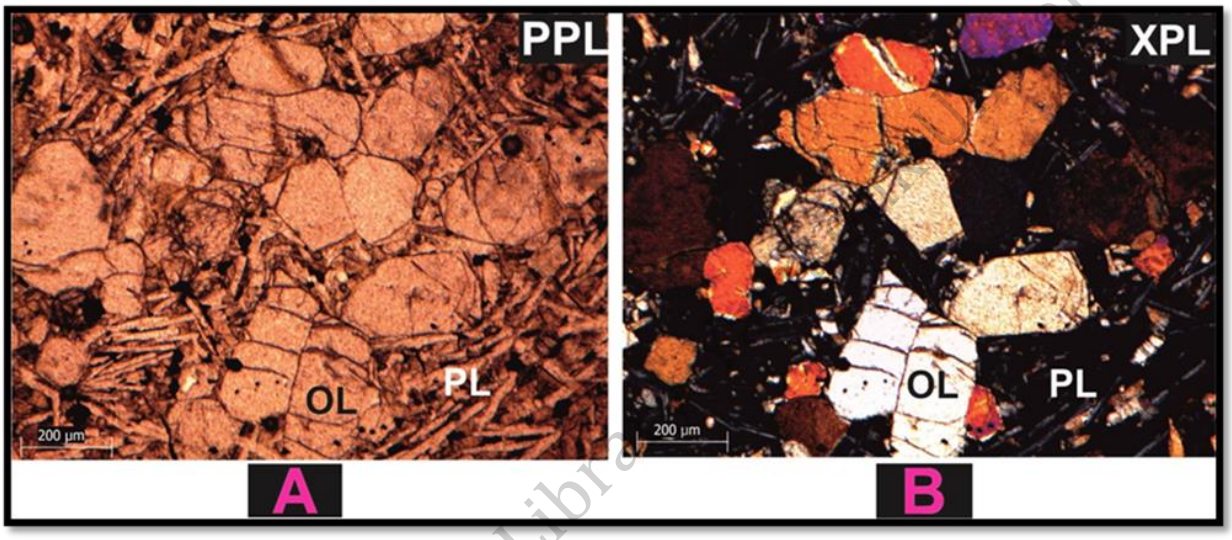

Figure (4.30): Photomicrograph images showing :(a) olivine grains are clustered into aggregates within plagioclase groundmass under PPL, (b) Same as (a) under XPL, 10x*10x magnification.

4.9.3 Amygdaloidal texture

Some smooth-walled vesicles may be filled with secondary minerals such as calcite, dolomite, barite and zeolite precipitated from fluid solutions percolating through the rock, producing amygdules and amygdaloidal texture (Figure 4.24 and Figure 4.25).

4.9.4 Intergranular texture

This term applied to an igneous texture, especially well developed in basalts, in which the wedge-shaped spaces between a meshwork of lath-

© Arabic Digital Library-Yarmouk University
المنارة للاستشارات
www.manaraa.com

shaped crystals, randomly oriented microlitic plagioclases (Figure 4.31) such as plagioclase, are filled with granules of other minerals.

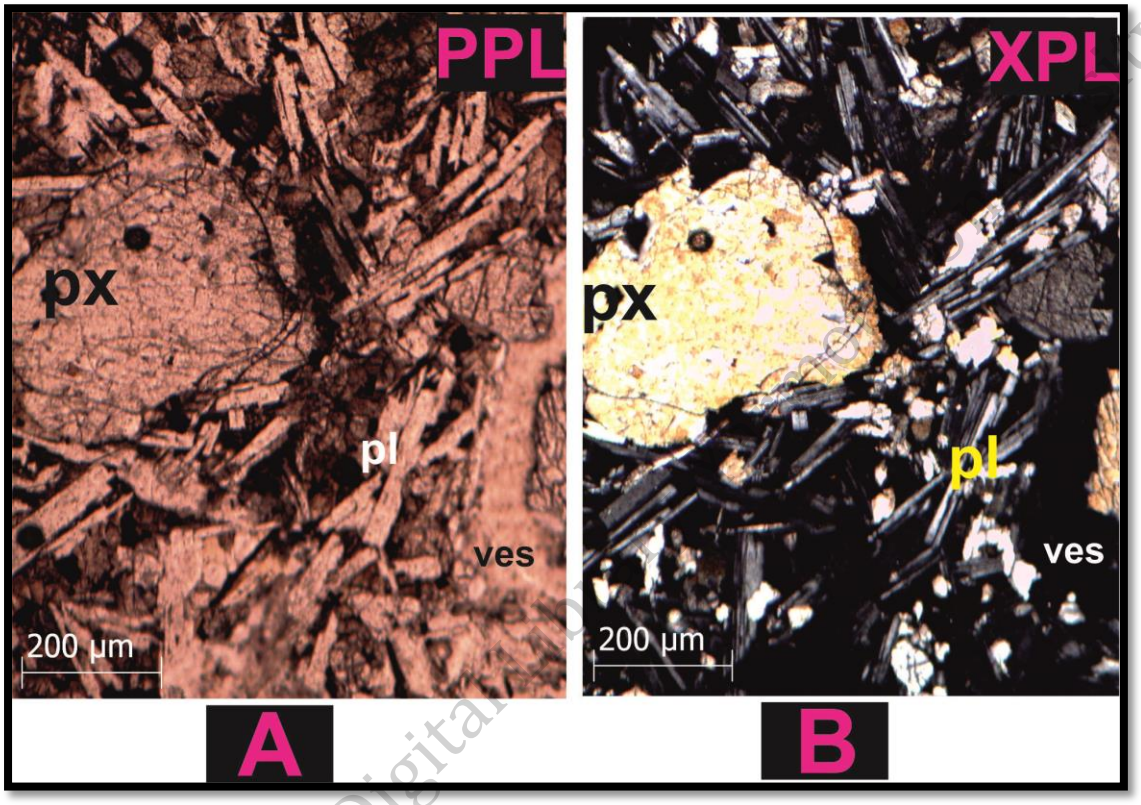

Figure (4.31): Photomicrographs of YR basalt showing intergranular textures of randomly lath crystal of plagioclase: (A) under XPL, 10x*10x magnification, (b) under XPL10x*10x magnification.

4.9.5 Pilotaxitic texture (felty texture)

Random orientation of fine elongate crystals in the groundmass of basalt. See (Figure 4.13, 4.17 and 4.29).

7.9.6 Trachytic texture

If feldspar microlites are oriented or aligned in a common direction due to the flow the texture is trachytic (Figure 4. 32).

© Arabic Digital University
المنارة للاستشارات
www.manaraa.com

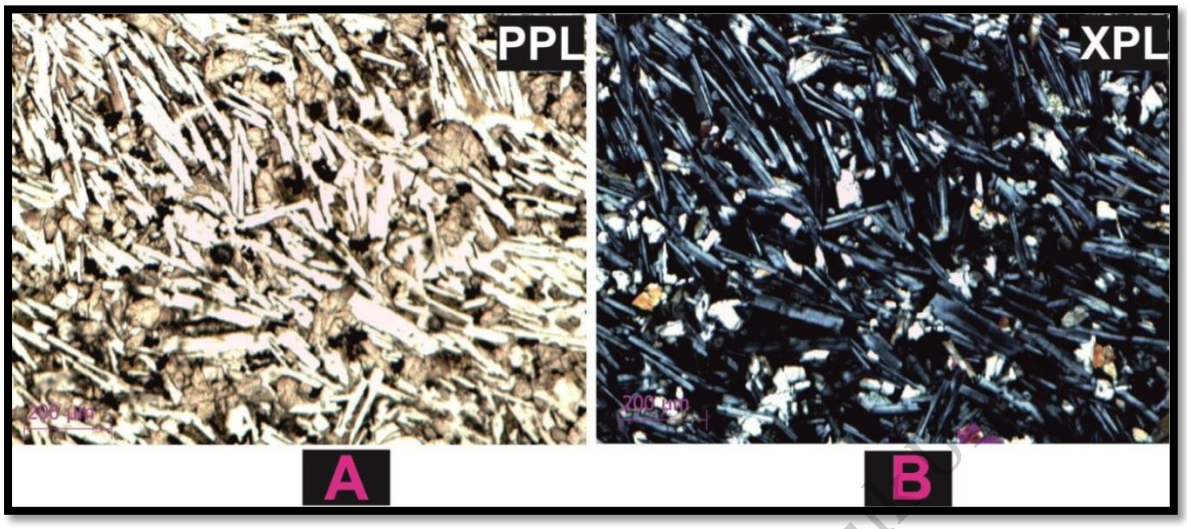

Figure (4.32): Photomicrograph images showing Trachytic texture :(a) plagioclase grains are aligned into same direction within under PPL, (b) under XPL, 10x*10x magnification.

4.9.7 Ophitic and Subophitic texture

These terms are describe magmatic texture in which large crystals of clinopyroxenes partially to completely enclose smaller, euhedral and randomly oriented crystals of plagioclases. The larger crystals form from fewer nuclei than the smaller enclosed mineral grains ophitic texture in rocks of basaltic composition (Figure 4.33).

© Arabic Digital Library-Yarmouk

www.manaraa.com

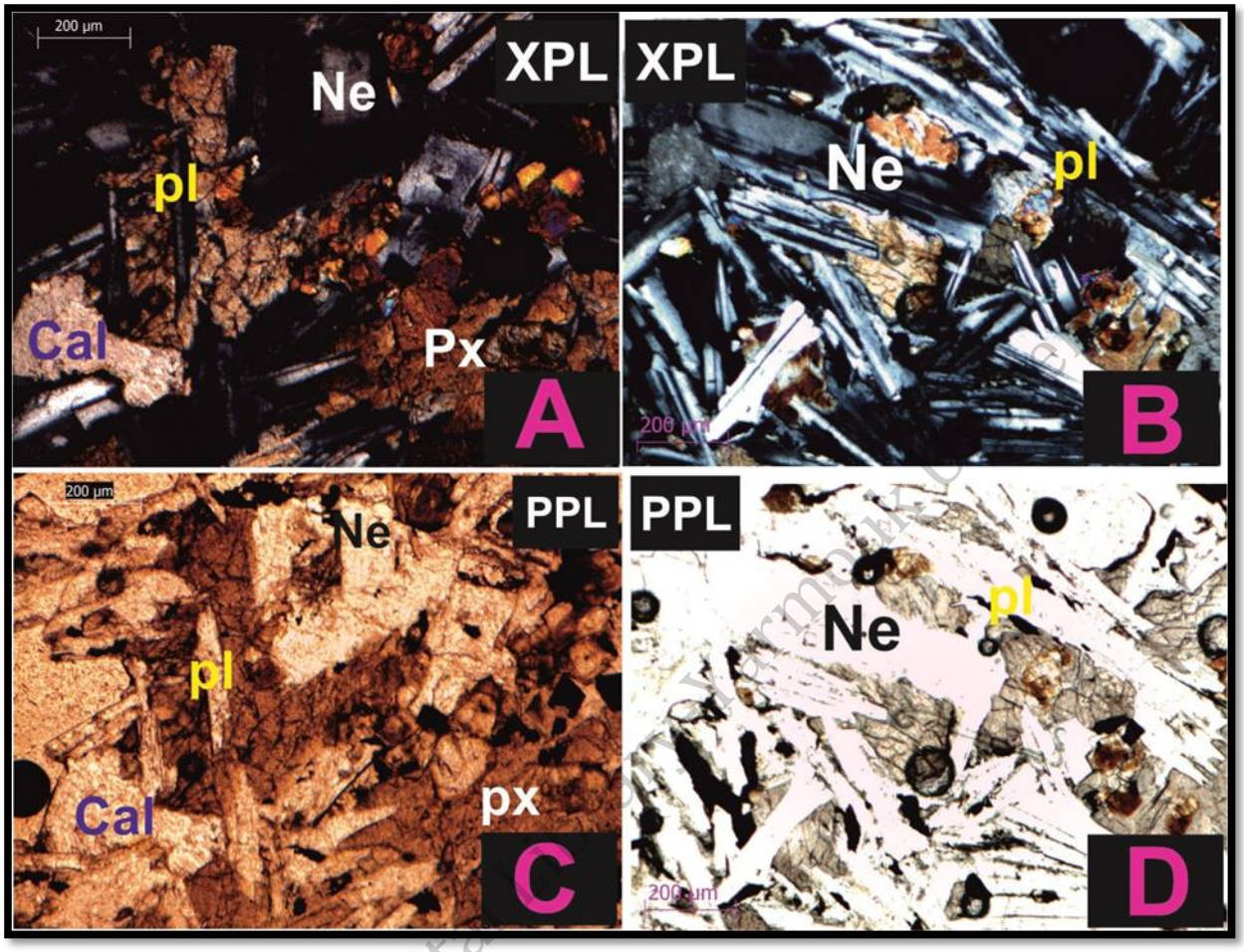

Figure(4.33): Microphotograph of Ophitic –supophitic texture in basalt euhedral multiply twinned plagioclase laths (grey interference colours) are enclosed by two augite oikocrysts with fi rst - order orange interference colours, under ppl 10x magnitude (c,d) under xpl 10x magnitude.

4.9.8 Seriate texture

Phaneritic, inequigranular magmatic texture in which grains range more or less continuously in size; contrast bimodal size distribution in porphyritic texture (Figure 4.34).

© Arabic Digital Library-Yarmouk University
المنارة للاستشارات
www.manaraa.com

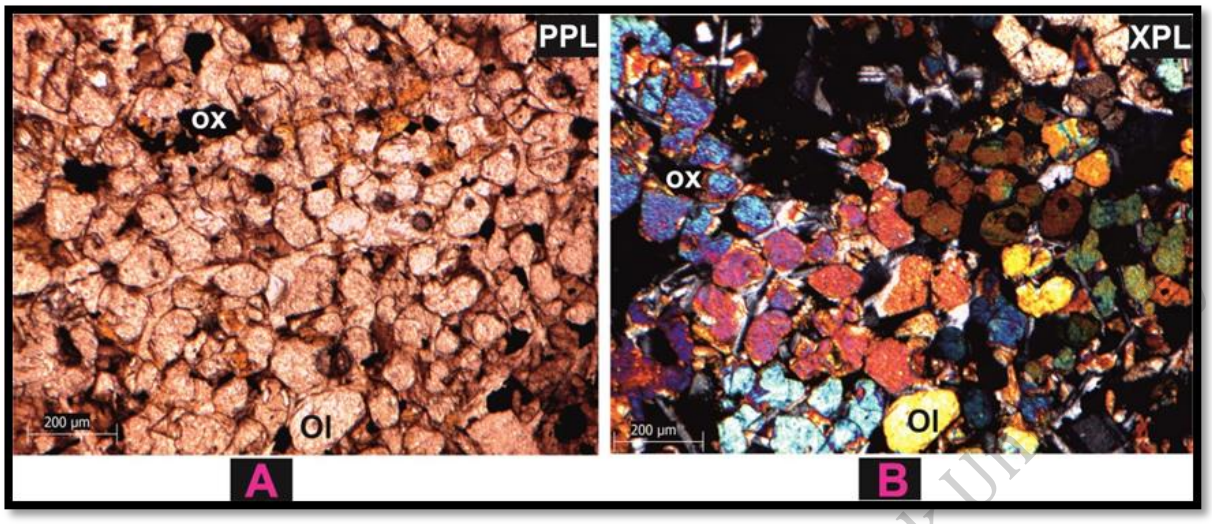

Figure (4.34): Microphotograph showing seriate and glomeroporphyritic texture in basalt sample grains range more or less continuously in size, (a) under ppl 10 x magnitudes (b) under xpl 10 x magnitudes.

4.9.9 Radiate texture

Needle-like crystals that radiate from a central point e.g. radial arrangement of plagioclase crystals diverging outward from a common centre (Figure 4.35).

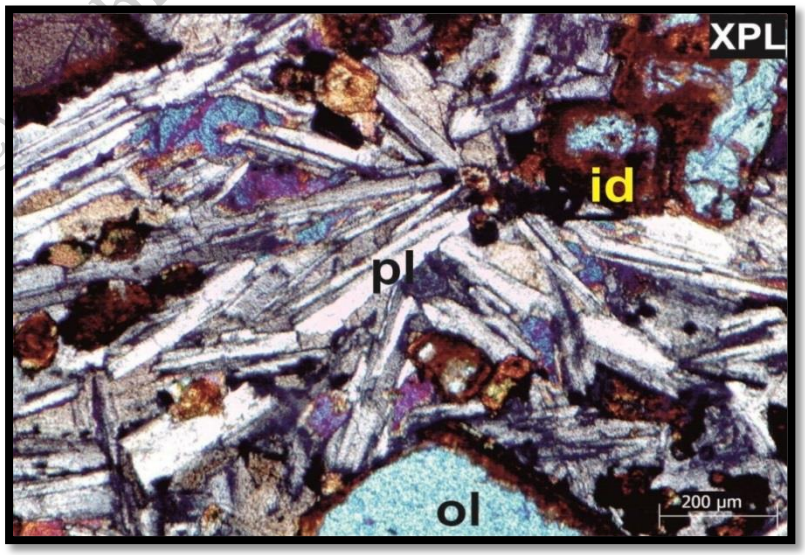

Figure (4.35): Microphotograph showing radiate texture in basalt sample under xpl 10 x magnitudes.

© Arabic Digital Library Yarmouk University

المنارة للاستشارات
www.manaraa.com

4.9.10 Vesicular texture

It is the most abundance texture appears in YR samples especially in flow four. This term refers to vesicles (cavities) within the igneous rock. Vesicles are the result of gas expansion (bubbles), which often occurs during volcanic eruptions. Pumice and scoria are common types of vesicular rocks. Volatile-fluid bubbles become vesicles as magma solidifies, see (Figure 4.23).

.

© Arabic Digital Library-Yarmouk University

المنارة للاستشارات
www.manaraa.com

Chapter Five

Geochemistry

5

© Arabic Digital Library-Yarmouk University

المنارة للاستشارات
www.manaraa.com

Chapter Five

Geochemistry

5.1introduction

After thin sections preparations finished for each sample for petrographic investigations. The geochemical preparation gets started in this chapter and representative fresh samples were selected from the massive parts of the flows for geochemical studies. Selected rocks were crushed using a tungsten carbide jaw crusher and the cleanest chips were hand-picked for fine crushing. These chips were then transferred to a tungsten carbide mill and ground to a fine powder for XRF analyses. Geochemists have determined the geologic, magmatic and/or tectonic affinities of igneous Rocks for decades to do this. X-ray fluorescence (XRF) analyses were carried out in Ministry of Energy and Mineral Resources (MEMR). XRF used for analysis of major and some trace elements (Ba, B, Nb, Pb, Sn, Sr, P, Zn, Zr, La, Li, Y, Cu, Mo, Cr, Co, Ce, V, Cu, Ni, and Be.) in YR samples. Other trace elements can be defined by using Inductive coupled plasma (ICP). In CIPW-norms were calculated for each sample.

Accordingly data were compiled and analyzed using Microsoft Excel, and Petrographic software to classify the rocks of the study area.

5.2 Major Elements Analysis

Major and minor elements are the main chemical constituents of magmas. Major minerals are present in high concentrations > 1.0 wt. %, miner elements

© Arabic Digital Library-Yarmouk University

المنارة للاستشارات
www.manaraa.com

0.1-1.0 wt.% and trace element are those <0.1 wt.%. The concentrations, of major oxides are expressed as weight percentage (wt. %) (SiO_2, TiO_2, Al_2O_3, Fe_2O_3, MnO, MgO, CaO, Na_2O, K_2O, and P_2O_5), are variable and range from a fraction of percent to some tens of percent's and trace elements are in ppm (Table 5.1), The basalts of the YR area represent broadly ultrabasic to basic rock in the Compositional range with their mean average value (46.3-47.7 % SiO_2, 1.81-2.74 % TiO_2, 13.3-14 % Al_2O_3, 11.7- 12.5 % Fe_2O_3, 0.16-0.18 % MnO, 8.4-10.6 % MgO, 8.56-10.7 % CaO, 2.19-2.94 % Na_2O, 0.59-1.37 % K_2O, 0.24-0.98 % P_2O_5 shown in (Figure 5.1) and (Table 5.2).

Table (5.1): Analytical data of the concentrations of major oxides are expressed as weight percentage wt. % of YRB samples.

S.ID.	**R1**	**R4**	**R6**	**Phase2-1**	**Phase2-4**	**Phase3**	**Phse4-3**
wt. %							
SiO_2	47.5	46.3	47.7	46.3	46.5	46.6	47.3
TiO_2	1.89	2.40	1.81	2.30	2.35	2.74	1.85
Al_2O_3	13.50	13.70	14.00	13.30	13.50	13.50	13.80
Fe_2O_3(t)	12.4	12	12	12.1	12.2	11.7	12.5
MnO	0.18	0.17	0.17	0.17	0.18	0.16	0.18
MgO	10.6	9.32	9.41	9.75	10.1	8.4	8.92
CaO	8.56	9.93	10.70	10.50	10.20	9.93	9.99
Na_2O	2.48	2.33	2.78	2.19	2.36	2.67	2.94
K_2O	0.65	1.08	0.65	0.65	0.59	1.37	0.68
P_2O_5	0.26	0.26	0.24	0.42	0.44	0.98	0.24
LOI	1.60	1.70	0.60	2.10	1.40	1.90	1.20
Total	99.62	99.56	100.06	99.78	99.82	99.95	99.6
Mg#	62.9	60.6	60.8	61.5	62.1	58.7	58.6

© Arabic Digital Library Yarmouk University

المنارة للاستشارات
www.manaraa.com

Table (5.2): Maximum, minimum, and mean average values of major oxide of the analyzed basalt samples from YR area

Oxides (wt %)	Minimum	Maximum	Mean average value
SiO_2	46.3	47.7	46.9
TiO_2	1.81	2.74	2.2
Al_2O_3	13.3	14	13.6
$(Fe_2O_3)_t$	11.7	12.5	12.1
MnO	0.16	0.18	0.17
MgO	8.4	10.6	9.5
CaO	8.56	10.7	9.97
Na_2O	2.19	2.94	2.54
K_2O	0.59	1.37	0.8
P_2O_5	0.24	0.98	0.5
LOI	0.6	2.1	1.5

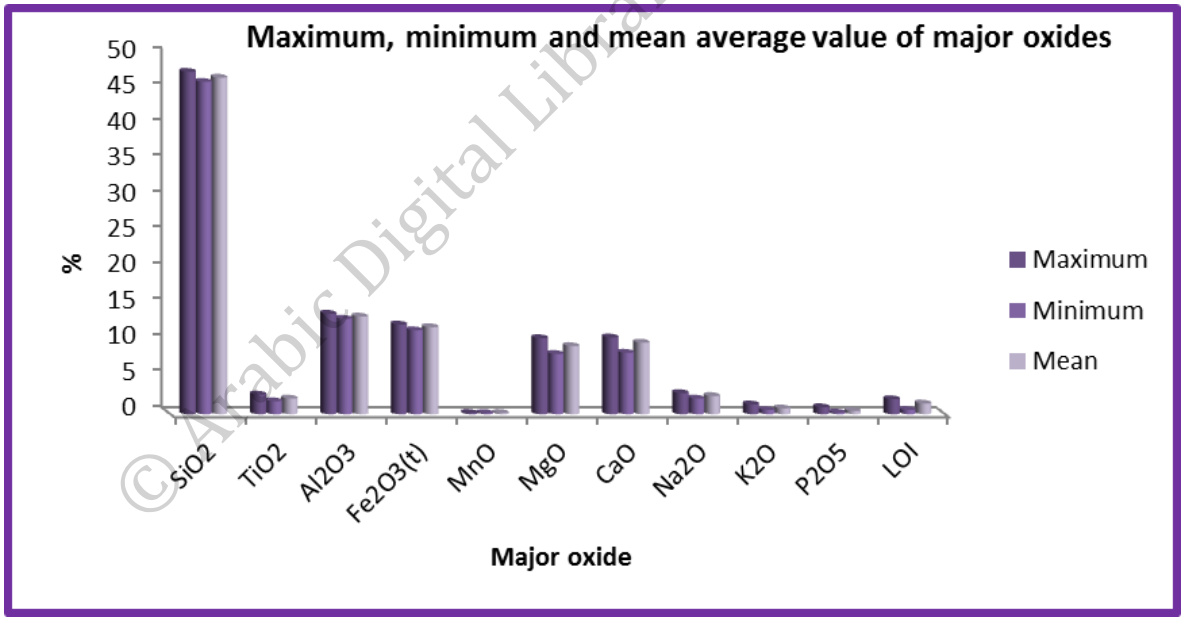

Figure (5.1): Bar Chart showing maximum, minimum and the calculated mean average values of Silicon dioxide and other oxide of the analyzed seven basalt samples from YRB area.

It's critically important to display geochemical data (major and trace elements) in a fashion that allows you to recognize trend in the variation to

© Arabic Digital Library-Yarmouk University

المنارة للاستشارات
www.manaraa.com

describe and interpret the processes responsible. The objects to find parameters that show you systematic variation is variation diagrams. There are two common formats for variation diagrams of chemical data in the first, the bivariate diagram (Cartesian, or x-y) plot: Two parameters are plotted one vertically called the ordinate, or y-axis) and one horizontally (called the abscissa, or the x-axis). In the second triangular diagram, we represent three parameters, one at each corner, but show only relative proportions, not absolute quantities, because three parameters must be normalized to sum 100%. These diagrams were applied to help in the classification, nomenclature and interpretation of the tectonic setting of Yarmouk River such as Harker diagram (Figure 5.2).

© Arabic Digital Library Yarmouk University

www.manaraa.com

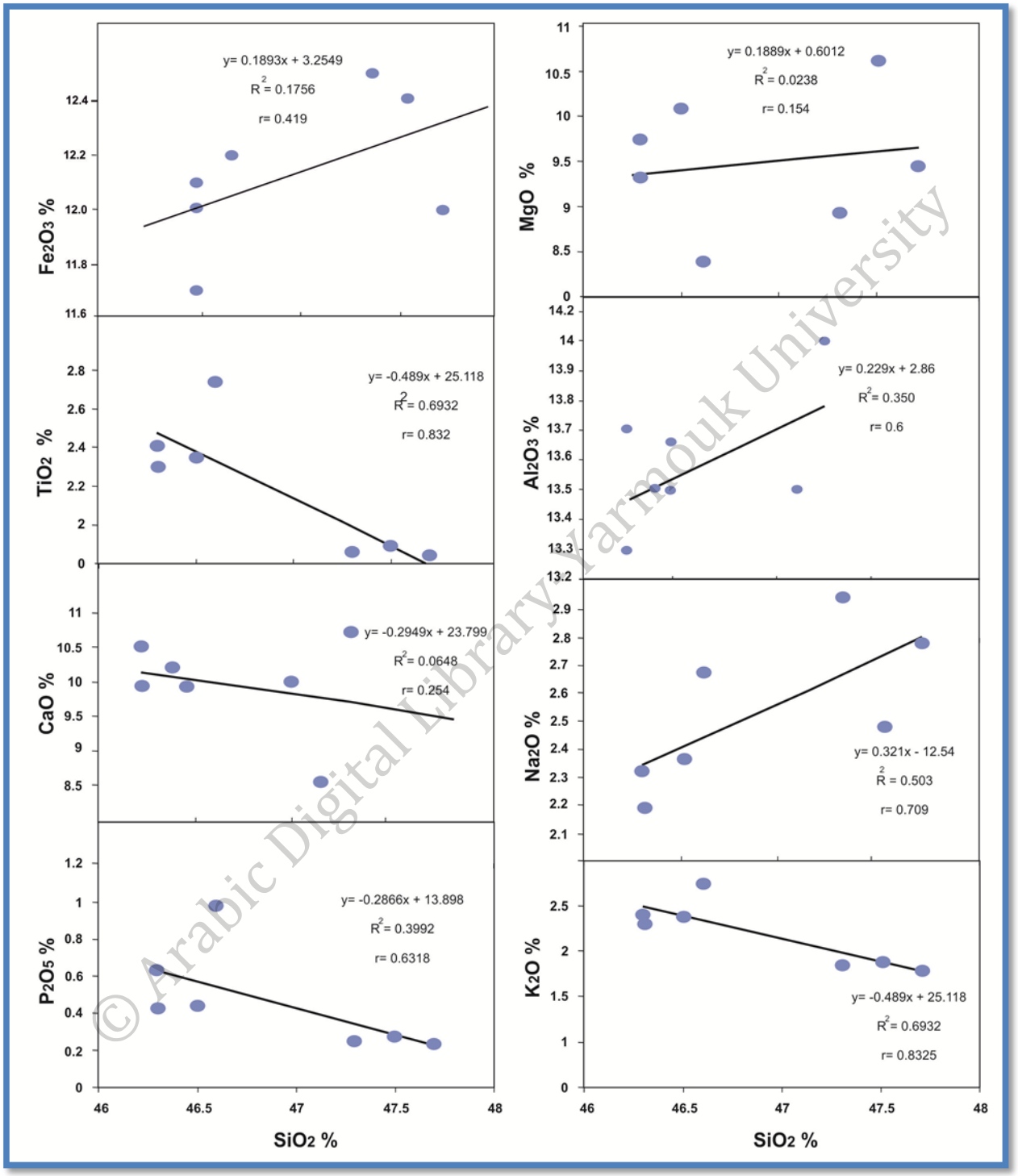

© Arabic Digital Library Yarmouk University

Figure (5.2): Harker variation diagrams for YRB samples. All the major oxides are characterized by their unique trend as SiO2 progress from 46.3-47.7 wt%.

المنارة للاستشارات
www.manaraa.com

5.2.1 Silicon dioxide (SiO_2)

(SiO_2) is the principal oxide constituent of basaltic rocks and serves as a basis for broadly defined classifications. The studied basaltic rocks show low span of silica contents. Its content of silicon dioxide ranges from 46.3 to 47.7 wt. % for all YRB with an average mean value of 46.88 wt. %. The low silica concentration of the studied rocks reflects their alkali character. Their SiO_2 ranges suggest that they are of basic to ultrabasic type (Best, 2003).

5.2.2 Magnesium oxide (MgO), Aluminium oxide (Al_2O_3) and Iron Oxide (Fe_2O_3)

The values of the studied magnesium oxide and Aluminium oxide (Al_2O_3) samples range from 8.4% to 10.6% with an average mean value of 9.5 % for MgO and 13.3% to 14% with a mean average of 13.61%, for Al_2O_3. According to magnesium and Aluminium oxide values the coefficient of determination (R^2) and the correlation coefficient r of MgO values, show weak positive linear relationship with Silicon dioxide in the studied basalt samples. The Mg number (Mg≠), defined as the molecular proportion of Mg^{2+}/ (Mg^{2+} + Fe^{2+}) (J;e nner et al. 1987), is usually used as a petrogenetic indicator for magma fractionation and its primitive volcanic rocks The YRB samples exhibited a high Mg≠, ranging between 58.6 and 61.9, with an average of 61.1. The Mg≠ calculation considers the Fe content in the rocks. It has been reported that values of Mg≠ > 7 can be considered as a threshold that characterizes primitive magmas, (Wilson, 1989). The Fe content of the YRB samples ranged between 7.36 wt%

© Arabic Digital Library-Yarmouk University

المنارة للاستشارات
www.manaraa.com

and 15.42 wt%, with an average of 12.93 wt%, indicating that the rocks were enriched in Fe.

Moderate (positive) linear relationship of Al_2O_3 value. Content generally increases as aluminum content decreases. Positive correlation between MgO and SiO_2 due to low degree of fractional crystallization temperature of olivine. The iron oxide content in the investigated rocks samples is high and ranges from 11.7% to 12.5 % with an average mean value of 12.3 %. The coefficient of determination (R^2) and the correlation coefficient r of iron Oxide values indicate weak (positive) linear relationship with Silicon dioxide in the studied basalt samples. The samples have a relatively high $(Fe_2O_3)_t$ content, which may indicate small degrees of melting at high pressure.

The sodium oxide (Na_2O) content ranges from 2.19% to 2.94% with a mean average value of 2.54%. The coefficient of determination (R^2) and the correlation coefficient r of sodium oxide values show moderate (positive) linear relationship with Silicon dioxide in the studied basalt samples.

5.2.3 Calcium Oxide (CaO), Diphosphorus pentaoxide (P_2O_5), Titanium dioxide (TiO_2) and Potassium oxide (K_2O)

CaO, P_2O_5 as well as K_2O and TiO_2 values show a general decrease with increasing SiO_2. calcium oxide samples varies from 8.56 % to 10.7 % with an average mean value of 9.97 %.The calcium oxide values show weak negative correlations with the silicon dioxide in the studied basalt samples. The values of the studied samples of titanium dioxide ranges from 1.81% to 2.74% with an

© Arabic Digital Library Yarmouk University

www.manaraa.com

average mean value of 2.19 %. The coefficient of determination (R^2) and the correlation coefficient r of titanium dioxide values show moderate (negative) linear relationship with Silicon dioxide. potassium oxide content value range from 0.59% to 1.37% with a mean average value of 0.81%. The coefficient of determination (R^2) and the correlation coefficient r of potassium oxide values show moderate (negative) linear relationship with Silicon dioxide in the studied basalt samples.

Diphosphorus pentaoxide content value range from 0.24 % to 0.98 % with a mean average value of 0.46 %. The coefficient of determination (R^2) and the correlation coefficient r of diphosphorus pentaoxide values show moderate (negative) linear relationship with Silicon dioxide in the studied basalt samples.

The decrease in CaO as SiO_2 increases is consistent with the removal of early-forming plagioclase and/or pyroxene from the cooling magma. The apparent constant to weekly negative correlation of Na_2O and K_2O with SiO_2 indicate the sodic affinity.

A general decrease with increasing SiO_2, as well as alkalies and TiO_2 values show little correlation. TiO_2 content varies from 1.89 to 2.52 wt%. All basaltic rocks have <48 wt% SiO_2 contents and high $Na_2O + K_2O$ (~3 – 5.3 wt %) contents. The samples have a relatively high FeO content, which may indicate small degrees of melting at high pressure (Wilson, 1989).

5.3 Inductive Coupled Plasma (ICP) analysis results.

© Arabic Digital Library Yarmouk University

المنارة للاستشارات
www.manaraa.com

Trace elements are those which occur in very low concentrations in volcanic rocks (usually < 0.1 % by weight). Their concentrations are therefore commonly expressed in parts per million (ppm; 1 ppm = 10^{-4} weight %). Unlike major elements, trace elements tend to concentrate in fewer minerals, and are therefore more useful in formulating models for magmatic differentiation, and partial melting, in some cases, in predicting the source of a particular magma. So we use for this purpose Inductive Couple Plasma (ICP) technique to get result. The occurrence of any trace element during the crystallization process is governed by the ionic radius, valency and ionic potential. According to their distribution coefficient (KD) trace elements are classified into two varieties: Compatible (KD>1) and incompatible (KD<1). Some elements behave as compatible and incompatible, e.g. Sr. These are some of trace elements: V, Ni, Cr, Co, Zn, Cu, Li, Rb, Ba, Sr, Ga, Zr, Nb, Hf, and Y listed in (Table 5.3). The presentation of the maximum, minimum and average values are given in (Table 5.4) (Figure 5.3).

© Arabic Digital Library Yarmouk University

www.manaraa.com

Table (5.3): Geochemical investigative results of trace elements of YRB samples

Sample ID	Phase 2 - 1	Phase 2 -4	Phase 3 a′a	Phase3-blocky pahoehoe	Phase 4
V	364	360	340	318	347
Cr	288	274	305	229	317
Ni	237	251	272	202	306
Co	116	81	86	78	82
Zn	124	128	135	146	124
Cu	71	63	70	59	55
Li	5	5	10	8	7
Sr	862	1370	703	1800	444
Ga	1073	1114	1197	1305	908
Ba	328	355	286	773	358
Nb	100	73	85	89	71
Zr	165	169	150	211	115
Hf	ND	ND	4	ND	ND
Y	28	32	31	32	27
La	34	30	36	58	18
Sm	934	1051	987	872	916
Sc	17	17	19	11	17

© Arabic Digital Library-Yarmouk University

المنارة للاستشارات
www.manaraa.com

Table (5.4): Maximum, minimum, and mean average values of trace elements of the YRB

Sample ID.	V	Cr	Ni	Co	Zn	Cu	Li	Sr	
Maximum	364	317	306	116	146	71	10	1800	
Minimum	318	229	202	78	124	55	5	444	
Average	345.8	282.6	253.6	88.6	131.4	63.6	7	1035.8	
Sample ID.	**Ga**	**Ba**	**Nb**	**Zr**	**Hf**	**Y**	**La**	**Sm**	**Sc**
Maximum	1305	773	100	211	4	32	58	1051	19
Minimum	908	286	71	115	4	27	18	872	11
Average	1119.4	420	83.6	162	4	30	35.2	952	16.2

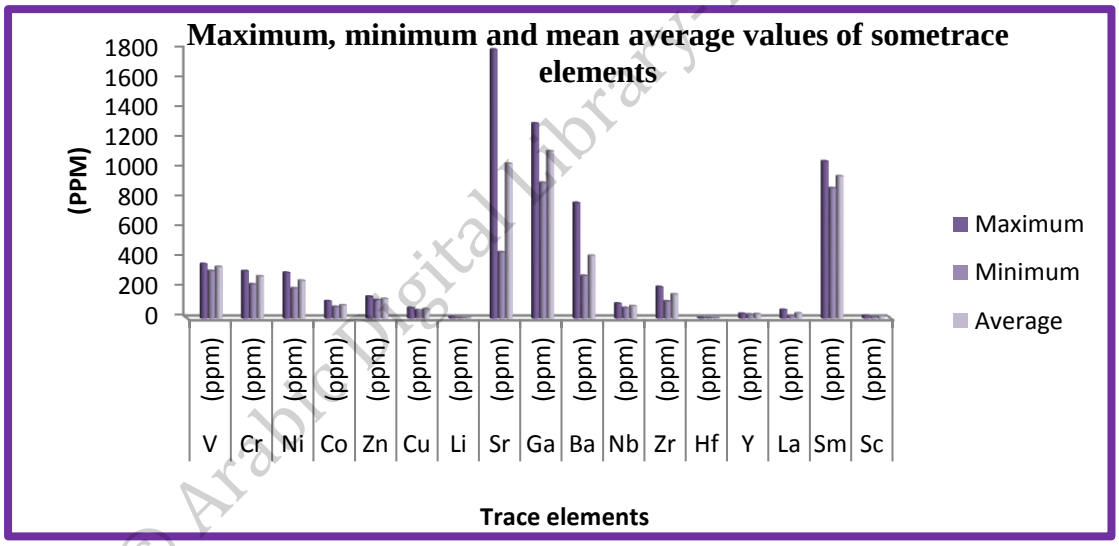

Figure (5.3): Representation of maximum, minimum, and average values of trace elements in samples of YRB.

5.3.1. Compatible elements (KD>1): Ferromagnesian elements (Ni, Cr, Co, Cu, and Li)

5.3.1.1 Transition Elements Abundance (TEA):

© Arabic Digital Library-Yarmouk University

www.manaraa.com

These elements are preferentially partitioned in crystals than in the coexisting melts. They are strongly partitioned into ultra-basic and basic rocks. . Upper mantle rocks are rich in olivine and pyroxenes and the elements, Cr, Co and Ni are compatible (enriched) in these phases relative to a silicate melt.

Cr^{3+}, $Ni^{2+}$and $Co^{2+}$are the most important ferromagnesian elements. In the studied rocks these elements are characterized by their high concentration, Cr content varies from 229 to 317ppm, and averages282.6.these averages exceed the average of 135ppm reported for Red Sea alkali basalt (Gass et al., 1973) and 300 ppm for alkali basalt from Aden reported by (Cox et al., 1970). On correlation diagram (Figure 5.4), Cr is negatively correlates with MgO. The average Cr content in the studied samples is lower that the published average of 347 ppm reported for alkali basalt in central Jordan by (Saffarinii *et al.*, 1987).

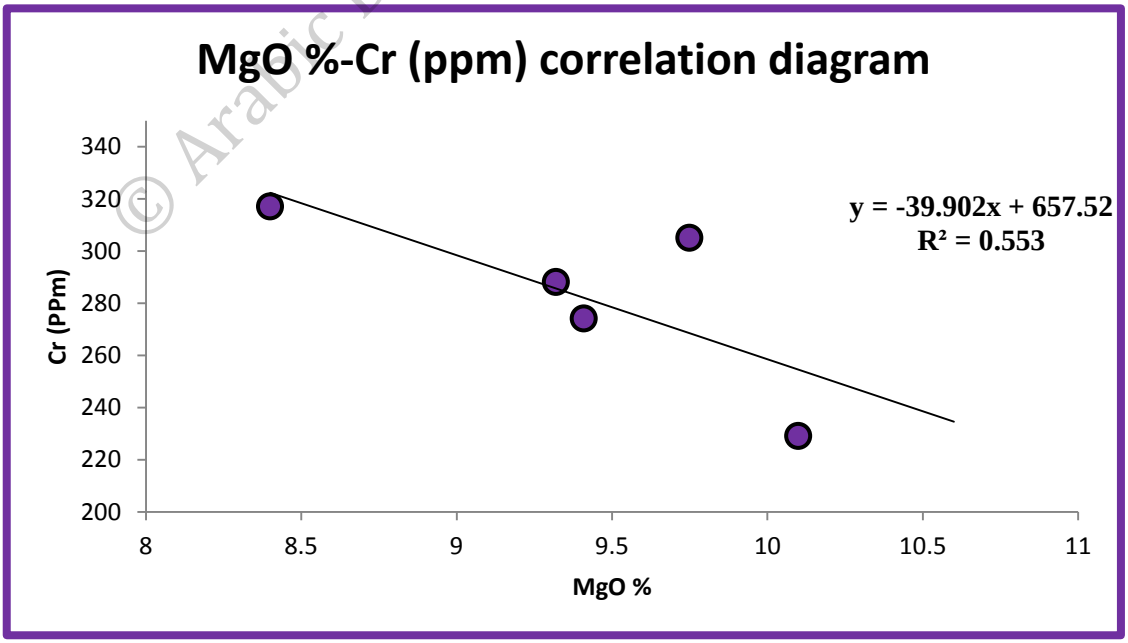

Figure (5.4): MgO% - Cr (ppm) Correlation diagram.

© Arabic Digital Library-Yarmouk University

www.manaraa.com

Nickel (Ni) content ranges between 202 and 306ppm, and averages 253.6ppm These average is higher than those for basalts of Al-Madina (101.6 ppm) reported by Camp and Robool, (1989).the average Ni content in the studied rock lies in the range of basanite (250-350) reported by (Sun&Hanson,1976). However, Nickel content show a moderate negative correlation with MgO and decreases sympathetically with MgO% is sample from all studied basalts (Figure 5.5). Moreover, Cr and Ni are positively correlated to each other (Figure 5.6), which reflects that they are petrogenetically related.

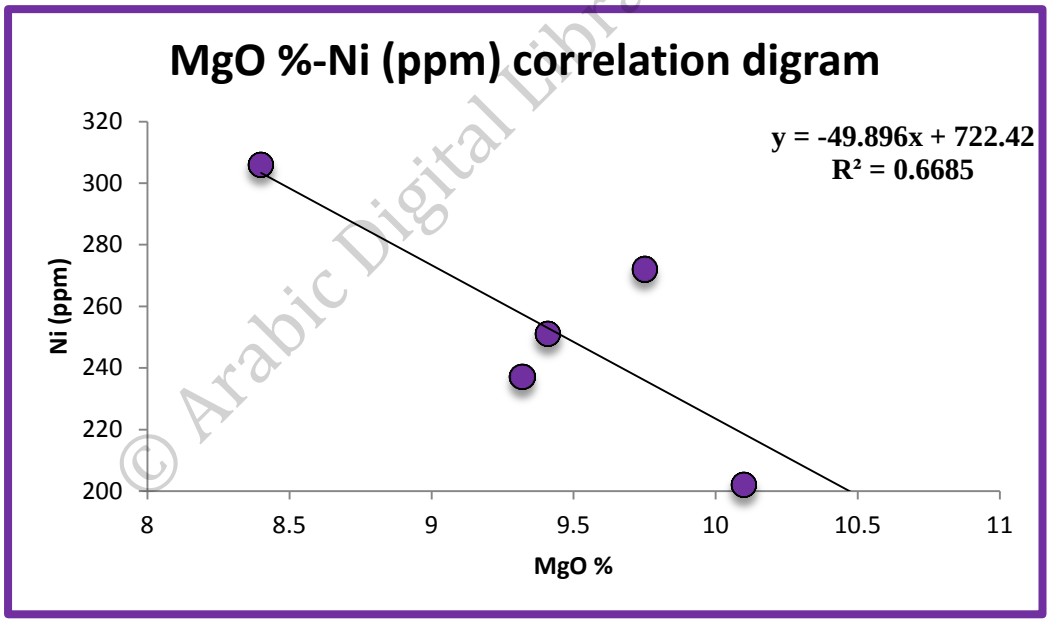

Figure (5.5): MgO% - Ni (ppm) Correlation diagram.

© Arabic Digital Library-Yarmouk University

www.manaraa.com

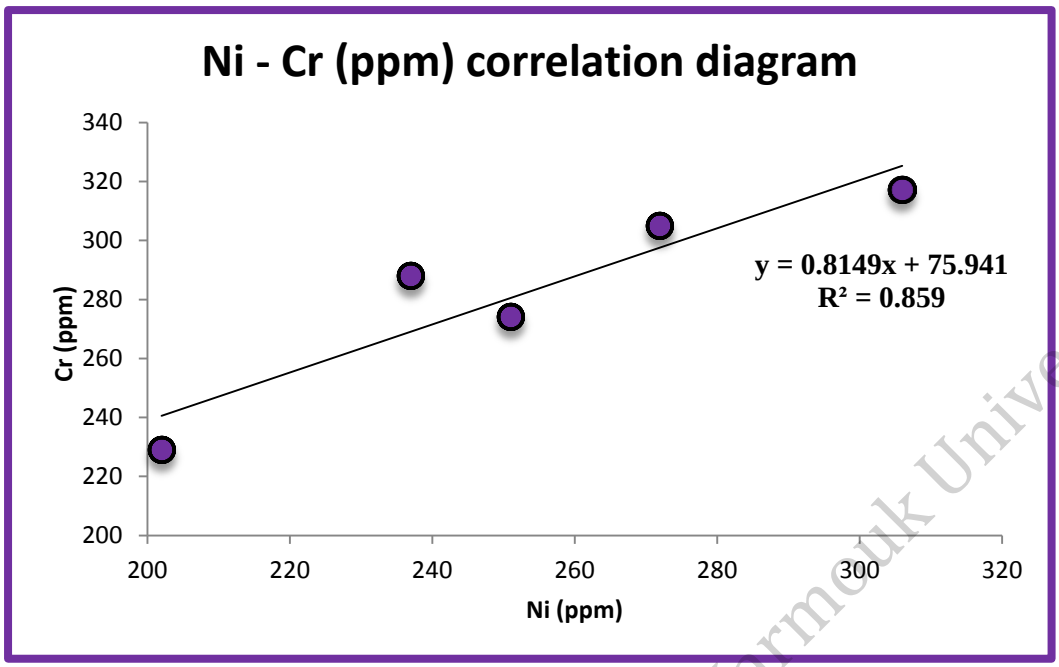

Figure (5.6): Ni –Cr (ppm) Correlation diagram.

Cobalt (Co) in the studied samples lies between 78ppm and 116ppm with an average of 88.6 ppm. The Co averages in the studied rocks are slightly higher than the average of 63 ppm for alkali basalt from NE-Jordan (Barberi et al., 1980).the samples are generally enriched in cobalt. This reflects that they didn't undergo high differentiation and reflect primitive nature of the rock. The Cr, Ni and Co contents may also indicate the derivation of the parental magma by partial melting of a peridotite mantle source (Wilson, 1989). Co is negatively correlates with MgO (Figure 5.7).

© Arabic Digital Library-Yarmouk University

المنارة للاستشارات
www.manaraa.com

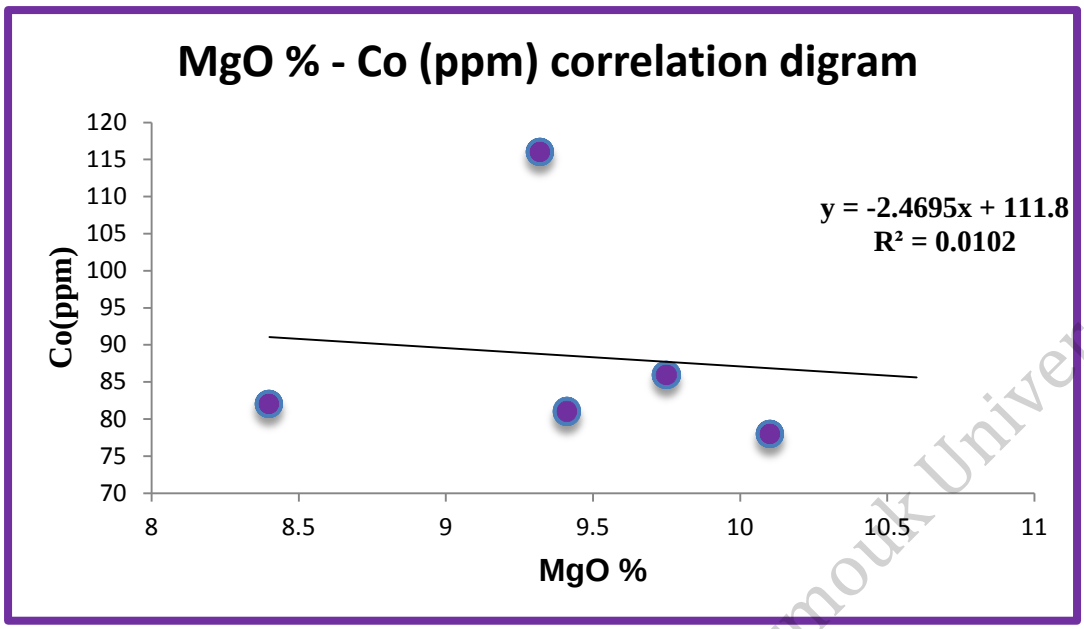

Figure (5.7): MgO% - Co (ppm) Correlation diagram.

5.3.1.2 Chalcophile Elements Abundance (CEA)

These elements are also compatible trace elements that rapidly substitute Fe^{2+} and Mg^{2+}, in early crystalized mafic minerals. For that they are reasonably classified as ferro-magnesian elements. These elements are: Cu, Zn, and Li. The highly concentrations of these elements may attribute to hydrothermal or lateral crystallization.

The distribution of Vanadium content in the studied rocks has an average of 345.8 ppm, and content range of 318 to 364 ppm. This average is higher than the published average of 230 ppm reported for alkali olivine basalt of Cenozoic Calatrara volcanic Spain. V show weak negative correlation and decreases sympathetically with MgO % is sample from all studied basalts (Figure 5.8).

© Arabic Digital Library Yarmouk University

www.manaraa.com

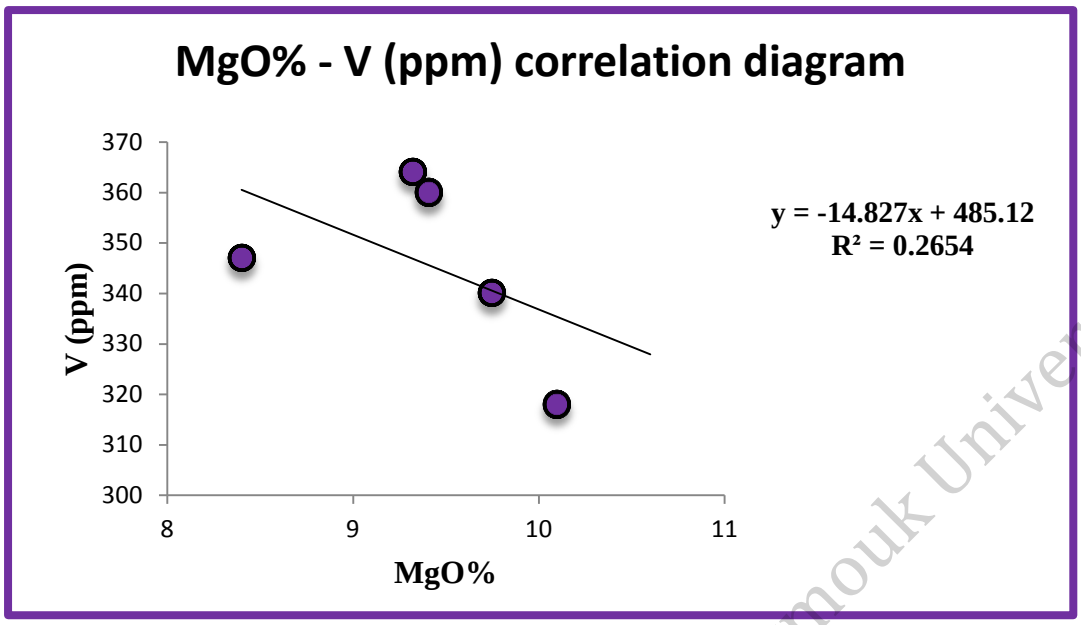

Figure (5.8): MgO % - V (ppm) Correlation diagram.

© Arabic Digital Library Yarmouk University

The Cu contents a range from 55 to 71 ppm, except with an average of 63.6 ppm. This average is lower than the average of 69 ppm reported for Alkali basalt from Harrat Madina in Saudi Arabia (Camp and Roobol, 1989).and 66 ppm reported for alkali basalt from Aden (COX et al., 1970) A weak positive correlation of Cu with MgO is detected in YR samples (Figure 5. 9).

In the samples from the studied rock, the average Zinc content is 131.4 ppm, and ranges from 124 ppm to 146 ppm. These averages exceed the Zn average of 40 ppm for alkali olivine basalt from Romania (Downes, 1995) and resemble the average of 101.25 ppm, for Spain basaltand similar to the average of 112 ppm for alkali olivine basalt, given by Wedepohl (1987). Zn is positively correlated with MgO and negatively correlated with Cu for all samples, (Figure 5.10 and 5.11).

المنارة للاستشارات
www.manaraa.com

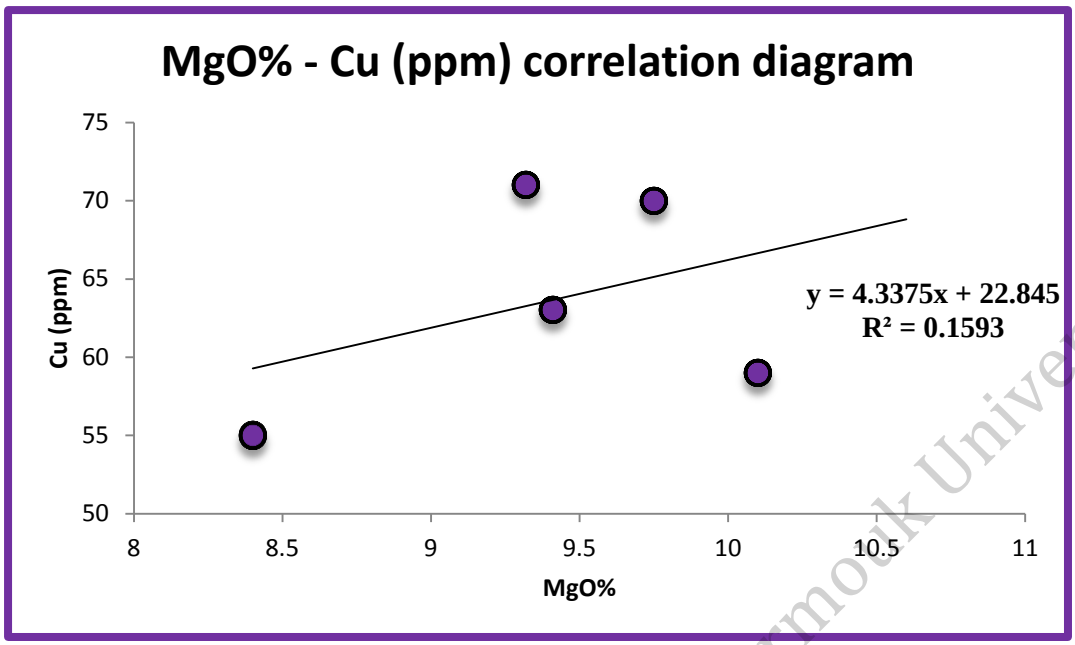

Figure (5.9): MgO% - Cu (ppm) Correlation diagram.

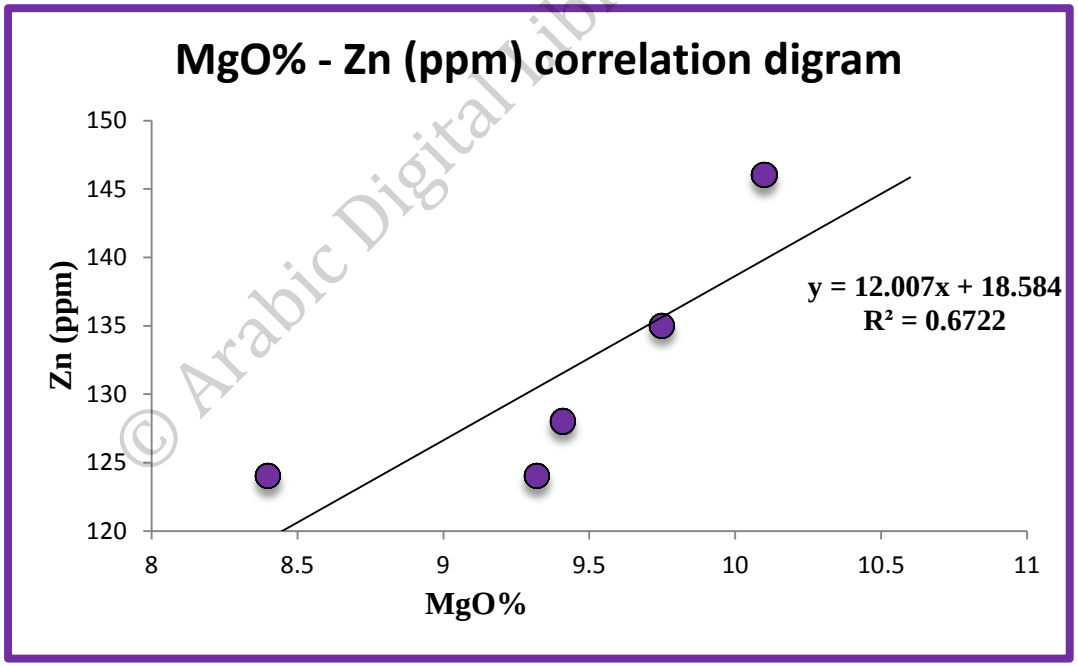

Figure (5.10): MgO% - Zn (ppm) Correlation diagram.

© Arabic Digital Library-Yarmouk University

www.manaraa.com

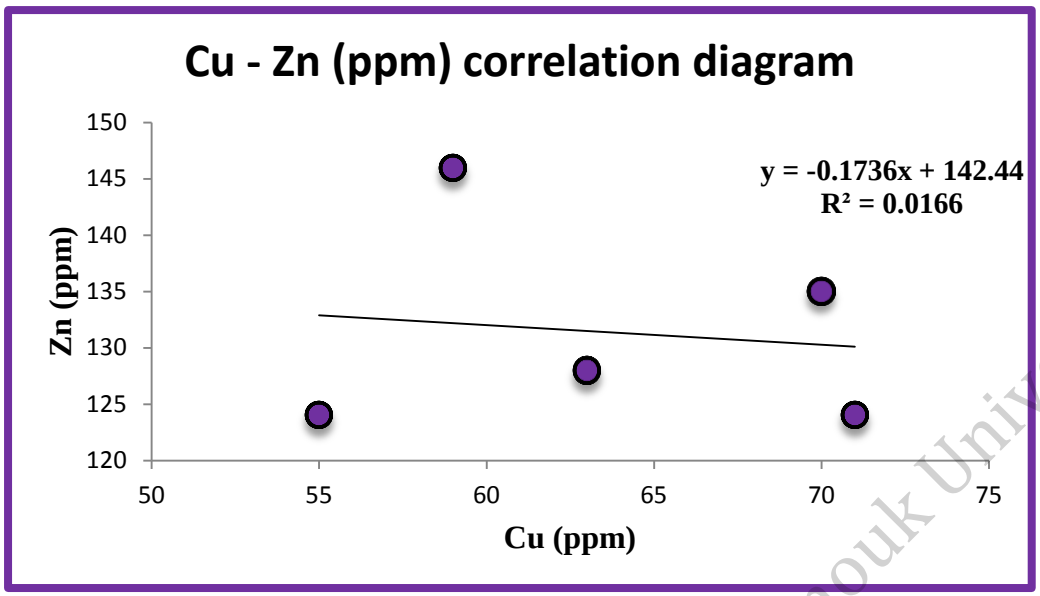

Figure (5. 11): Cu (ppm) - Zn (ppm) Correlation diagram.

The Lithium content in the studied samples varies between 5 ppm and 10 ppm and has an average of 7 ppm. The average is lower than the published average value of 10 ppm for alkali basalt (Taylor, 1968). Li has weak positive correlation with MgO for all samples, (Figure 5.12).

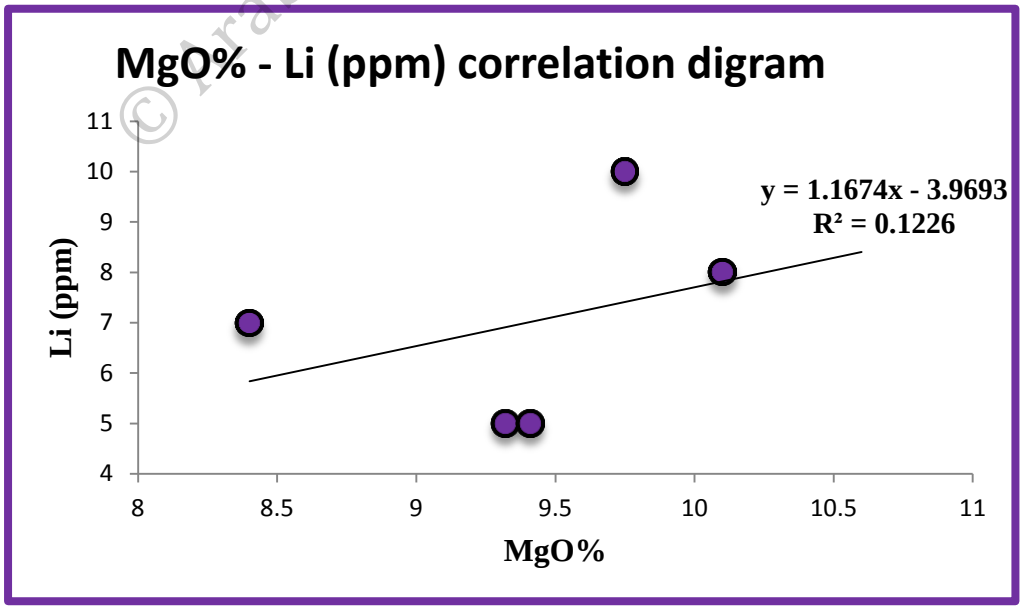

Figure (5.12): MgO% - Li (ppm) Correlation diagram.

© Arabic Digital Library- Yarmouk University
www.manaraa.com

5.3.2 Incompatible elements (KD < 1): Rb, Sr, Ba, Ga Zr, Nb, Y and HF

Incompatible elements are grouped as: 1) low - field strength elements (LFSE) such as Rb, Sr, Ba, Ga also called large ion lithophiles elements (LILE). These elements are characterized by large ionic radii, and low charges, and will therefore preferentially concentrate in the liquid until a particular phase with large enough sites to accommodate them begins to crystallize. 2) High - field strength elements(HFSE) such as: Zr, Nb, Hf andY These are elements which have large cations, but also large charges, and are also excluded from mantle phases and more concentrated in residual liquids and immobile in such fluids.

5.3.2.1 Low - field strength elements (LFSE): Rb, Sr, Ba and Ga

These elements are also calledthe large ion lithophile elements (LTLEs) which are characterized by their low valency and greater tendency to be mobilized in aqueous fluids (Al-Malabeh, 1993).

Strontium content in the studied basalt ranges from 444 to 1800 ppm in YRB samples and averages 1035.8 ppm, The average of Strontium (Sr) content in Al-Madina basalt rocks is 539 ppm which reported by Camp and Roobol (1989) and in Jebal Remah was 1214wich reported by (Al-Malabeh, 1993).

Barium content in the studied basalt ranges from 286 to 773 ppm in YRB samples and averages 420 ppm, The average of Strontium (Sr) content in Al-

© Arabic Digital Library-Yarmouk University
المنارة للاستشارات
www.manaraa.com

Madina basalt rocks is 539 ppm which reported by Camp and Roobol (1989) and in Jebal Remah was 1214wich reported by (Al-Malabeh, 1993). Ba shows a moderate positive correlation with Sr figure (5.13). Ba and Sr have negative correlation with K_2o content figure (5.14&5.15)

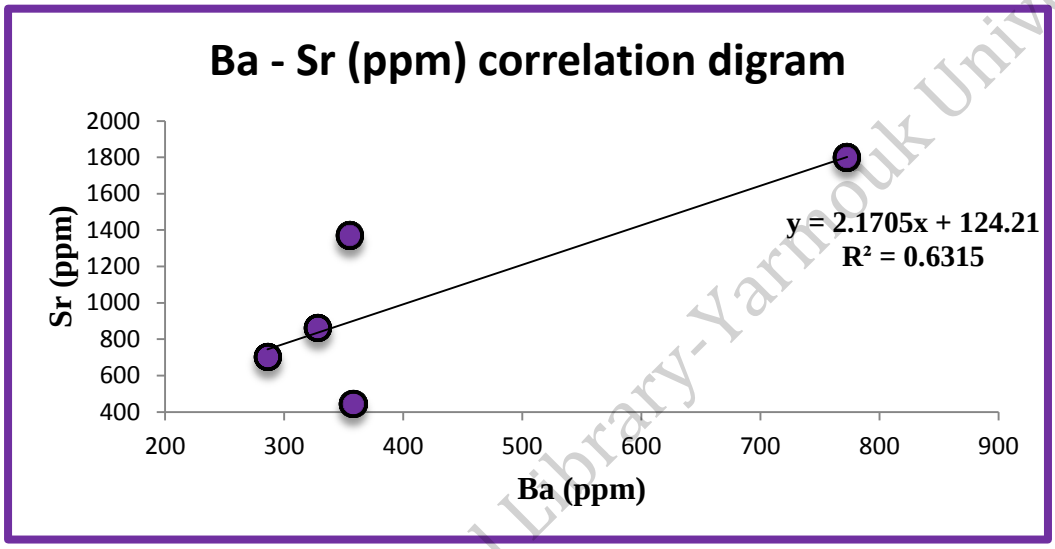

Figure (5.13): Ba-Sr correlation diagram.

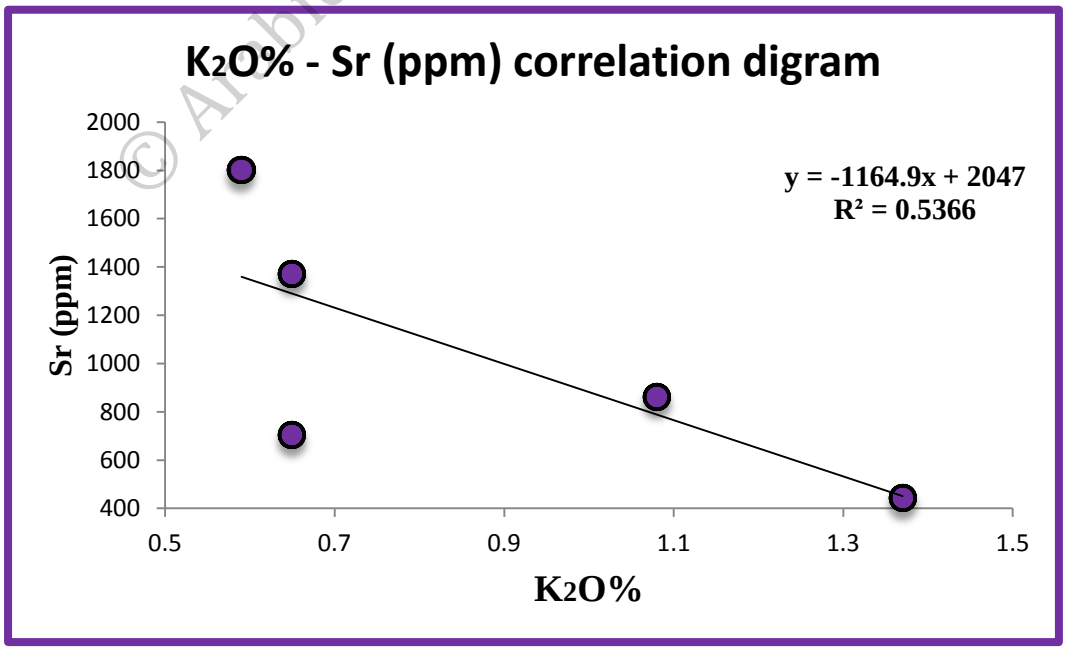

Figure (5.14): K_2O-Sr correlation diagram.

© Arabic Digital Library-Yarmouk University
www.manaraa.com

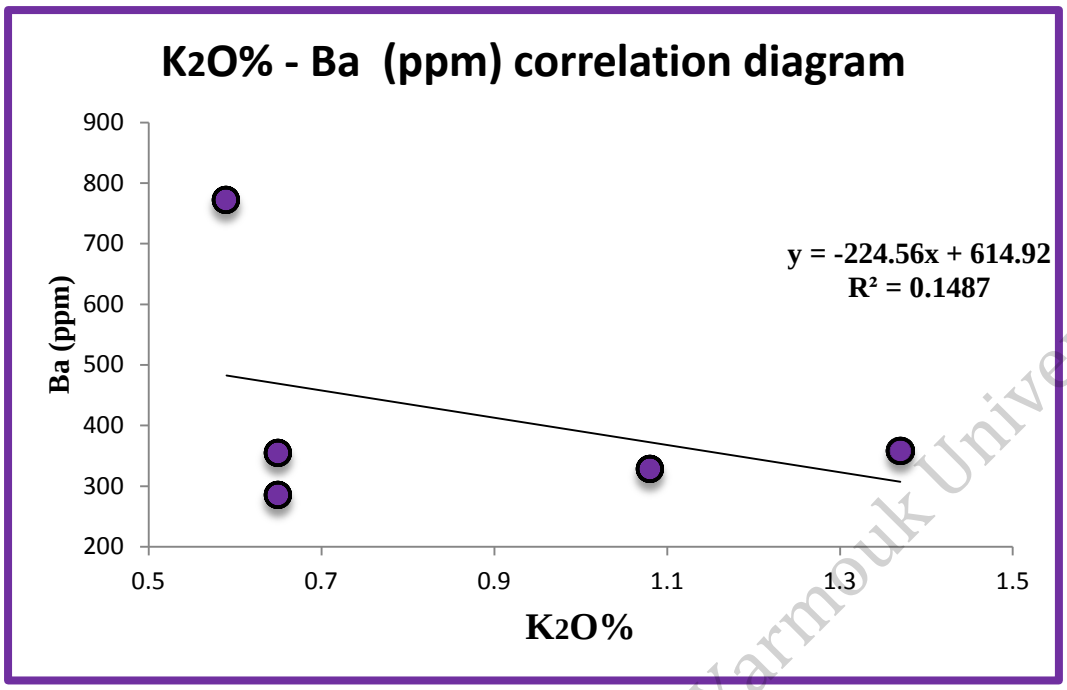

Figure (5.15): K_2O-Ba correlation diagram.

Gallium (Ga) is coordinated geochemically with Aluminum because it exhibit easy substitution for aluminum. Ga content in the studied samples varies between 908ppm and 1305 ppm, and averages 1119.4 ppm. Al_2O_3 and Ga has negative correlation with Ga content (Figure 5.16).

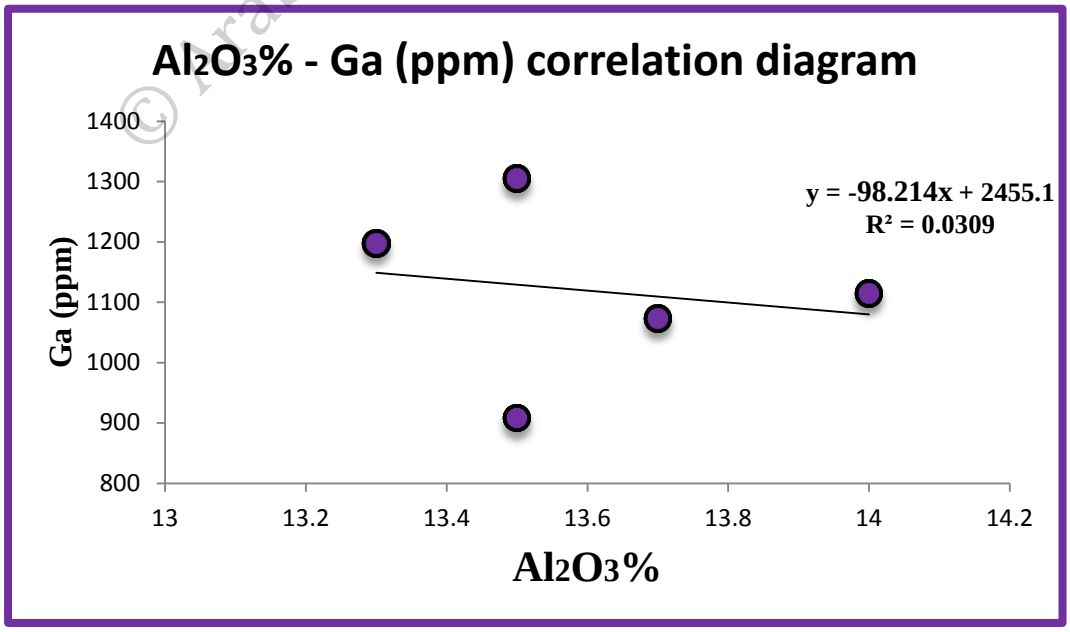

Figure (5.16): Al_2O_3-Ga correlation diagram.

© Arabic Digital Library-Yarmouk University
www.manaraa.com

5.3.2.2 High - field strength elements (HFSE) such as: Zr, Nb, Hf andY

These elements are also called Large highly charged cations (KD < 0.5). These elements do not have large IR, because of their high charge and the consequent difficulty in achieving charge balance. They are generally immobile in aqueous fluids.

The Zr content of the analyzed rocks exhibits some variability. It ranges from 115 to 211 ppm, and averages 162 ppm. This average exceeds the Zr average of 140 ppm for alkali olivine basalt from Harrat El-Jabban (Khalil, 1991). Zr is negatively correlated with TiO_2, K_2O and P_2O_5 (Figure 5.17, 5.18 & 5.19).

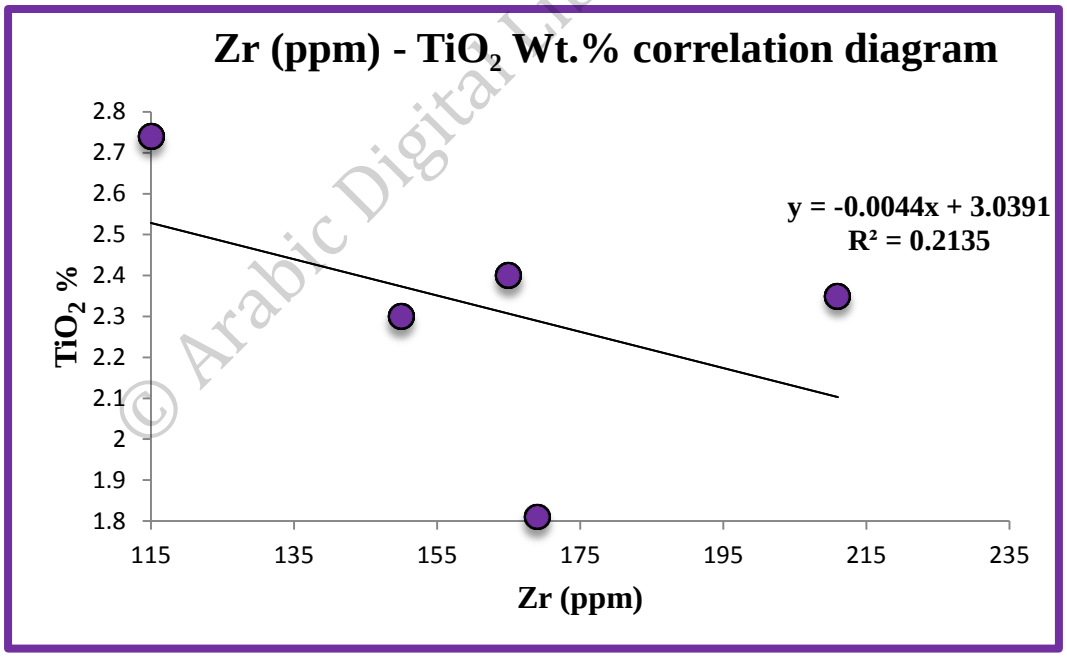

Figure (5.17): Zr -TiO_2 correlation diagram.

© Arabic Digital Library-Yarmouk University

www.manaraa.com

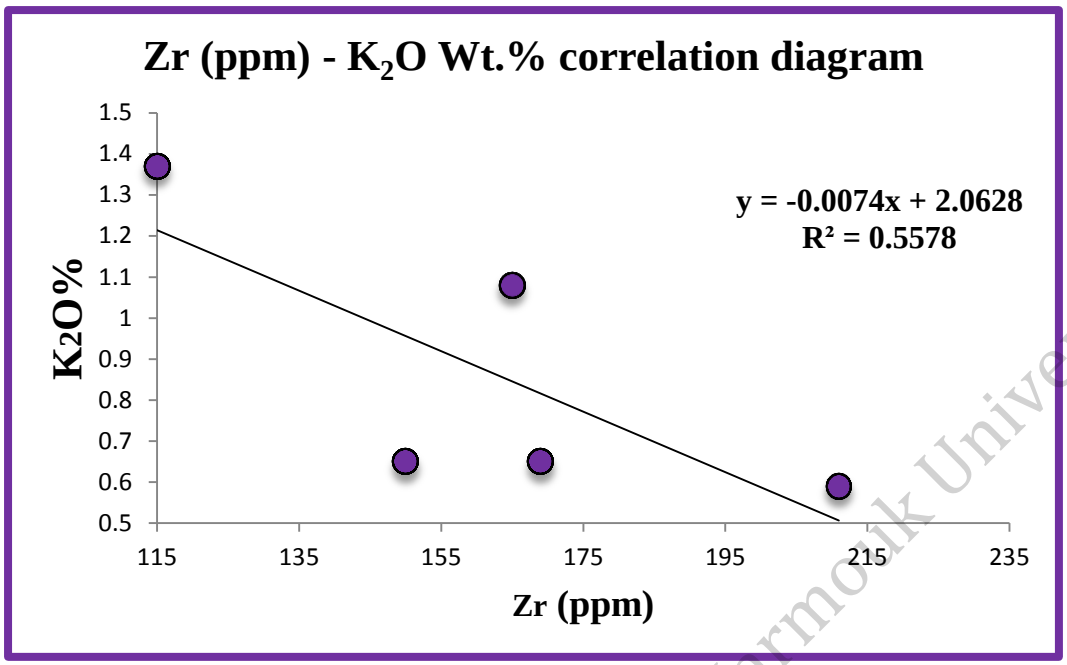

Figure (5.18): Zr –K_2O correlation diagram.

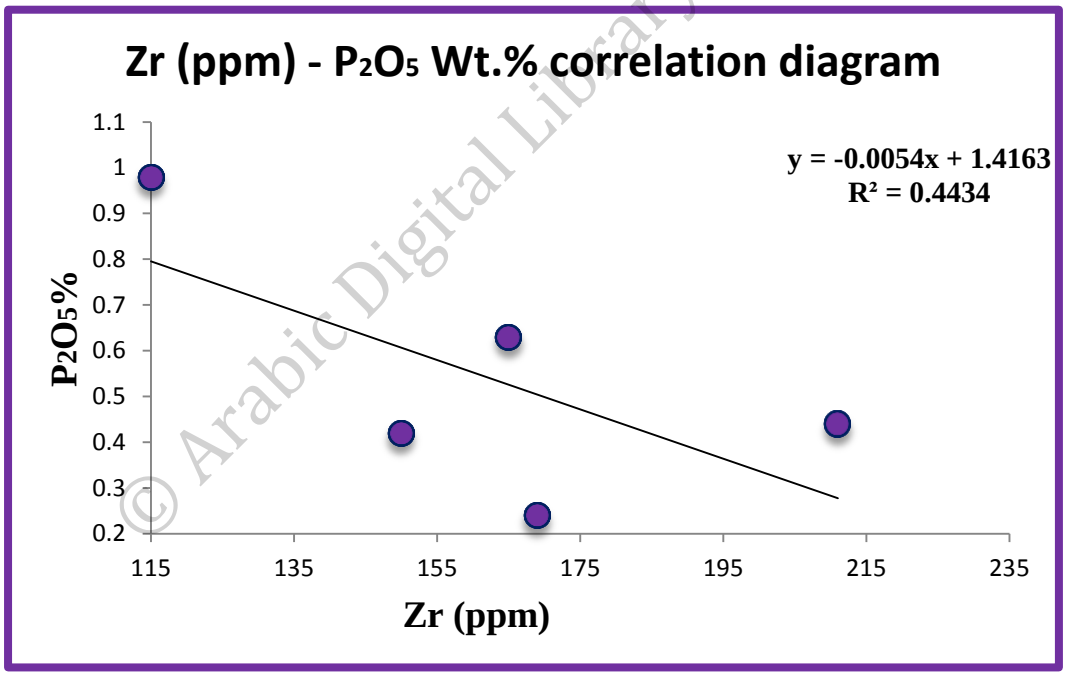

Figure (5.19): Zr –P_2O_5 correlation diagram.

Niobium content (Nb) in the studied rocks ranges from 71 to 100 ppm, with an average of about 83.6 ppm. These averages are higher than the published average of 23.3 ppm reported for alkali olivine basalt of the Rahat.

© Arabic Digital Library-Yarmouk University

www.manaraa.com

(Camp and Roobol, 1989). Nb is positively correlated with Zr in all samples from YR (Figure 5.20).

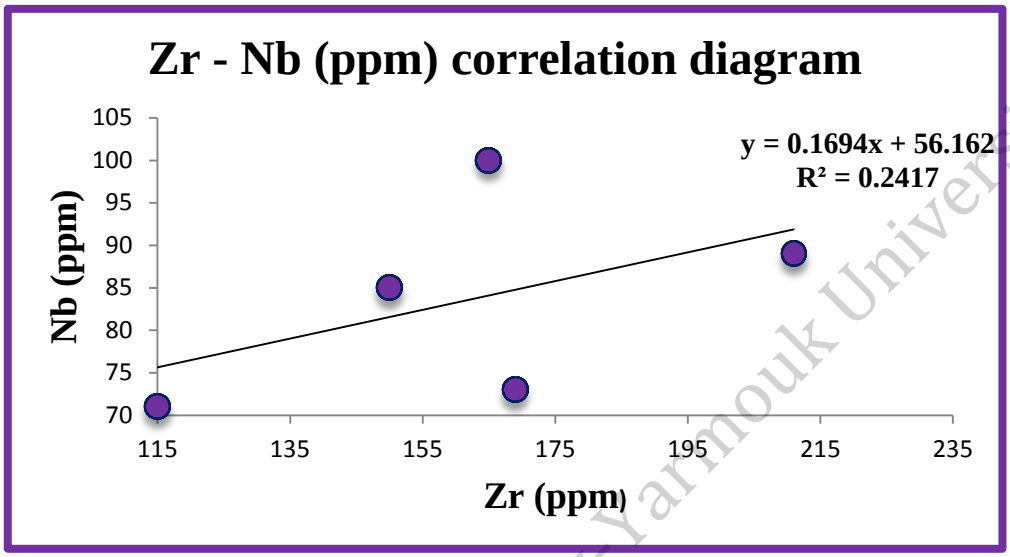

Figure (5.20): Zr –Nb correlation diagram.

Hafnium content (Nb) in the studied rocks ranges from4 to 4 ppm, with an average of about 4 ppm. This average is equal to the published average of 4 ppm reported by Horn & Adams (1966) for alkali basalt.

Niobium content (Y) in the studied rocks ranges from27 to 32 ppm, with an average of about 30 ppm. These averages are the same of the published average of 31 ppm reported for alkali olivine basalt from Snake River plain. (Thompson et al, 1983). Y is positively correlated with Zr in all samples from YR (Figure 5.21).

© Arabic Digital Library-Yarmouk University

www.manaraa.com

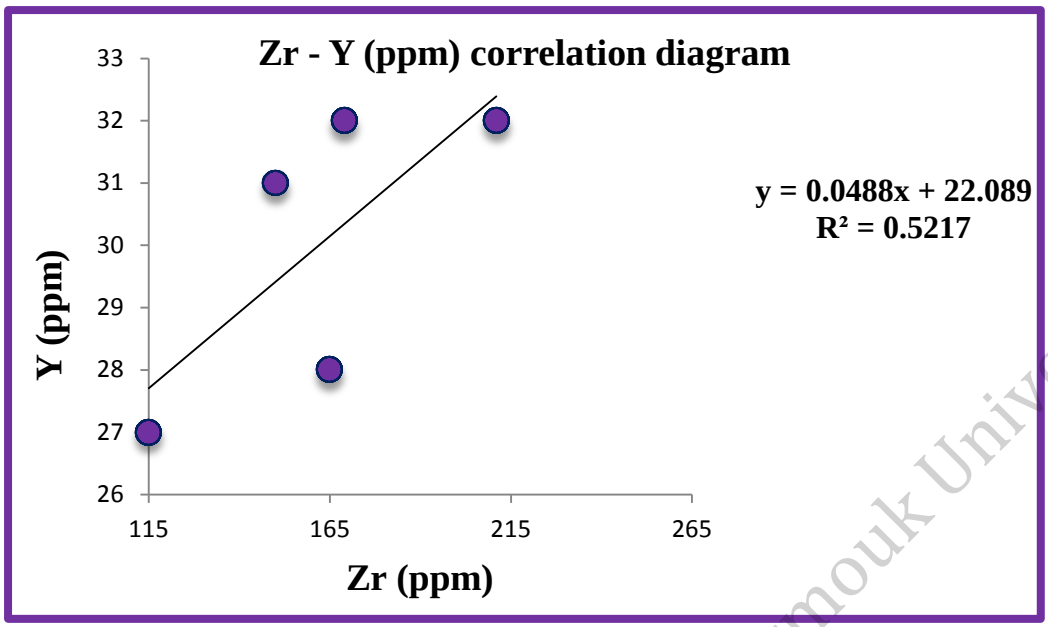

Figure (5.21): Zr –Y correlation diagram.

5.4 Classification and discussion of YRB

It's critically important to display geochemical data (major and trace elements) in a fashion that allows you to recognize trend in the variation to describe and interpret the processes responsible. The objects to find parameters that show you systematic variation is variation diagrams. There are two common formats for variation diagrams of chemical data in the first, the bivariate diagram (Cartesian, or x-y) plot: Two parameters are plotted one vertically called the ordinate, or y-axis) and one horizontally (called the abscissa, or the x-axis) figure (5..In the second triangular diagram, we represent three parameters, one at each corner, but show only relative proportions, not absolute quantities, because three parameters must be normalized to sum 100%. These diagrams were applied to help in the classification, nomenclature and interpretation of the tectonic setting of Yarmouk River.

© Arabic Digital Library-Yarmouk University

www.manaraa.com

5.4.1 Total Alkalis Silica (TAS) classification

The data of all the basaltic samples are listed in table (1) was plotted on the TAS diagram after Le Bas et al (1986). The Cartesian diagrams, especially for chemical classification and nomenclature of volcanic rocks, is the total alkalies (Na2O + K2O) versus silica (SiO2) diagram. It's modified by Le Base et al., (1986) and alkaline/ subalkaline line that included by Irvine and Baragar (1974). On this diagram all of YRB samples occurred in the basalt fields and belong to the subalkaline series (Figure 5.22).

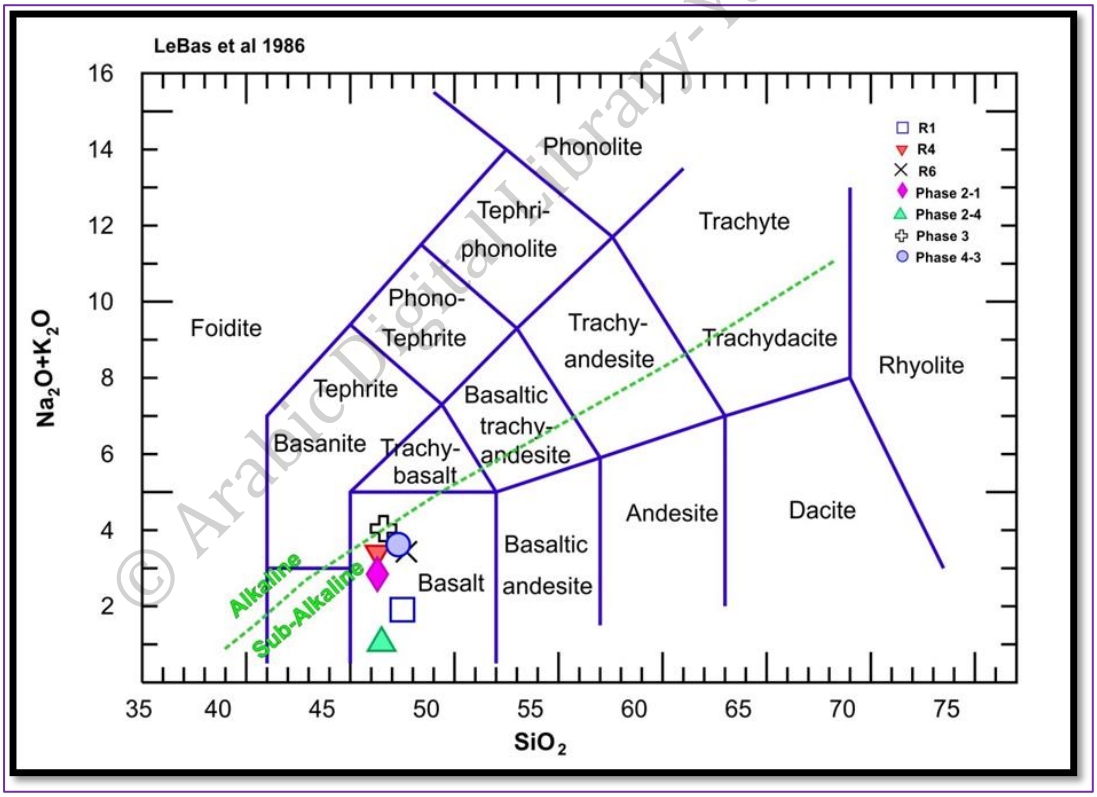

Figure (5.22): Analyzed samples plotted on TAS diagram according to (Le Bas et al., 1986). Discrimination line of alkaline and sub-alkaline rock fields after Irvine and Baragar (1971).

5.4.2 Subdivision of Alkaline Magma Series

© Arabic Digital Library-Yarmouk University

www.manaraa.com

A.Normative An–Ab–Or diagram

Irvine and Baragar (1971) suggested new classification of alkali series divided into sodic and potassic series (Figure 5.23). Potassic series those in which K_2O (wt.%) exceeds Na_2O (wt.%). subdivision of subalkaline rocks according to K_2O versus SiO_2. (Redrawn from Ewart, 1982).

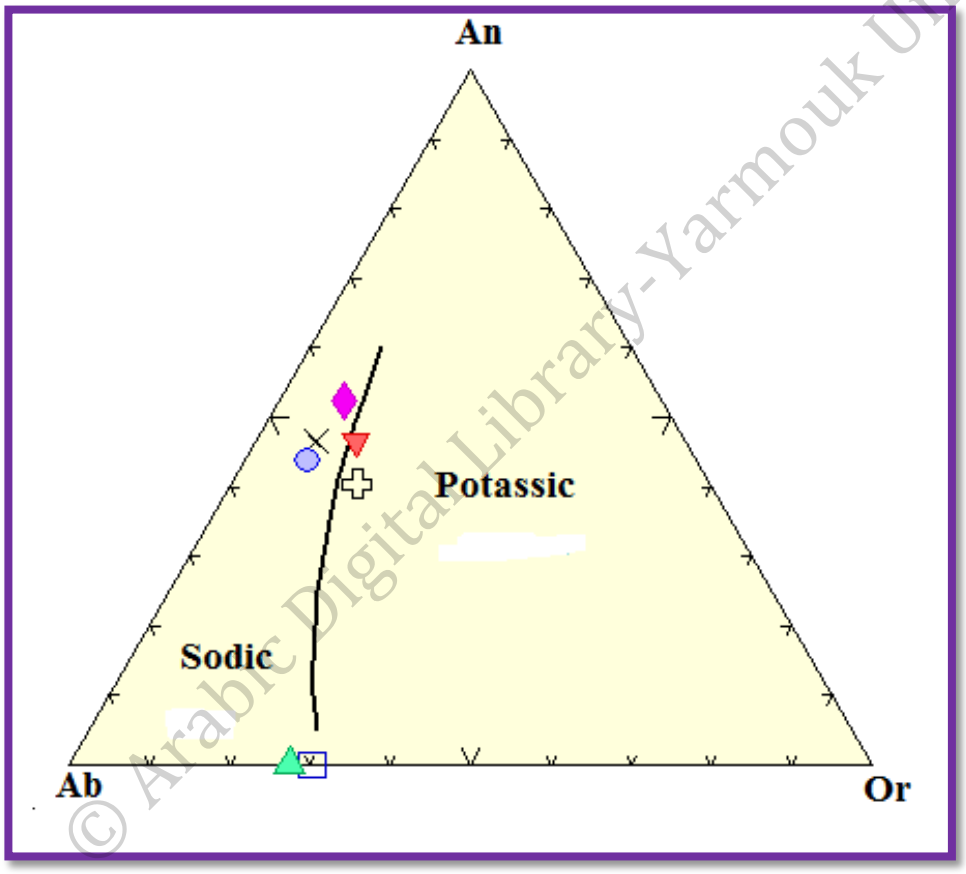

© Arabic Digital Library-Yarmouk University

Figure (5.23): Normative An-Ab`-Or projection (Irvine and Barger, 1971) from the studied basaltic showing the sodic and potassic series.

B. K-series

Moreover, using the diagram of alkalinity that proposed by different authors (e.g. Redrawn from Ewart, 1982.), which used to discriminate between various degrees of alkaline affinities subdividing the alkaline YRB samples into

المنارة للاستشارات
www.manaraa.com

High-K-, K-, and low K-sub-series. The studied samples fall in the alkaline and sub alkaline field (Figure 5.24).

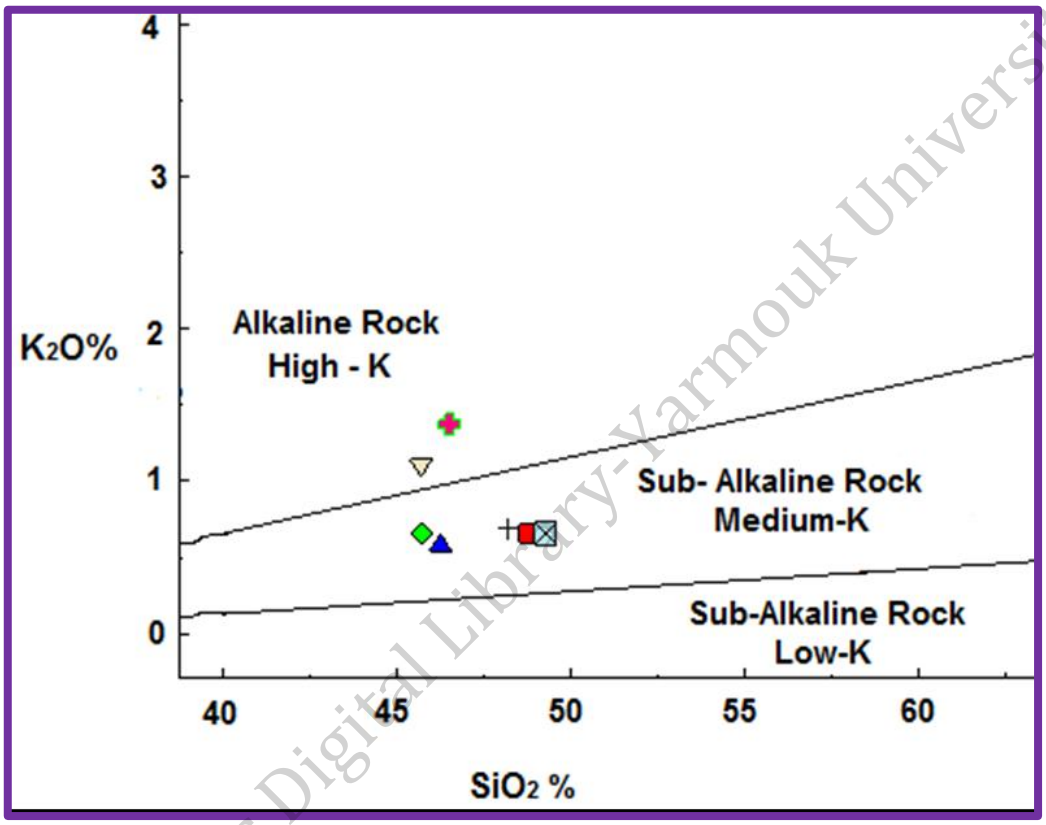

© Arabic Digital Library-Yarmouk University

Figure (5.24): K_2O vs. SiO_2 diagram subdividing the alkaline and subalkaline YRB samples into High-K-, K-, and low K-sub-series (After Redrawn from Ewart, 1982).

5.4.4 SiO_2 Saturation (Shand's Classification)

Three basalt rock types can be recognized according to their degree of silica saturation: 1. Quartz-hypersthene normative (Q _ Hy) quartz tholeiite (silica-oversaturated) 2. Olivine-hypersthene normative (Ol _ Hy) olivine tholeiite (silica- saturated) 3.Nepheline-normative (Ne) alkaline basalt (silica-undersaturated). The alkaline and subalkaline rocks, when plotted on Ne-Ol-

المنارة للاستشارات
www.manaraa.com

Qtz diagram (Figure 5.25) using the normative minerals include nepheline, olivine and quartz, are marked by the dividing line that is close to the critical plane of silica under saturation (Proposed by Irvine and Baragar, 1971). Alkaline rocks plot to the left of this plane and are silica undersaturated, while the subalkaline rocks are plotted on the right and are silica oversaturated. The IGB samples falls in undersaturated area.

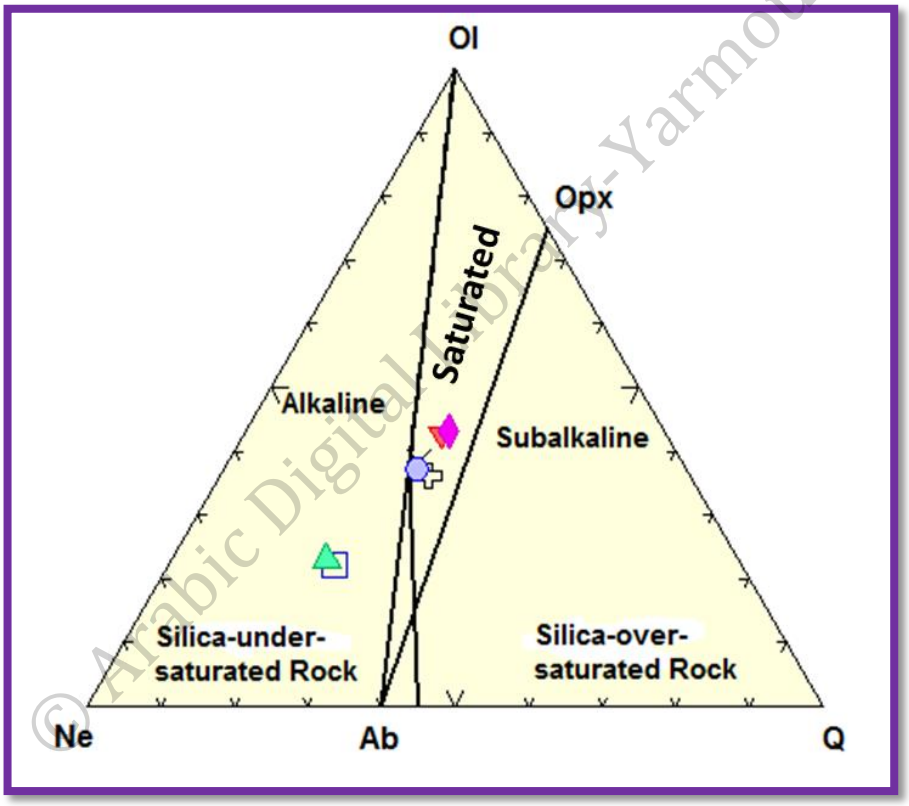

Figure (5.25): A Ne-Ol-Q base of the basalt tetrahedron illustrating YRB samples in highly saturated to undersaturated alkaline field (Modified after Irvine and Baragar).

© Arabic Digital Library-Yarmouk University

www.manaraa.com

Chapter Sex

Physical Properties

6

© Arabic Digital Library-Yarmouk University

المنارة للاستشارات
www.manaraa.com

Chapter 6

Physical Properties

6. 1Introduction

Basalt has been used as building materials in historical and modern buildings due to their natural beauty and availability. The diversity of their applications increased constantly since depending on location of origin. As any other building material, basalt rock today has to fulfill the physical and technical requirements required by architects and civil engineers.

Various physical and mechanical laboratory tests such as specific gravity, dry and bulk density, dry unit weight (UW), water absorption (WA), water content, degree of saturation, porosity(P), void ratio and ultra-sonic velocity were carried out on core samples obtained from block rocks of the YRB.

The mechanical properties discussed here are uniaxial compressive strength (UCS) and abrasiveness (Los Angeles test).

Basalt resists water absorption, oxidation, freezing, collapse and friction. Its show a durable color resisting changes and does not show excessive vitreous property. Furthermore it avoids stains and fissures in building for a long time and its acid resistance. Because of these properties, basalt has been used commonly in building of historical walls, mosques, taverns, traditional baths, houses and roads. More resistant non-porous basalt, on the other hand,

© Arabic Digital Library Yarmouk University

www.manaraa.com

was used in walls, columns, column headers, frames, thresholds and side beams of pools.

Basaltic rocks have been widely used as aggregate for various purposes. They show a variety of textural and mineralogical individuality that may affect their physical and mechanical properties as well as their use as construction material.

6.2 Physical Properties

Investigation of the physical properties of basalt rock is very important to develop an engineering classification system for intact rock, and also to develop an index related to important physical characteristics.

Laboratory tests were conducted on twelve intact basalt samples extracted and collected from representative sites in the study area. Physical tests were performed on in the engineering geology laboratory at the Department of Earth and environmental Science at Yarmouk University. Cores were cut perpendicular to bedding planes and prepared for further testing at the Jordan University of Science and Technology/Irbid.

6.2.1 Specific gravity (relative density), water absorption and bulk density:

© Arabic Digital Library Yarmouk University

www.manaraa.com

Table (6.1): indicate bulk and apparent specific gravity as well as absorption of the tested basalt samples from the YRB.

Core No.	**C1**	**C2**	**C3**	**C4**	**C_5**	**C_6**	C_7	C_8	**C9**	**C10**	**C11**
Sample No.	1	2	3	4	5	6	7	8	9	10	11
Bulk Density (oven dry basis)	2.63	2.62	2.85	2.54	2.82	2.79	2.84	2.60	2.80	2.61	2.89
Bulk Density (S.S.D dry basis)	2.66	2.65	2.86	2.57	2.85	2.79	2.84	2.64	2.80	2.64	2.90
Apparent Density (oven dry basis)	2.71	2.69	2.86	2.62	2.89	2.81	2.86	2.70	2.81	2.68	2.91
Absorption (%)	1.14	0.93	0.14	1.22	0.91	0.25	0.30	1.38	0.21	0.95	0.22

The bulk specific gravity of the tested basalt samples was determined using the balance standards. The oven dried samples show an average value ranging from 2.54 to 2.89 and 2.57 to 2.90 for the saturated and surface dried samples. The apparent density values ranges from 2.62 to 2.91 (table 6-1).

The minimum value of basalt specific gravity recorded by Jumikies, (1983) and Touloukian *et. al*., (1981) was 2.21 and 2.04 respectively. Values obtained from the YRB don't exceed those values and are matching well with the range of this value.

The values of specific gravity are comparable with the northern Jordan basalt that was described by Humidi (1993) who reported a specific gravity with an average value of 2.65 comparable with values obtained from Irbid (2.71), Ramatha (2.621), Al-Mafraq (2.582), Al-Azraq (2.67) and Um-Qays (2.731) basalts described by Taqieddin, 2017. Values of the specific gravity can also be compared with the values of apparent, dry and SSD specific

© Arabic Digital Library-Yarmouk University

المنارة للاستشارات
www.manaraa.com

gravities for the coarse aggregates (2.800, 2.650, and 2.700 respectively), obtained from Al-Rjoub quarry in the northern part of Jordan. Those values are also comparable with Al- Hashimiyya basalt reported by Al-Zyoud (2005). She gives an average specific gravity of 2.59. Abu-Mahfouz et.al, 2016 gave an apparent specific gravity values ranging from 2.70 to 2.90 and a bulk specific gravity ranging from 2.60 – 2.84. Those values are also compared with results obtained by Al-Baijat, 2008. Values of apparent, dry and SSD specific gravities of the coarse aggregate are 2.917, 2.765 and 2.814 respectively.

The plagioclase phyric basalt yields the highest specific gravity due to its massive and compact nature as well as the presence of magnetite/ilmenite minerals, samples that have low specific gravity vale due to the presence of pores.

6.2.2 Water absorption

It is used to describe the rock texture and it is an indirect measure of the permeability of an aggregate. It can also be used to calculate changes in the weight of an aggregate and are also used to calculate the amount of water absorbed by aggregates during Portland concrete mix preparation. According to Collis and Fox, 1985, water absorption can also be related to other physical characteristics such as mechanical strength. It could be also related to mechanical strength and reliability. Aggregates having high water absorption are generally considered as unsuitable building materials unless they pass other properties tests such as strength, impact and hardness.

© Arabic Digital Library-Yarmouk University

المنارة للاستشارات
www.manaraa.com

The studied basalt samples present water absorption values ranging from 0.14 to 1.38. The minimum value (0.14%) was recorded in sample C_3 from the porphyritic basalt which is dense and massive, while the maximum value (1.38%) was recorded from the vesicular basalt sample C_8 table (6.2). table (6.3) indicating that the basalt in the study area shows a crystalline texture

In general, less absorptive basalt or aggregates often tend to be more resistant to mechanical forces and weathering. Low absorption values might be considered as less than 1% and it is essential to clarify that water absorption limits should not be imposed unless it has been established, for a particular material, which relates closely to some other undesirable properties. However, ASTM C127, C128, state that the upper limit for concrete aggregate water absorption should not exceeds two percent.

Table (6.2): Absorption % of the tested core samples of the YRB.

Sample. no	Core Samples	% Absorption
1	C1	1.14
2	C2	0.93
3	C3	0.14
4	C4	1.22
5	C5	0.91
6	C6	0.25
7	C7	0.30
8	C8	1.38
9	C9	0.21
10	C10	0.95
11	C11	0.22

Basalt absorption is affected by the texture and fabric of the samples. It was qualitatively used to describe the texture of the rock. According to Duncan,

© Arabic Digital Library-Yarmouk University

المنارة للاستشارات
www.manaraa.com

(1966 and 1969), the tested basalt samples show a crystalline texture whereas the percentage of the absorption averages 0.70%. Jumikis, (1983) provide a relationship between the percentage of absorption and the textures of the tested rock samples, as shown in Table (6.3).

Table (6.3): Relationship between rock textures and absorption values, (Jumikis, 1983).

Absorption %	Texture Description
0 - 2	Crystalline, Crystalline – Indurated, Indurated
2-8	Strongly Cemented
8-10	Fairly Cemented, Fairly Compacted
10-15	Weakly Cemented, Weakly Compacted
>15	Very Weakly Cemented, Very Weakly Compacted

The obtained values of basalt absorption are correlated with the absorption values of the continental basalt, which ranges from (0.1 to 0.3%). The values of absorption are also comparable with Abu-Mahfouz et al, 2016 values, ranging from (0.33 to 1.60%) and indicating also a crystalline texture and good rock to use in concrete and as building materials.

6.2.3 Unit weight

It's defined as the weight per unit volume. Highly porous rocks and relatively poor arrangement of grains (less packing) usually have relatively less densities and vice versa. The bulk unit weight considers the bulk (total) volume of rocks whereas the solid unit weight considers volume excluding the pores and fissures. For porous rocks the unit weight of solid rocks would be relatively

© Arabic Digital Library-Yarmouk University

www.manaraa.com

higher than the bulk unit weight as the value in the denominator is relatively lower due to exclusion of pores and micro fractures.

Bulk unit weight depends on the type of rock, its porosity and the geological processes affecting it. Bulk unit weight of a rock may vary locally, sometimes from one site to another within the same geological formation. Bulk unit weight of basalt is revealed in table (6.4).

Table (6.4): Average bulk unit weight for some common rocks.

Sample. no	Rock Name	Average Bulk unit weight (KN/m^3)
1	Granite	27
2	Basalt	30
3	Gneiss	27
4	Marble	27
5	Schist	26
6	Sandstone	26
7	Hard coal	15

Results of the unit weight tests are shown in Table (6.5) and were correlated with the standard set by the International Association of Engineering Geologists (I.A.E.G.).

Table (6.5): Bulk unit weight of the tested YRB samples

Sample. no	Core No.	Unit Weight (KN/m^3)	Unit Weight (g/cm^3)
1	C1	25.73964	2.63
2	C2	25.71852	2.62
3	C3	27.95911	2.85
4	C4	24.86645	2.54
5	C5	27.6331	2.82
6	C6	27.29717	2.78
7	C7	27.78993	2.84
8	C8	25.49709	2.60
9	C9	27.40711	2.79
10	C10	25.58326	2.61
11	C11	28.31341	2.89

© Arabic Digital Library-Yarmouk University
المنارة للاستشارات
www.manaraa.com

The tested basalt samples can be classified as having higher unit weight values ranging from 2.54 to 2.89 gram/cm^3 with an average value of 2.73 gram / cm^3 due to its low porosity and void ratio values. (table 6.6). This value can be compared with the value 2.717 gram/cm^3 obtained by AL-Zyoud (2005) from Al- Hashimiyya basalt and by Abu-Mahfouz et. al,(2016) 2.69 gram/cm^3. This value is slightly higher than that value (2.605gram/cm^3) reported by Humidi, (1993), from north Jordan. However, the difference between the solid unit weight and the bulk unit weight is negligible, due to the fact that, the volume of voids in the tested basalt samples is very small.

Table (6.6): Rock classification criterion according to (I.A.E.G, Lama, 1978)

Sample no.	Unit weight (gram/cm^3	Description
1	less than 1.8	very low
2	1.8 – 2.2	Low
3	2.2 – 2.55	Moderate
4	2.55 – 2.75	High
5	more than 2.75	very high

© Arabic Digital Library-Yarmouk University

6.2.4 Porosity, Apparent Porosity and Void Ratio

The porosity of a rock is that fraction of a given volume of material that is occupied by void space, or interstices, and is mathematically defined as a fraction of the volume of voids divided by its total volume; it ranges between 0 to 100 %.

6.2.5 Void Ratio

المنارة للاستشارات
www.manaraa.com

Void ratio (e) is the percentage of volume of voids of solid volume of the sample, e calculated after (Brown, 1981). The results of porosity and void ratio of tested samples are presented in Table (6.7).

Table (6.7): Porosity and void ratio of YRB samples.

Sample. no	Type	Porosity (0-1)	Porosity (0-100)	Void ratio
1	C1	0.0299	2.99	0.0308
2	C2	0.0243	2.43	0.0249
3	C3	0.0040	0.4	0.0040
4	C4	0.0310	3.1	0.0320
5	C5	0.0256	2.56	0.0263
6	C6	0.0071	0.71	0.0071
7	C7	0.0085	0.85	0.0086
8	C8	0.0359	3.59	0.0372
9	C9	0.0059	0.59	0.0060
10	C10	0.0248	2.48	0.0254
11	C11	0.0063	0.63	0.0064

According to (Anon, 1979 engineering classification) most of the basaltic samples have low porosity. Many factors such as grain size grain shape, sorting of the grains, crystal arrangement, degree of packing and cementation all affect porosity. Porosity decreases with increasing of pressure and therefore, deep seated deposits with large overburden pressure tend to have relatively low porosity compared with surface depositions.

The results of porosity and void ratio values of the studied basalt samples show variation in porosity values, and slightly variation in void ratio values. Based on rock densities and porosity, the (IAEG) proposed a classification of rocks into five classes, as shown in Table (6.8), the average value of this basalt porosity is 1.8 %, which considered classifying as low porous rock, of class 4

© Arabic Digital Library-Yarmouk University

المنارة للاستشارات
www.manaraa.com

of the IAEG classification. von Moos and Quervain (1948) classified rocks into six categories as shown in table (6.8).

The obtained values of porosity (0.4 to 3.59%), and void ratios (0.004 to 0.0372) were compared with (Abu-Mahfouz et. al**,** 2016) and by (Taqieddin, 2017) for Irbid, Ramatha, Al-Mafraq, Al-Zarqa and Um-Qays basalt. These values are 1.95, 3.1, 2.32, 2.4, and 1 respectively. Effects voids present in the aggregate at a given degree of compaction (Waqa, 2004).

Table (6.8): Rock classification criterion according to (IAEG), (Jumikis, 1983) and (von Moos and Quervain, 1948)

Basalt	**According to IAEG**		**According to von Moos and Quervain**	
Class	Porosity%	Description	Porosity%	Description
1	Over 30	Very high	more than 20%	a lot of pore space
2	30-15	High	10–20%	many pores
3	15-5	Medium	5–10%	significantly porous
4	5-1	Low	2.5–5%	slightly porous
5	Less than 1	Very low	1–2.5%	a few pores
6	-	-	<1%	Compact

6.2.6 Ultrasonic wave velocity

It measures the travel time of an ultrasonic pulse passing through the cylindrical basalt rock specimen, having a length to diameter ratio (L/D) greater than 3. The velocity is determined from the known relation of time, distance and velocity. The ultrasonic P-wave Velocity measurements are applied to determine the quality of the basalt samples, in order to demonstrate its homogeneity or its degree of alteration (Mamillan, 1972).

© Arabic Digital Library-Yarmouk University

المنارة للاستشارات
www.manaraa.com

The important dominant factors are rock type, mineralogical composition, rock texture and structure, grain size, shape of the grains, density, porosity, anisotropy, pore water, confining pressure, temperature, weathering, alteration zones, bedding planes, and joint properties (Yasar and Erdogan, 2004: as cited in Moradian, 2009). This test was conducted for the following reasons:

- Evaluating the uniformity and the quality of rocks.

-locating internal voids and cracks

- estimating severity of deterioration.

-estimating compressive strength (with correlation of Uniaxial Strength tests).

Results of the ultrasonic velocity of the studied basalt core-samples are shown in table (6.9) indicating a range of 3141–5514 m/s. The variation of the velocity values may be attributed to high variation of water content of the studied samples. Furthermore, porosity, density, micro fractures, mineral composition and dry density may affect the velocity of basalt rock samples.

Table (6.9): Results of Ultrasonic Wave Velocities (UWV) of the tested basalt samples extracted from different locations at YR North Jordan.

Sample. no	Length (m)	Time (s)	Velocity (m/s)
R1	19.3	35	5514
R2	20.3	63	3222
R3	19.4	36	5389
R4	20.1	60	3350
R5	20.1	59	3407
R6	20.1	64	3141

© Arabic Digital Library Yarmouk University

المنارة للاستشارات
www.manaraa.com

According to the (IAEG) and Anon 1976, the basalt samples show high ultrasonic wave velocity of class 4, due to its compact dense and low pours nature (table 6.10). Taqieddin, 2017 reported from north east Jordan average values of ultrasonic wave velocity for the studied basalt rocks in Irbid, Ramatha, Al-Mafraq, Al-Azraq and Um-Qays area basalt as followed 5480, 5302, 5465, 5496, and 5306 m/s respectively, the ultrasonic averege values in the study area is (4003 m/s) slightly less than those of Al- Hashimiyya basalt that averages 5067 m/s, but both readings are within the continental basalt range of ultrasonic wave velocity that is (5400-6400) m/s .

Table (6.10): Rock classification criterion using ultrasonic wave velocity by (I.A.E.G), Lama (1978), and Anon (1979).

Class	Ultrasonic Velocity (m/s)	Description	Grade of weathering
1	Less than 2500	Very low	Very strongly weathered
2	2500 - 3500	Low	Strongly weathered
3	3500 - 4000	Moderate	Moderately weathered
4	4000 - 5000	High	Slightly weathered
5	Over 5000	Very High	Fresh

© Arabic Digital Library-Yarmouk University

المنارة للاستشارات
www.manaraa.com

The results of some physical properties conducted on YRB compared with other basalt localities in Jordan and in the world are listed in table (6.11|).

Table (6.11): Physical properties of YRB and other area

Physical property	The average value of YRM	Harrat Irbid North Jordan	North Jordan basalt					Average values of Al-Hashimiyya basalt	Continental basalt
			Irbid	**Ramatha**	**Al-Mafraq**	**Al-Azraq**	**Um-Qays**		
Specific gravity	**2.73**	**2.72**	**2.72**	**2.629**	**2.582**	**2.67**	**2.731**	**2.58**	**2.65**
Unit weight (gm/cm3)	**2.73**	**2.69**	**-**	**-**	**-**	**-**	**-**	**2.717**	**2.605**
Absorption (%)	**0.70%**	**0.97%**	**-**					**0.24**	**-**
Porosity (%)	**1.8%**	**0.96%**	**1.95**	**3.1**	**2.32**	**2.4**	**1**	**2.46**	**3.2**
Ultrasonic wave velocity(m/s)	**4003**	**4549**	**5480**	**5302**	**5465**	**5496**	**5306**	**5067**	**5399**

© Arabic Digital Library-Yarmouk University

www.manaraa.com

6.3 Relationships between the physical properties

6.3.1 Dry density vs. Porosity

The Coefficient of Determination (R2) and The correlation coefficient (r) indicates a moderate (negative) linear relationship Figure (6.1) show an inversely proportional linear relationship, indicating that a decrease in porosity is associated with an increase in density.

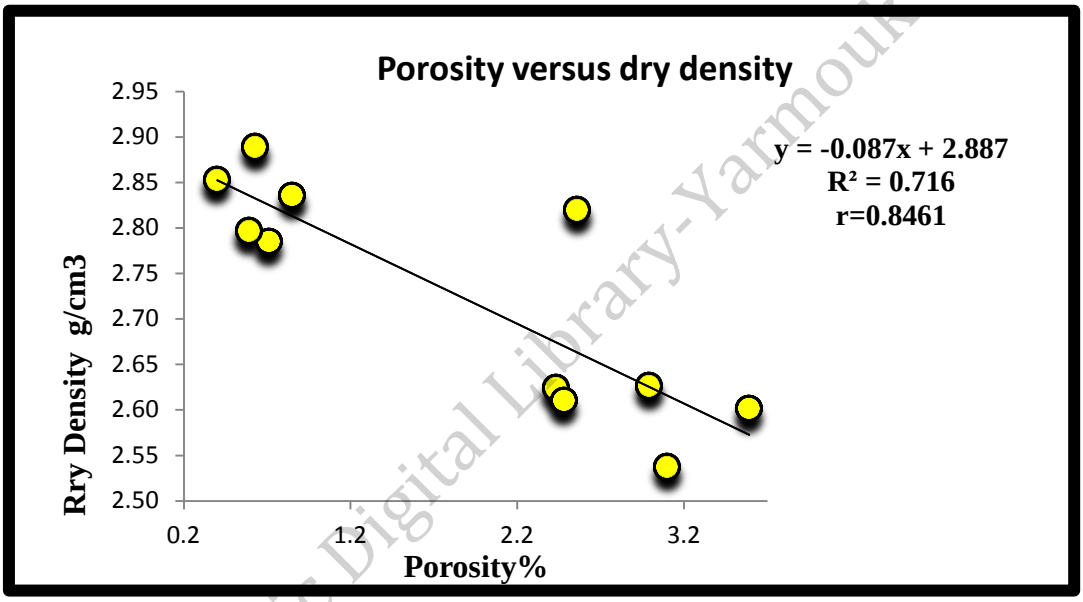

Figure (6.1): Porosity versus dry density for basalt samples.

6.3.2 Relationship between absorption and porosity

The Coefficient of Determination (R2) and the correlation coefficient (r) indicates a strong (positive) linear relationship Figure (6.2) show a direct proportional linear relationship, indicating that an increase in porosity is associated with an increase in absorption.

© Arabic Digital Library-Yarmouk University

المنارة للاستشارات
www.manaraa.com

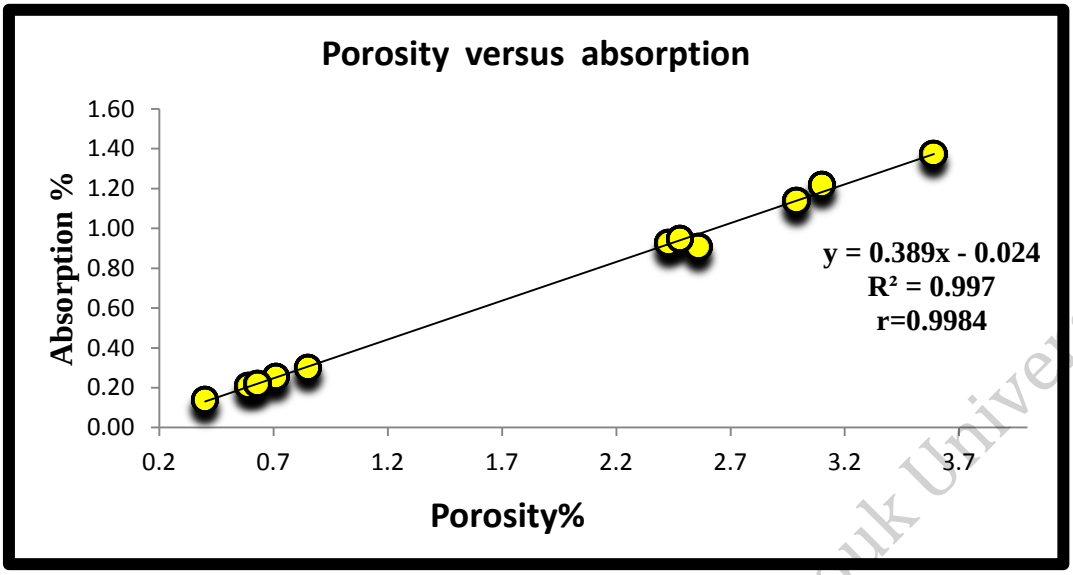

Figure (6.2): Relationship between porosity % and absorption %.

6.3.3 dry density and absorption

The Coefficient of Determination (R2) and the correlation coefficient(r) indicates a moderate (negative) linear relationship (Figure 6.3). Show an inversely proportional linear relationship, indicating that an increase in dry density is associated with a decrease in absorption.

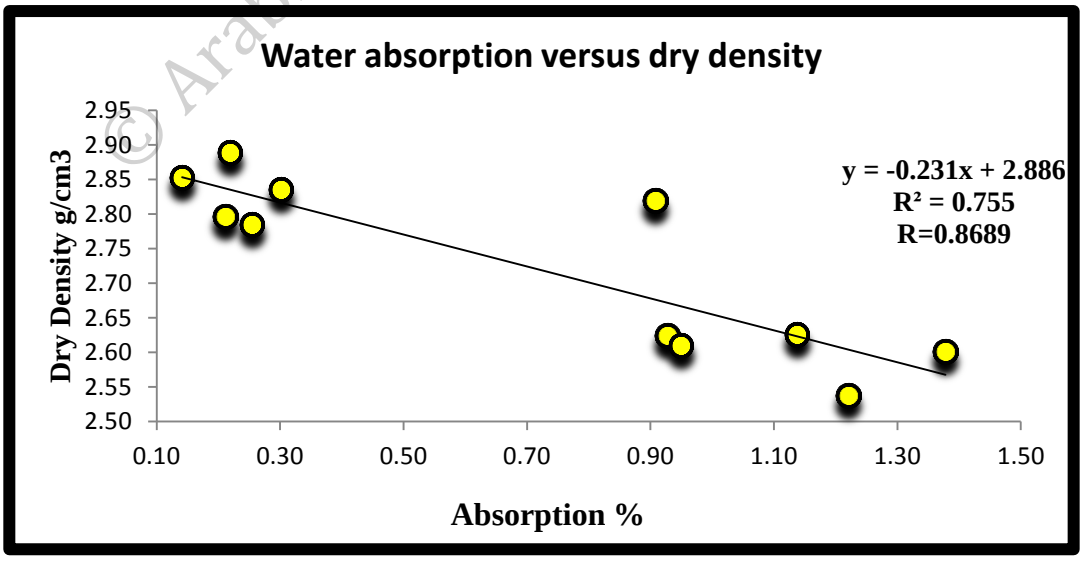

Figure (6.3): Absorption versus dry density for basalt samples.

© Arabic Digital Library-Yarmouk University
www.manaraa.com

6.3.4 Porosity and void ratio

The Coefficient of Determination (R2) and the correlation coefficient (r) indicates a perfect positive linear relationship (figure 6.4). Show direct proportional linear relationship, indicating that an increase in porosity is associated with an increase in void ratio.

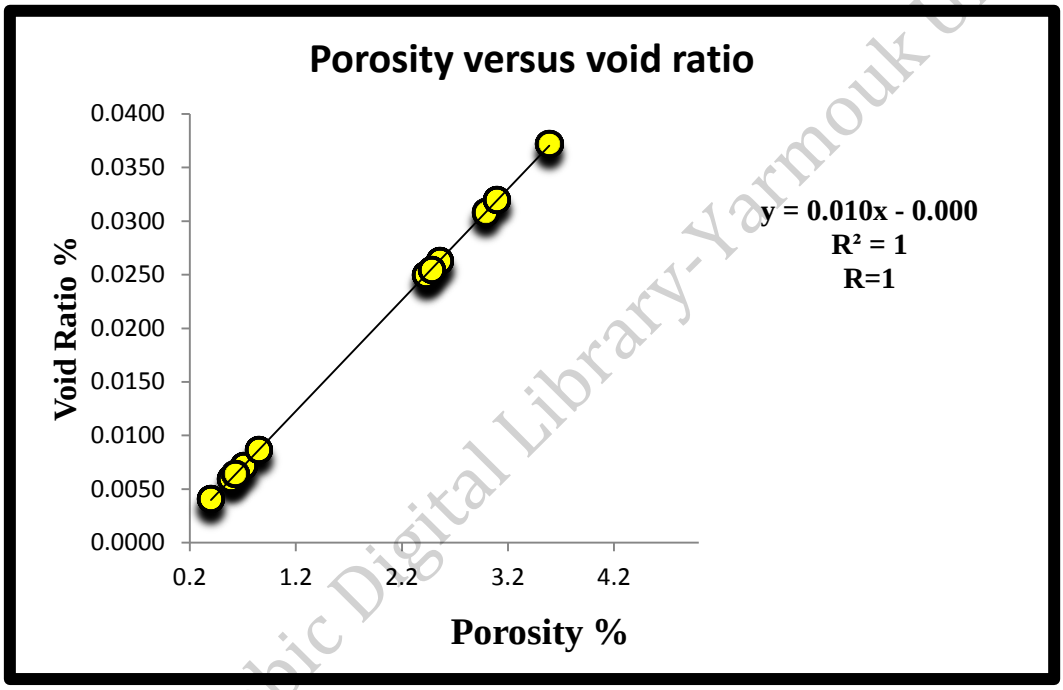

Figure (6.4): Relationship between porosity % versus void ratio %.

© Arabic Digital Library-Yarmouk University

6.3.5 Velocity versus bulk density relationships

The Coefficient of Determination (R2) and the correlation coefficient (r) indicate a weak (negative) linear relationship (Figure 6.5). Show inversely proportional linear relationship, indicating that an increase in bulk density is associated with a decrease in ultrasonic velocity.

www.manaraa.com

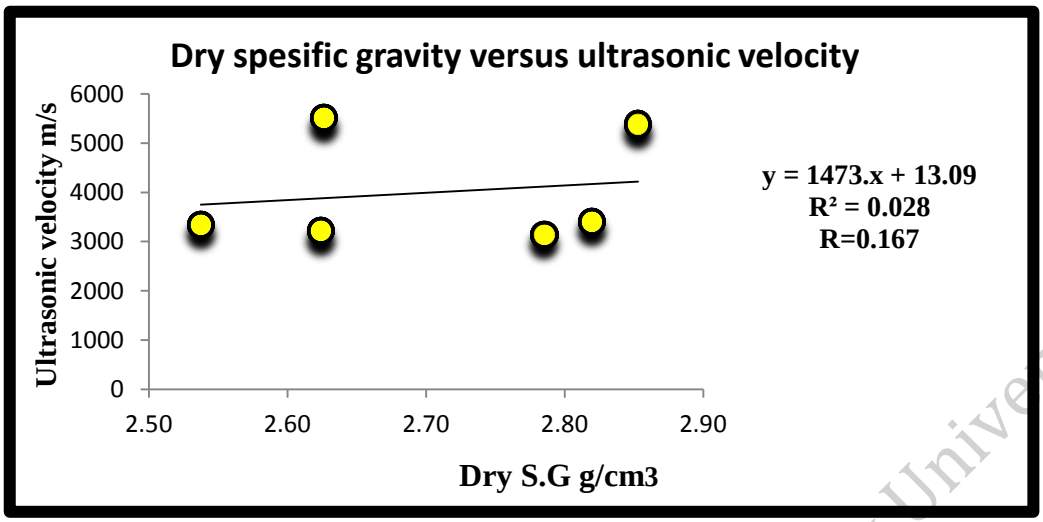

Figure (6.5): Relationship between dry density g/cm^3 and ultrasonic velocity m/s.

6.3.5 Ultrasonic wave velocities (Vp) vs porosity

The Coefficient of Determination (R2) and the correlation coefficient (r) indicates a moderate (negative) linear relationship, (Figure 6.6) show an inversely proportional linear relationship, indicating that a decrease in porosity is associated with an increase in ultrasonic velocity.

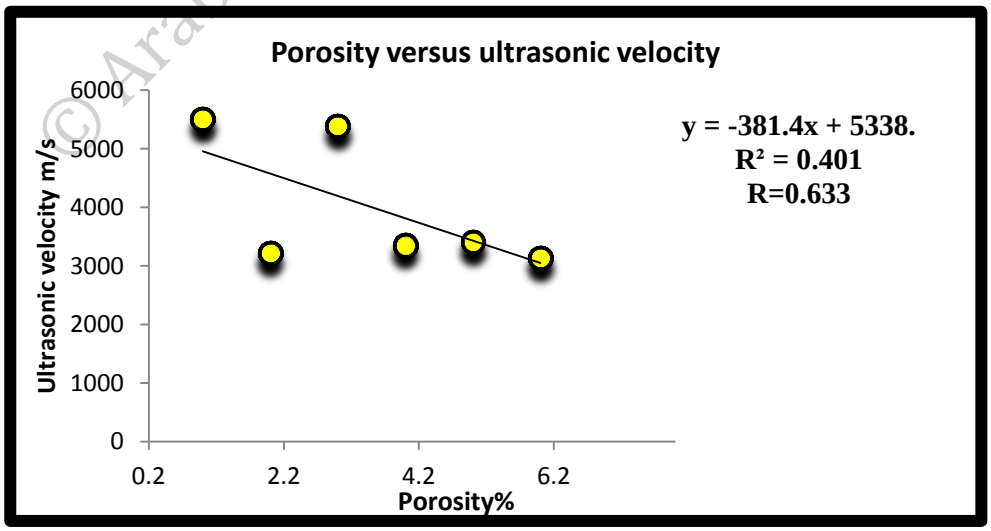

Figure (6.6): Relationship between porosity and ultrasonic velocity m/s.

© Arabic Digital Library Yarmouk University
www.manaraa.com

Chapter Seven

Mechanical properties

7

© Arabic Digital Library-Yarmouk University

المنارة للاستشارات
www.manaraa.com

Chapter 7

Mechanical properties

7.1 Mechanical properties

7.1.1 Unconfined compressive strength Uniaxial compressive strength, (UCS).

The Uniaxial Compressive Strength test is one of the most important contribution parameters used in rock engineering. it is essential to understand rock nature and rock deformation behaviour under loading, which is established by applying compressive load until failure occurs in the core sample (Figure 7.1) by a fracture in the middle (table 7.1).

Table (7.1): Uniaxial Compressive Strength of the tested basaltic core samples.

Sample. no	Weight (kg)	Diameter (cm)	Height (cm)	Area (cm^2)	Volume (cm^3)	Load (kg)	UCS (MPa)
R1	557.83	5	10.1	19.63	198.21	68	353.33
R2	487.83	4.9	10.2	18.85	192.25	106	573.49
R3	503.7	4.9	10.2	18.85	192.25	87	470.69
R4	549.8	4.9	10	18.85	188.48	79	427.41
R5	507.9	4.9	10.2	18.85	192.25	88	476.10
R6	513.9	4.9	10.3	18.85	194.13	113	611.36

© Arabic Digital Library-Yarmouk University

www.manaraa.com

Figure (7.1): Crack and failure pattern in basalt core.

The Uniaxial Compressive Strength values of the tested basalt samples ranges from 353.33 to 611.36 MPa. The maximum value of the unconfined compressive strength was recorded from sample R6, while the lowest value was recorded in the R1 sample (table 7.1). The corresponding engineering classification by Anon (1979) and Deer and miller, (1966) shows that all of the tested basaltic corresponds to class A (>250 MPa) indicating very high strength and extremely hard rock its, (Figure 7.2), table (7.2) & table (7.3).

The average value of the studied samples YRB samples was 485.40 MPa were obtained by using the Uniaxial Strength method. This value was compared with results obtained from Al- Hashimiyya basalt 106.83 MPa (AL-Zyoud 2005), and Abu Mahfouz 108.94 MPa. Compared with northern Jordan values by (Taqieddin, 2017) in Irbid, Ramatha, Mafraq, Zarqa and Um- Qays, their average values were 105.89, 90.90, 87.92, 92.58 and 97.97

© Arabic Digital Library Yarmouk University

المنارة للاستشارات
www.manaraa.com

respectively. The continental basalt uniaxial compressive strength shows an average value of (100-300 MPa).

Table (7.2): Show the Hardness and unconfined compressive strength of the tested samples.

Types of rocks	Typical range in unconfined compressi strength (MPa)
Very soft rock or hard, soil -like materia	0.60 –1.25
Soft rocks	1.25 –5.0
Moderately soft rocks	5.0 –12.5
Moderately hard rocks	12.5 – 50
Hard rocks	50 –100
Very hard rocks	100 – 250
Extremely hard rocks	> 250

Table (7.3): classification of the intact rock in accordance to the basis of strength (Deere and Miller, 1966)

Class	Uniaxial compressive strength (Mpa)	Type of strength
A	> 220	Very high strength
B	110-220	High strength
C	55 - 110	Medium strength
D	28 - 55	Low strength
E	< 28	Very low strength

Several factors such as porosity, tectonic deformations, and the degree of weathering may affect the test results, flatness of the end faces of core, moisture content, rate of loading; specimen size and shape have great influence on the test results significantly. This is attributed to the following external and internal factors:

© Arabic Digital Library-Yarmouk University
www.manaraa.com

- The external factores includes: Specimen geometry bearing surfaces, shape and size, rate of loading, platens conditions and surfaces and non-isotropy.

- The internal factors includes: Mineralogical composition, porosity, moisture content and texture.

The relationship between porosity, compressive strength and deformability indicates that the YRB show low porosity of 1.8% and can be clasifyed as extremely strong and slightly deformable table (7.4). Low strenght value due to some samples suffered from slight altration ,contains some secndery minerals(calcite, zeolite) and are moderately fractured.

Table (7.4): Relationship between porosity, compressive strength and deformability of the tested vesicular basalt (modified after Turk and Dearman 1983).

Porosity (%)	Strength	Deformability
0–5	Extremely strong	Very slightly deformable
5–10	Very strong	Very slightly deformable
10–20	Very strong	Slightly deformable
20–30	Strong	Slightly deformable
30–50	Strong	Moderately deformable
>50	Moderately strong	Very deformable

© Arabic Digital Library Yarmouk University

www.manaraa.com

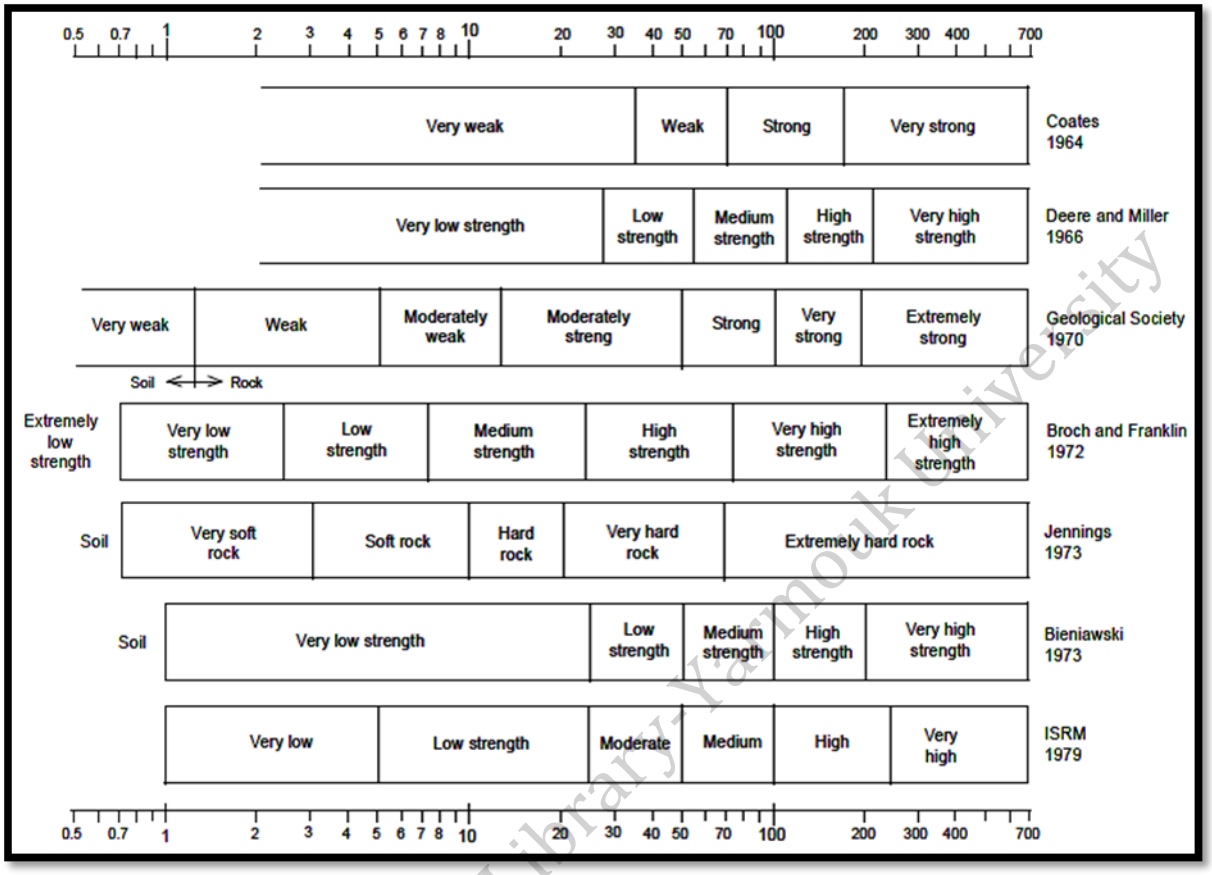

Figure (7.2): Classifications of the strength of the tested basalt rock samples according to (Deere and Miller, 1966).

7.1.2 Los Angeles Abrasion test

It is a common technique used to evaluate the toughness and abrasion characteristics of crushed basaltic rock used in aggregate, concrete and road construction. It measures also the degradation of a coarse aggregate sample that is placed in a rotating drum with steel spheres. Once the test is completed, the calculated mass of the crusched aggregate is expressed as a percentage of the total mass of these aggregates.

According to Farmer, 1983 this property depends on the mineral content and the strength of the chemical bonds.

© Arabic Digital Library-Yarmouk University
www.manaraa.com

Abrasion is calculated as a percentage using the following equations:

$$\% A = (Iw - R w)/ Iw$$

Where:

%A : Abrasion percent

Iw :Iinitial weight of the sample.

Rw : Retained weight on sieve No.12.

Table (7.5): Show thee abrasion test results of the TRB.

Sample .no.	% Abrasion For 100 Revolution	%Abrasion For 500 Revolutions	Uniformity of wear (100/500)
1	4.3%	22%	0.195
2	4.5%	22.7%	0.198

© Arabic Digital Library-Yarmouk University

www.manaraa.com

The uniformity of wear ratio (100/500) which is very important in engineering constructions. Results obtained for the uniformity of wear ratio ranges from 0.195 to 0.198% with an average value of 0.1965%, while the abrasion for the 500 revolution cycle is in the range of 22.355 (table 7.5).

This test was conducted to determine the suitability of basalt for concrete and road constructions. The wear ratios of the YR basalt were compared with the north Jordan values obtained by Taqieddin, 2017 showing average values of 0.19, 0.23, 0.20, 0.22 and 0.20 respectively.this test indicated the basalt rock good forusing as construction materials. Low Los Angeles Abrasion value due to some samples suffered from slight altration ,contains some secndery minerals(calcite, iddingsite) and are moderately fractured.

7.2 Simple regression analysis of physical and mechanical properties

An attempt was used to correlate Uniaxial Compressive Strength, ultrasonic Velocity, bulk density, open porosity, Los Angeles and water absorption of the volcanic rocks of the study area.

7.2.1 Relationship between porosity and uniaxial compressive strength

The Coefficient of determination (R2) and the correlation coefficient (r) indicates a moderate (negative) linear relationship (Figure 7.3).

© Arabic Digital Library-Yarmouk University

www.manaraa.com

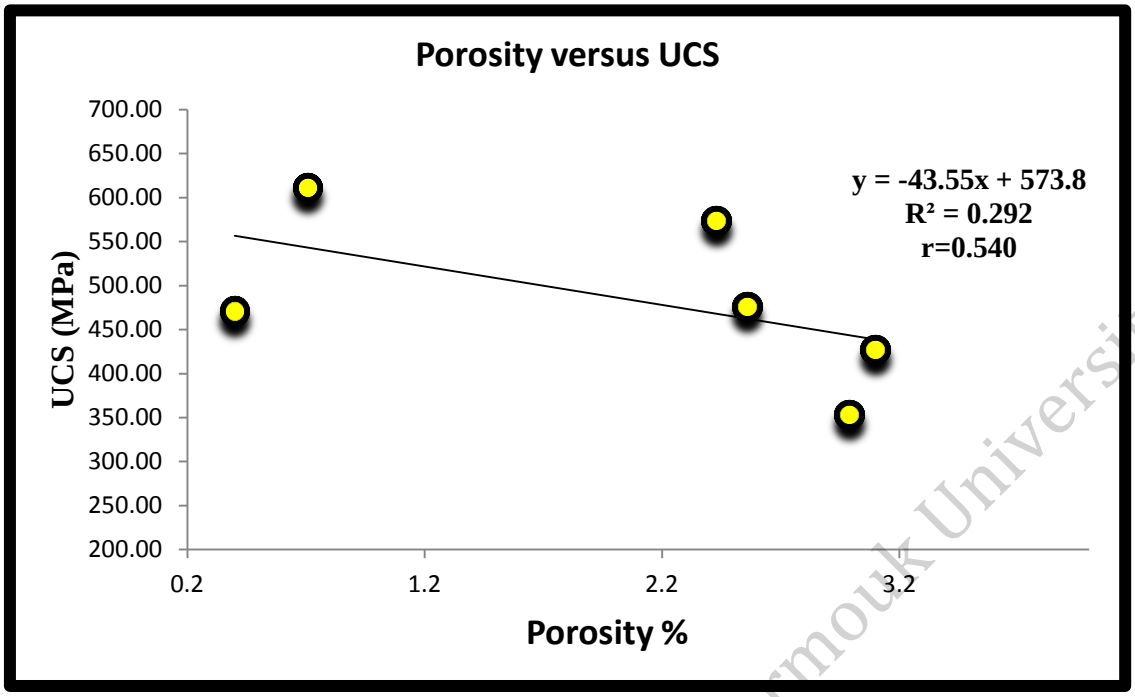

Figur (7.3): Show an inverse proportional linear relationship, indicating that the rapid decrease in the uniaxial compressive strength is related to the increase in the determined porosity.

7.2.2 relationship between ultrasonic velocity and uniaxial compressive strength

The Coefficient of determination (R^2) and the correlation coefficient (r) indicates a moderate (negative) linear relationship**.** Figure (7.4) show an inversely proportional linear relationship, indicating a rapid decrease in the compressive strength obtained with an increase in the determined velocity.

© Arabic Digital Library-Yarmouk University

www.manaraa.com

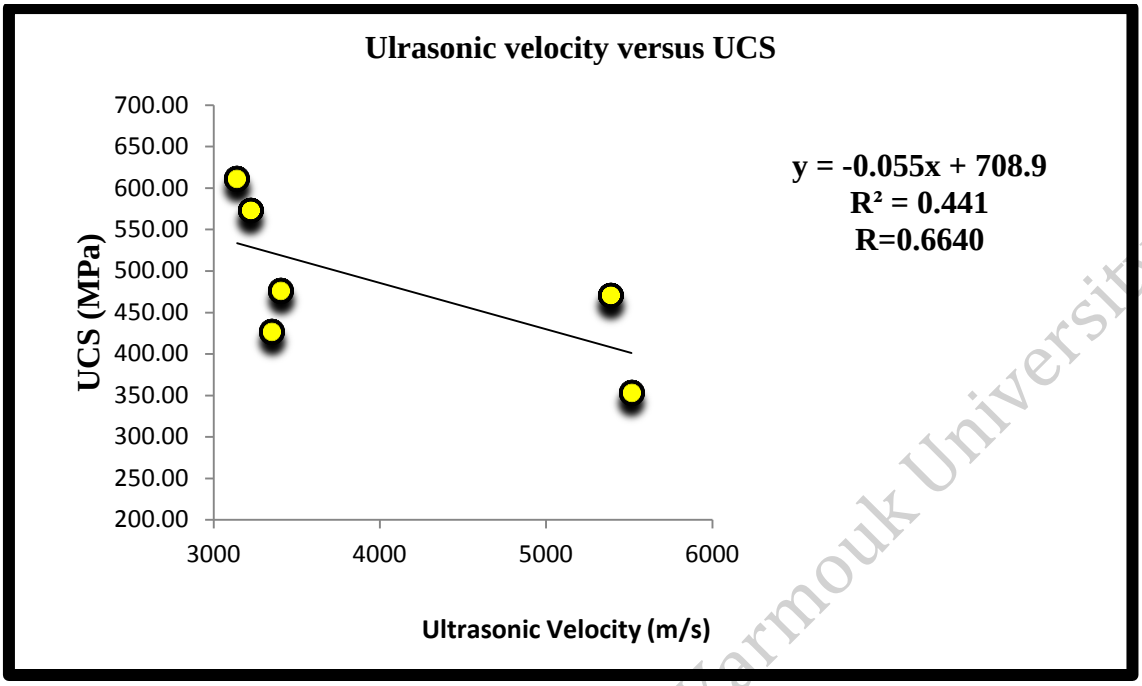

Figure (7.4): Showing the relationship between the ultrasonic velocity versus Uniaxial Compressive Strength.

7.2.3 Relationship between specific gravity and uniaxial compressive strength

The Coefficient of determination (R2) and the correlation coefficient (r) indicates a weak (negative) linear relationship. Figure (7.5) show an inversely proportional linear relationship, indicating that a rapid decrease in the compressive strength obtained is related to an increase in the specific gravity. An increase in the compressive strength values was obtained in samples with lower bulk density values and a decrease for samples with higher bulk densities.

© Arabic Digital Library-Yarmouk University

www.manaraa.com

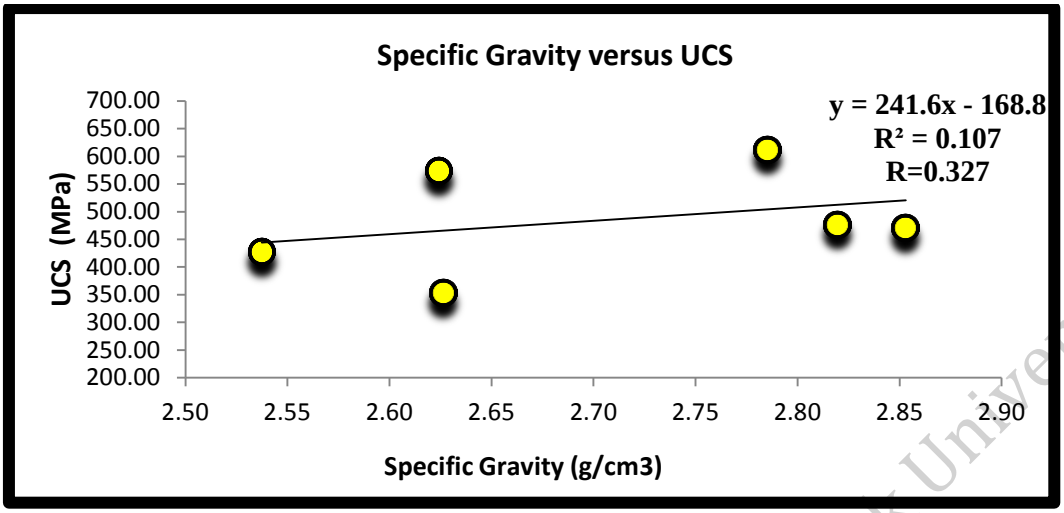

Figure (7.5): correlation of specific gravity versus Uniaxial Compressive Strength.

7.2.4 Relationship between Los Angeles and absorption

The Coefficient of determination (R2) and the correlation coefficient (r) indicates a perfect positive linear relationship. Figure (7.6) show a direct proportional linear relationship, indicating that an increase in the Los Angeles values obtained is related to an increase in the absorption.

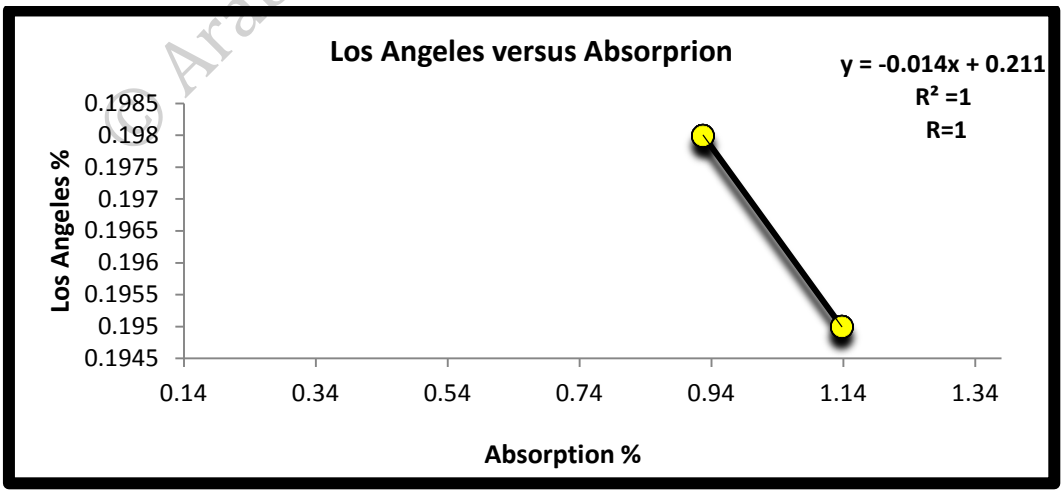

Figure (7.6): Correlation of the obtained Los Angeles values with absorption.

© Arabic Digital Library-Yarmouk University
المنارة للاستشارات
www.manaraa.com

Chapter Eight

Conclusions and Recommendations

© Arabic Digital Library-Yarmouk University

المنارة للاستشارات
www.manaraa.com

Chapter 8

Conclusions and Recommendations

8.1 Conclusions

Many different naturally accessible geological materials were used for different purposes after subjecting them to definite modifications and changes. The scarcity of commonly used geological materials such as granite, marble, etc., and the increasing demand of construction materials have led to intense and new investigations resulting in the use of naturally occurring basaltic rocks as construction materials.

In this work all the available geochemical, geological, physical, mechanical and petrographical data from the literature, field observation, intensive laboratory works have been gathered and synthesized to draw the following conclusions, because a better understanding of the engineering properties of rocks can provide a base for a more rational approaches to use these rocks in civil engineering works. Understanding of the physical and mechanical properties of those rocks can be useful both for initial selection and for diagnosis of the deterioration processes of building stone.

8.1. Conclusions

8.1.1 The YRB flows cover an area of about 1 km. It is exposed as massive, sheeted and vesicular basalt with thicknesses ranging from few meters up to 122 m and has four successive flow units. These basalt flows are:

© Arabic Digital Library-Yarmouk University

www.manaraa.com

A. Flow 1 has a thickness of 35 m that characterize by sheeted and cliff basalt.

B. Flow 2 has 27 m thickness of massive, blocky and jointed basalt.

C. Flow 3 is about 23 m in thickness of Pahoehoe lava 15 m in thickness and a'a lava 8m in thickness.

D. F4 is columnar an exfoliated basalt with 8 m thick.

The abundance of vesicular basalt, give us clues that the basalt in the study area was caused by a volcanic eruption that flows in the YR area from wadi al Ragaad in Syria.

8.1.2 Mineralogically, the using OM, XRD and SEM show that the rocks are characterized by a high content of the minerals diopside and olivine with a low or without nepheline and high content of plagioclase Labradorite , and low content percent of orthoclase, magnetite, apatite, and illmenite.

The XRD analysis indicated that the main mineral is pyroxene (clinopyroxene) especially augite, pigeonite, sodalite and diopside olivine (forsterite) also appeared as primary rock forming minerals calcite and zeolite as secondary rock forming mineral.XRD also indicated that plagioclase, feldspathoids, opaque minerals are present (such as magnetite, illmenite as trace minerals).

Mineralogically, the main mineral constituent of basaltic rock includes plagioclase, pyroxene (augite, pigeonite, and diopside and hypersthene),

© Arabic Digital Library Yarmouk University

www.manaraa.com

olivine, and opaque minerals. The secondary minerals included calcite, zeolite, iddingsite and serpentine.

Microscopic classifications indicated that YRB types are related to as pyroxene phyric basalt, olivine- pyroxene phyric basalt and olivine Phyric basalt type.

Petrographically the common textures of the YRB were trachytic, glomeroporphyritic, vesicular, and amygdaloidal, porpherytic, ophitic to sub ophitic texture, intergranular and taxitic texture, and melanocraitic, hypocrystalline, hypidiomorphic fine to medium grained.

8.1.3 Geochemically, YRB is of subalkaline type and was produced from the saturated primitive magma, and showing sodic series.

8.1.4. The physical properties tests have shown that:

(a) Apparent Specific gravity ranges between (2.62 – 2.91) gm/cm^3.

(b) Bulk Specific gravity (oven dry basis) ranges between (2.54 – 2.89) gm/cm^3.

(c) Bulk Specific gravity (S.S.D dry basis) ranges between (2.57 – 2.90) gm/cm^3.

(d) Absorption values range between (0.14 –m 1.38) % according to Jumikis, (1983) the values of absorption indicating a crystalline texture

(e) The porosity ranges between (0.4 to 3.59%), which considered classifying as low porous rock, of class 4 of the IAEG classification.

© Arabic Digital Library Yarmouk University

المنارة للاستشارات
www.manaraa.com

(g) The void ratio was (0.004 to 0.0372) %.

(h) Ultrasonic velocity values range between (3141–5514) m/s.

6. According to the International Association of Engineering Geologists (IAEG), the basalt samples can be classified as very high ultrasonic wave velocity of class 5, which gives an average of 4003 m/s, specific gravity is consider to be high, and porosity gives low porous basalt classification.

8.1.5 The engineering properties tests have shown that:

(a) The Uniaxial Compressive Strength values of the tested basalt samples ranges from 353.33 to 611.36 MPa with an average was 485.40 MPa. The corresponding engineering classification by Anon (1979) and Deere and miller, (1966) shows that all of the tested basaltic corresponds to class A (>250 MPa) indicating very high strength and extremely hard rock its

(b) Basalt uniformity of wear ratio ranges from 0.195 to 0.198% with an average value of 0.1965%.

According to (Turk and Dearman, 1983), the relationship between porosity, compressive strength and deformability indicates that the YRB show low porosity of 1.8% and can be classified as extremely strong and slightly deformable.

© Arabic Digital Library-Yarmouk University

www.manaraa.com

8.2 Recommendations

The studied area basalts have been used as construction material both for aggregate and dimension stone/cut stone without any physical and mechanical characterization. This leads to failure of the engineering structures before the design life. The present study identified important physical, chemical and mechanical properties of the YRB in general. However, the following recommendations are suggested to be considered:

1. It's recommended to study other locations and types of basalt in Jordan which are still to be studied.
2. It's recommended study the petrogenesis of YRB and other chemical properties such as Alkali Silica Reactivity (ASR) .
3. Its recommended to study isotopes analyses and rare earth elements should be made to determine the exact age of basalt and their interrelationships
4. It's recommended to study permeability, freezing and thawing tests, flatness index and elongation index should be carried out.
5. It's recommended to study Thermal conductivity, confined compression strength, flexural strength, point load Strength Dynamic elastic modulus (Young's modulus) should be carried out.

© Arabic Digital Library-Yarmouk University

www.manaraa.com

6. It's recommended to make feasibility studies and economic values of the basalt rocks for utilization in different construction applications merits further investigations.
7. It's recommended to make Environmental Impact Assessments (EIA) of the construction stone quarry sites on environment.

© Arabic Digital Library-Yarmouk University

المنارة للاستشارات
www.manaraa.com

References

- Abu-Mahfouz, I. (2009). "Petrogensis of Irbid District basalt rocks (Al-Tura – Beit Ras); Northern Jordan, and their engineering evaluation as building and Construction material". M.Sc. thesis, Hashemite University, Jordan.
- Abu-Mahfouz, I. Al-Malabeh, A. and Rababeh, S. (2016). "Geo-Engineering Evaluation of Harrat Irbid Basaltic Rocks, Irbid District-North Jordan *" Arabian Journal of Geosciences*" Vol. 8,no.4, 230-236
- Al-Baijat, H. (2008): "The Use of Basalt Aggregates in Concrete Mixes in Jordan", *Jordan Journal of Civil Engineering*, Volume 2, No. 1.
- Al-Baijat, H. and Benedetti, A. (2013). "Comparison between Composite Column Using Limestone and Basalt Concrete". *Open Journal of Civil Engineering*, Vol. 3, 1-6
- Abu-Mahfouz, I., Al-Malabeh, A. and Rababeh, S. (2016). "Geo-Engineering of Harrat Irbid Basaltic Rocks, Irbid District-North Jordan". Arabian Journal of Geosciences, Vol. 8, No. 4.
- Al-Hunjul, N. (2001): "The Geology of Qasr Al Harrana". Natural Resources Authority, Geologic Directorate, Geological Mapping Division, Bulletin 49, Amman, 29.
- Al-Amoush, H. (2010). "Integration of Vertical Electrical Sounding and Aeromagnetic Data Using GIS Techniques to Assess the Potential of Unsaturated Zone and Natural Basalt Caves for Groundwater Artificial Recharge in NE-Jordan". *Jordan Journal of Civil Engineering*, Vol. 4, No. 4, pp. 387-389.
- Al-Malabeh, A. (1989): "The volcanic succession of Jabal Aritain volcano, NE – Jordan: A field, petrographic and geotechnical study". M.Sc. thesis, Yarmouk University, Jordan, p.p182.
- Al-Malabeh, A. (1993): "The volcanolgy, mineralogy and geochemistry of selected pyroclastic cones from NE – Jordan and their evolution for possible industrial applications", pp.330.
- Al-Malabeh, A. (1994): "Geochemistry of Two Volcanic Cones from the Intracontinental plateau Basalt of Harra El-Jabban, NE-Jordan". In Basaltic rocks of Various Tectonic Setting, Special Issue of the Geochemical Journal, Japan Vol. 28: 542-558.
- Al-Malabeh, A., El-Hasan, T., Lataifeh, M. and Shea, M. (2002). "Geochemical and Mineralogical Related Magnetic Characteristics of the Tertiary-Quaternary (Umm Al-Qutein) Basaltic Flows from the Basaltic Field of Harrat El-Jabban Northeast Jordan". *Physica B*: *Condensed Matter*, 32, 396-403
- Al-Malabeh, A., (2003). "Geochemistry and Volcanology of Jabal Al-Rufiyat, Strombolian Monogenic Volcano". Jordan, Dirasat, 30: 125-14
- Al-Malabeh, A. (2004): "Physico-Mechanical Evaluations and Economic Potential of Umm Qays Basalts for Construction Purposes". 5th On Eastern Mediterranean Geol. Abstr. Band P.7, Athen-Greece.

© Arabic Digital Library-Yarmouk University

www.manaraa.com

- Al-Malabeh, A. (2005): "New discoveries supporting eco-tourism in Jordan". *1st Economic Jordanian Forum. Abstracts*. Book, p. 6.
- Al-Malabeh, A. (2009). "Cryptic Mantle Metasomatism: Evidences from Spinel l Herzolite Xenoliths/Al-Harida Volcano in Harrat Al-Shaam, Jordan". *American Journal of Applied Sciences*, Vol. 6, No. 12, 2085-2092.
- Alnawafleh, H., Tarawneh, K., Ibrahim, K., Zghoul, K., Titi, A., Rawashdeh, R., Moumani, K. and Masri, A. (2015). "Characterization and Origin of the Miocene Mudawwara-Quwayra Basaltic Dike, Southern Jordan". *International Journal of Geosciences*, 6, 869-881.
- Al-Oufi, A., Al-Malabeh, A. and Al-Tarazi, E. (2012). "Characterization of Lava Caves, Using 2D Induced Polarization Imaging, Umm Al Quttein area, NE Jordan". *15th International Symposium on Vulcanospeleology*, March 15-22, 71-83.
- Anon, P. (1979). "Classification of rocks and soils for engineering geological mapping", Part I: Rock and soil materials, *Bulletin of International Association of Geology*, No.19, 364-371
- Al-Zyoud, S. (2005). "Geochemistry and Physico-Mechanical Evaluations of Al-Hashimiyya Basaltic Rocks-Jordan". M.Sc. thesis, Hashemite University, Jordan.
- Bany Yaseen, I. Al-Hawari, Z. and Diabat, A. (2010). "Petrology, Geochemistry, Petrogenesis and Reactivation of Volcanic Tuffs at Dair El-Kahif Area, NE-Jordan". J*ordan Journal of Civil Engineering*, Vol. 4, No. 4, pp. 336-350.
- Bany Yaseen, I. (2014). "Petrography and Mineral Chemistry of the Almanden Garnet, and Implication for Kelyphite Texture in the Miocene Alkaline Basaltic Rocks, North East Jordan". *International Journal of Geosciences*, Vol. 5, pp.222-237.
- Barberi, F. Capaldi, G. Gasperini, P. Marinelli, G. Santacroce, R. Scandone, R. Treuil, M. and Varet, J. (1979). "Recent basaltic volcanism of Jordan and its implications on the geodynamic evolution of the AfroArabian rift system". *Accademia Nazionale Dei Lincei, Atti Del Corvegni Lincei*, 47, Rome, pp. 667–683.
- Barberi, F., Civetta, L. & Varet, J. (1980). "Sr isotopic composition of Afar volcanics and its implication for mantle evolution.- - Earth Planet. Sci. Lett, 50: 247- 259, 7 Fig., 2Tab.; Amsterdam.
- Bender, F. (1974). "Geology of Jordan". Supplementary edition in English with minor revision. Gebr. Borntraeger, pp.196.
- Best, M. (2003). "Igneous and Metamorphic Petrology". Second Edition, *Library of Congress Cataloging-in-Publication Data*, USA, Vol. 7, pp. 153-163.
- Brown, E. T. (1981). "Rock Characterization testing and monitoring", Peramon Press Ltd.
- Camp,V.E.& Roobol, M.J. (1989). "The Arabian contienental alkali province": Part I. Evolution of Harrat Rahat, Kingdom of Saudi Arabia.- - Geol. Soc. Am. Bull., 101: 71-95., 18 Fig.4Tab.; Boulder.
- Camp, V. and Roobol, M., (1992). "Upwelling asthenosphere beneath western Arabia and its regional implications", *Journal of Geophysical Research*, 97: 15255-15271.

© Arabic Digital Library-Yarmouk University

www.manaraa.com

- Central Intelligence Agency (CIA), U.S. (2004). "Jordan (Physiography) 2004 Map". Retrieved November 23, 2014, from Psi Phi: Perry-Castañeda Library Map Collection of University of Texas Education Web Site: http://www.lib.utexas.edu/maps/jordan.html.
- Coleman, R., and McGuire, A., (1988). "Magma systems related to the Red Sea opening", Tectonophysics, 150:77 –100.
- Cox, K.G., Gass, I.G. & Mallick, D.I. (1970). "The peralkaline volcanic suite of Aden and Little Aden", South Arabia. - -J .Petrol., 11: 433- 462; Oxford.
- Deere, D.U. and Miller, R.P. (1966). "Engineering classification and index properties of intact rock". Tech report. No. AFWL-Tr-65-116, USAF Weapons lab. Kirtland Air force Base, NM.
- Downes, H. et. al., (1995). "Petrology and geochemistry of late Tertiary/Quaternary mafic alkaline volcanism in Romania", Lithos, 35, 65-81.
- Derucher, K.N., and Heins, C.P.(1981)."*Materials For Civil And Highway Engineers", Prentice Hall, Inc*
- Dubertret, L. (1929). "Edute des regions volcaniques du Haouran", du Djebel Druze et du Diret –et-touloul. pp. 321.
- Duncan, N. (1966)."Rock mechanics and earthwork engineering". Part 5: Excavation assessments: Quantitative classification of rock materials. Muck Shifter., 24, No. 10, P.39-47.
- Duncan, N. (1969). "Engineering Geology and Rock Mechanics", 2 Vols. London, Leonard Hill.
- El-Hasan, T., and Al-Malabeh, A. (2008). "Geochemistry, Mineralogy and Petrogenesis of El-Lajjoun Pleistocene Alkali Basalt of Central Jordan". *Jordan Journal of Earth and Environmental Sciences*, Vol. 1, No. 2, pp. 53-62.
- Ewart, E. (1982). "The mineralogy and petrology of Tertiary– recent orogenic volcanic rocks with special reference to the andesite – basaltic composition range". In: Thorpe RS, ed. Andesites. New York, John Wiley and Sons: 25–87.
- Farmer, I. (1983). "Engineering Behavior of Rocks", 2nd edition. Chapman and Hall Ltd.
- French, W.J. (1991). "Concrete petrography: a review". *Quarterly Journal of Engineering Geology*, 24, 17–48.
- Gass, I.G, Mallick, D.I. & Cox, K.G. (1973). "Volcanic island of Red Sea".- -J. Geol. Soc. London, 129: 275-310, 11 Fig., 6 Tab.; London.
- Goodman, R.E. (1993). "Rock in Engineering Construction, Engineering Geology", Wiley, New York, pp. 412.
- Horn, M.K. & Adams, J.A. (1966). "Computer-derived geochemical balance on element abundances".- -Geochim. Cosmochim. Acta., 30: 279 – 297; Oxford.
- Humidi, H. (1993). "Engineering properties of some selected basalt rocks in Northern Jordan".M.Sc. thesis, Jordan University of Science and technology, pp. 133.
- Ibrahim, K. (1993). "The geological framework for Harrat Ash – Shaam basaltic super group and its volcano tectonic evolution". Bulletin 25. NRA, Amman, Jordan.

© Arabic Digital Library Yarmouk University

www.manaraa.com

- Ibrahim, K., Rabba', I. and Tarawneh, K. (2001). "Geological and mineral occurrences map of the northern Badia region, Jordan, scale 1:250,000". *A Joint Report of the Higher Council for Science and Technology and the NRA*, p. 136.
- Ibrahim, K. Tarawneh, K. and Rabba', I. (2003). "Phases of activity and geochemistry of basaltic dike systems in northeast Jordan parallel to the Red Sea". *Journal of Asian Earth Sciences* 21, 467-472pp
- Ibrahim, K., Faisal, S. and Jamil, N. (2007)." Use of basalt in asphalt concrete mixes". Construction And Building Materials doi:10.1016/ j.conbuildmat.2007.10.026
- Ibrahim, K. Moh'd, B. Masri, A. Al-Taj, M. Musleh, S. and Alzughoul, K. (2014). "Volcanotectonic evolution of central Jordan: Evidence from the Shihan Volcano". *Journal of African Earth Sciences*, Vol. 100, pp. 541–553.
- Ilani,S. Harlvan,Y. Tarawneh, K. Rabba`, I. Weinberger, R. Ibrahim, K. Peltz, S. and Steinitz, G. (2001). "Dating of the Harrat Ash – Shaam basalts, Northeastern Jordan", Geological Society of America, Geology, Vol. 29; No. 2, 171-174.
- Irvine, T., and Barager, W. (1971). "A guide to the chemical classification of the common rocks". Canadian *Journal of Earth Sciences*, Vol. 8, pp. 523-548.
- Jenner, G., Gawood, P., Rautenschlein, M. and White, W., (1987). "Composition of back-arc basin volcanics", Valufa ridge, Lau basin: evidence for a slab-derived component in their mantle source, J. Volcanol. Geotherm. Res., 32: 209-222.
- Jumikis, A.R (1983). "Rock Mechanics "," Trans Tech Publications, second edition, 1983, U.S.A., PP. 37-40.
- Kempe, S. and Al-Malabeh, A. (2005). "Newly discovered lava tunnels of the Al-Shaam plateau basalts, Jordan". Geophysical Research Abstracts, European Geosciences Union, Vol. 7.
- Kempe, S. Al-Malabeh, A. and Henschel, H. (2012). "Jordanian lava caves, an overview". *15th International Symposium on Vucanospeleology*, March 15-22, pp. 38-43.
- Khalil, I. (1991). "Geochemische and petrographische Untersuchungen and teriären bis quartären kontinentalen Intraplattenbasalten Nordost – Jordaniens". - - Unpuble. Ph. D. thesis. Claustal University, Germany. 119p., 25 Fig., 19 Tab.; Claustal.
- Kretz, R. (1983). "Symbols of rock-forming minerals". American Mineralogist, Vol. 68, pp. 277-279.
- Lama, R. D., Vutukuri, V. S. (1978). "Hand book on Mechanical Properties of Rocks", Trans Tech Publications, Vol. 1, 2 & 4.
- Lartet, L. (1869). "Essai Sur La geologie de la Palestine et des contres avoisinantes", telles que Egypt et I Arabic, These, Fac. Sci. Paris, 316p; Paris.
- Le Bas, M., Le Maitre, R., Streckeisen, A. Zanettin, B. (1986). "A chemical classification of volcanic rocks based on the total alkalis-silica diagram". *Journal of Petrology*, Vol. 27, pp. 745-750.
- Mamillan, M. (1972). "Connaissances actuelles pour mesurer le degre d'alteration des pierres et l'efficacite des methodes de traitement", 1st. International Symposoium on the deterioration of building stones, La Rochelle, pp. 47-56.

© Arabic Digital Library Yarmouk University

www.manaraa.com

- Mcann, D.M. & Fennin G P.J. (1995). "Estimation of rippability and excavation conditions from seismic velocity measurements". In: Engineering Geology of Construction. The Geological Society, London. Engineering Geology Special Publication 10: 335-343.
- Meiler, M., (2011). "The Deep Geological Structure of the Golan Heights and the Evolution of the Adjacent Dead Sea Fault System". PhD thesis, Tel-Aviv, Tel-Aviv, 150 p.
- Meiler, M., Reshef, M. and Shulman, H., (2011). "Seismic Depth-Domain Stratigraphic Classification of the Golan Heights", Central Dead Sea Fault. Tectonophysics, 510: 354-369.
- Moffat, R. (1988). "Describing the uncertainties in experimental results". *Experimental Thermal and Fluid Science*, Vol.1, pp. 3-17
- Moh'd, Basem K. (1997). "Geological Map of Irbid (3155II)". 1:50,000, Natural Resources Authority, Amman, Jordan.
- Moh`d, B. (2000). "The Geology of Irbid and Ash Shuna Ash Shamaliiyya (Waqqas) map". Sheets no.3154-IIand 3154-III Bulletin 46. NRA, Amman, Jordan.
- Pick, R., Deniel, C., Coulon, C. Yirgu, G. and Marty, B., (1999). "Isotopic and trace element signatures of Ethiopian flood basalts: evidence for plume-lithosphere interactions", Geochimicaet Cosmo-chimicaActa, 63: 2263-2279.
- Powell, J H. (1989)." Stragraphy and Sedimentation of The Phanerozoic Rocks in Center and".Ph.D. thesis, Amman, Jordan.
- Raymond, Loren A. (2002). "The Study of Igneous, Sedimentary and Metamorphic Rock". Library of Congress Cataloging-in-Publication Data, New York, NY: McGraw-Hill.
- Saffarini, G., Khoury, H., & Rascha, H. (1987). "Detection of compositional variations and differentiation trend in Cenozoic Jordanian basalts". - - Dirasat, 12: 193-210, 12 Fig., 2Tab.; Amman.
- Siegesmund, S. and &Dürrast, H. (2011). "Stone in Architecture, Properties, Durability: Geoscience Center", Universität Göttingen, Göttingen, Germany, Naturstein, Bauchemie und Bauphysik in der Denkmalpflege, Bamberg, Germany.
- Spear, F. (1993). "Metamorphic Phase Equilibria and Pressure-Temperature-Time Paths". *Monograph 1, Mineralogical Society of America*, Chantilly, Virginia.
- Sun, M. (1957), "The nature of iddingsite in some basaltic rocks of New Mexico", Am. Mineral., Vol. 42, pp. 526–532.
- Sun, S.S & Hasnson, G.N (1976). "Rare earth element evidence for differentiation of Mc Murdo volcanics", Ross Island, Antarctica.- -Contrib. Mineral. Petrol., 45:139-155; 10 Fig. 4Tab.; Amsterdam.
- Swain, C. (20.1). "Determination of Rock Strength from Slake Durability Tests, Protodyakonov Impact Tests and Los Angeles Abrasion Resistance Tests". M.Sc. thesis, National Institute of Technology, (Deemed University), Rourkela.

© Arabic Digital Library-Yarmouk University

www.manaraa.com

- Taqieddin, S. (2017)." Physical and Engineering Properties of Some Selected Jordanian Basalt". PhD thesis ,Jordan university of science and technology ,pp.34
- Tarawneh, K. ShimonI, Rabba, I. Harlavan, Y. Peltz, S. Ibrahim, K. Weinberger, R. and Steinitz, G. (2000). "Dating Of the Harrat Ash Shaam Basalts/ NE Jordan (Phase 1)". NRA-GSI Report, p. 65.
- Taylor,S.R. (1968). "Geochemistry of andesites".- - In: Originand distribution of the element. Ed. L.H. Ahrns, 551- 584; Peryamon.
- Thompson, R.N.,Morrison, M.A., Dickin, A.P. &Hendry, G.L. (1983). "Continental flood basalt, Arachnids rule OK"?.- - In Hawkeseorth, C.J. & Norry, M.J. (eds) ,continental basalts and mantle xenoliths , 158 – 185, Cheshire (Shiva).
- Touloukian, Y, S. (1981). "Physical properties of rocks and minerals", Megraw-Hill., New York.
- Turk, N.T., Dearman, W.R., (1983). "A practical classification of rocks for engineering purposes". Bull. Int. Assoc. Eng. Geol. 28, 161–167.
- Van Den Boom, G. and Sawwan, O. (1966). "Report on Geological and Petrological Studies of The Platue Basalt in NW Jordan". Germ. Unpubl. Germ. Geol. Mission in Jordan. 42p.
- Von Moos, A., De Quervin. F., (1948). "Technische Gesteinskunde. Birkhäuser, Basel. Vos BH (1978) Hygric methods for the determination of the behaviour of stones". Int Symp Deterioration of Stone Monuments. UNESCO-RILEM, Paris.
- Waqa, I. R. (2004). "Geological and Geo-technical Characterisation of Aggregate Source
- Rocks from Selected Sites in Viti Levu Fiji". M.Sc. thesis, University of Canterbury (unpubl.)
- Winter, john D. (2001). "An Introduction to Igneous and Metamorphic Petrology". *Library of Congress Cataloging-in-Publication Data*, New Jersey, NJ: Prentice Hall .
- Wedepohle, K.H. (1987). "Kontinentaler Intraplatten Vulkanismus am Besipiel der tertiären Basalte der Hessischen Senke". - - Forschr. Mineral. 6:19-47, 10 Fig., 6 Tab.;Stuttgart.
- Wilson, M. (1989). “Igneous Petrogenesis, a Global Tectonic Approach”. Unwin Hyman, London.
- Weismann, G. And Abdullatif, A. (1963). "Geology of the Yarmouk Area, North Jordan". GGM Report, 81p.
- Yasar, E. and Erdogan, Y. (2004). "Correlating sound velocity with the density, compressive strength and Young’s modulus of carbonate rocks". Int. J. Rock Mech. Min. Sci., 41-5, 871-875.

© Arabic Digital Library-Yarmouk University

المنارة للاستشارات
www.manaraa.com

© Arabic Digital Library-Yarmouk University

المنارة للاستشارات
www.manaraa.com